Synthesis and mechanism of biological action of morpholinyl-bearing arylsquaramides as small-molecule lysosomal pH modulators

Tao Zhang [#a], Xiao-Qiao Hong [#b], Hai-Tao Zhi [a], Jinhui Hu [a,*] and Wen-Hua Chen [a,*]

[a] *School of Biotechnology and Health Sciences, Wuyi University, Jiangmen 529020, Guangdong, P. R. China*

[b] *School of Pharmaceutical Sciences, Tsinghua University, Haidian Dist, Beijing 100084, P. R. China*

[#] *These authors contributed equally to this work.*

Supporting Information

1. Experimental procedures

Preparation of EYPC vesicles

Vesicles for chloride efflux and size distribution measurements were prepared based on the reported protocols. [1] Specifically, a solution of EYPC in chloroform (0.5 mL, 40 mg/mL) in a test tube was concentrated with N_2 and subsequently dried under vacuum overnight. A solution of NaCl in 25 mM HEPES buffer (500 mM, pH 7.0, 1 mL) was added to the tube. The resulting mixture was vortexed for 1 min. The dispersion was then incubated at room temperature for 5 min, followed by another 1 min of vortexing and 20 min of incubation at ambient temperature. The sample was subjected to seven freeze/thaw cycles (77 K/325 K), followed by extrusion through a 100 nm Nuclepore membrane (15 times). After extrusion, the dispersion was incubated at room temperature for 30 min, and subject to gel filtration [Sephadex G-25, eluted with 25 mM HEPES buffer (500 mM $NaNO_3$, pH 7.0)] to exchange the non-entrapped NaCl.

The vesicles for cation and anion selectivity experiments were prepared in a similar fashion. Exceptionally, the vesicles used for cation selectivity experiments were formed in 25 mM HEPES buffer (500 mM MCl, pH 7.0; M = Li, Na, K, Rb or Cs) and the external solution was 25 mM HEPES buffer (500 mM $NaNO_3$, pH 7.0). The vesicles used for anion selectivity experiments were formed in 25 mM HEPES buffer (500 mM NaCl, pH 7.0), whereas the external solution was 25 mM HEPES buffer (500 mM $NaNO_3$, $NaHCO_3$, or 250 mM Na_2SO_4, pH 7.0).

Vesicles for calcein leakage experiments were prepared in a similar fashion, except that they were formed in a 100 mM calcein solution in 25 mM HEPES buffer (500 mM NaCl, pH 7.0); and 25 mM HEPES buffer (500 mM NaCl, pH 7.0) was used to elute the Sephadex G-25 column to remove the non-entrapped calcein.

Measurement of anionophoric activity [2-7]

Chloride anion efflux

To 1.78 mL of 25 mM HEPES buffer (500 mM $NaNO_3$, pH 7.0) was added the vesicle

dispersion (0.2 mL), followed by the addition of each compound in DMSO (20 μL). A chloride ion selective electrode was used to monitor the concentration of chloride anions. After 330 s, 10 wt% aqueous Triton X-100 (50 μL) was added. The relative chloride efflux was calculated using the following formula:

$$Relative\ chloride\ efflux\ (\%) = \frac{C - C_0}{C_{total} - C_0} \times 100\%$$

OR

$$Relative\ chloride\ efflux = \frac{C - C_0}{C_{total} - C_0}$$

Wherein C_0, C and C_{total} represent the concentration of chloride anions of the dispersion at the initial time, after a period of time and after the addition of 10 wt% aqueous Triton X-100, respectively.

Cation and anion selective transport

The experiments were tested in a similar fashion with chloride anion efflux. Exceptionally, for cation selectivity experiments, the liposome dispersion encapsulated with 500 mM MCl solution in 25 mM HEPES buffer (pH 7.0) was added to 500 mM $NaNO_3$ in 25 mM HEPES buffer (pH 7.0). Whereas for anion selectivity experiments, the liposome dispersion was added to 500 mM $NaNO_3$, $NaHCO_3$ or 250 mM Na_2SO_4 in 25 mM HEPES buffer (pH 7.0). The concentration of compound **12** was fixed at 5 mol%.

Calcein leakage experiments

200 μL of vesicle suspension was added to 1780 μL of 25 mM HEPES buffer (500 mM $NaNO_3$, pH 7.0). The resulting mixture was mixed well, and the fluorescence intensity was monitored against time. After 30 s, a solution of compound **12** in DMSO (20 μL) was added, and 50 μL of Triton X-100 solution (10 wt%) was added after 5.5 min. The relative fluorescence intensity was calculated according to the following formula.

$$FI = \frac{F - F_0}{F_\infty - F_0}$$

Wherein F_0, F and F_∞ represent the fluorescent intensity at the initial time, after a period of time and after the addition of 10 wt% aqueous Triton X-100, respectively.

Measurement of particle size distribution

A solution of compound **12** in DMSO was added to the vesicles for the measurement of size distribution (20 μL) diluted with 25 mM HEPES buffer solution (500 mM $NaNO_3$, 25 mM HEPES buffer, pH 7.0). The final concentrations of EYPC and compound 12 were 1.32 mM and 5 mol%, respectively. The resulting mixtures were stirred at room temperature for 5 min. Then the mixture (400 μL) was analyzed for the particle size distribution, by using a particle size analyzer.

U-tube experiments

A solution of compound **12** (1.0 mM) and $TBAPF_6$ (2.0 mM) in nitrobenzene (5 mL, 2 mM $TBAPF_6$) was placed at the bottom of a U-shaped tube. Then 3 mL of $NaNO_3$ aqueous solution (500 mM, 25 mM HEPES, pH 7.0) was added to one end of the tube, and 3 mL of NaCl aqueous solution (500 mM, 25 mM HEPES, pH 7.0) to the other end of the tube. The nitrobenzene solution was stirred continuously. The concentration of chloride anions in the receiving phase was measured at intervals of 12 h, by using a chloride ion selective electrode.

MQAE assays

The experiments were conducted following the protocols reported in literatures. [2, 5, 7] Specifically, HeLa cells were seeded in a 96-well flat-bottom culture plates (Corning) at the density of 1.2×10^4 cells/well (per 100 μL) and incubated in a 5% CO_2 incubator at 37 ℃ for 24 h. A solution of MQAE (5 mM) was added to each well, followed by incubation for additional 4 h. Extracellular dye was removed by washing with PBS buffer thrice. Then, a solution of compound **12** of varying concentrations in DMEM was added, and the cells were incubated for additional 2 h. DMSO (1%) was used as a control. The fluorescence of MQAE was measured by using a multifunctional microplate reader (λ_{ex} = 350 nm, λ_{em} = 460 nm).

MQAE-MP assays

The experiments were conducted following the protocols reported in literatures. [8] Specifically,

HeLa cells were seeded in a 96-well flat-bottom culture plates (Corning) at density of 1.2×10^4 cells/well (per 100 μL) and incubated in a 5% CO_2 incubator at 37 ℃ for 24 h. A solution of compound **12** of varying concentrations in DMEM was added, and the cells were incubated for additional 4 h. DMSO (1%) was used as a control. Then, a solution of MQAE-MP (5 mM) was added to each well, followed by incubation for additional 0.5 h. Extracellular dye was removed by washing with PBS buffer thrice. The fluorescence of MQAE-MP was measured by using a multifunctional microplate reader (λ_{ex} = 350 nm, λ_{em} = 460 nm).

Acridine orange (AO) assays

The experiments were conducted following the protocols reported in literatures. [9-12, 15] Specifically, HeLa cells were seeded on a 6-well plate for 24 h and then treated with compounds **1-12** of varying concentrations for 3 h. DMSO was used as a negative control. Then the cells were washed thrice with PBS buffer, and incubated in a solution of AO (5 μg/mL) at 37 ℃ in the dark for 30 min. Finally, the cells were washed with PBS buffer thrice and examined by fluorescence on a confocal microscope. ImageJ software (Media Cybernetics) was used to calculate the area integral intensities in each cell. The EC_{50} was obtained by fitting the ratios of red to green fluorescent intensity against the concentrations of each compound with GraphPad Prism 8 software.

BCECF-AM assays

The experiments were conducted following the protocols reported in literatures. [13] Firstly, a calibration curve for intracellular pH levels was determined after incubation of BCECF-loaded cells with 25 mM HEPES buffer (145 mM KCl, 0.8 mM $MgCl_2$, 1.8 mM $CaCl_2$, and 5.5 mM glucose, 10 μM nigericin) at pH varying from 7.0 to 9.5. The pH levels were adjusted using 1 M NaOH.

HeLa cells were seeded at 5,000 cells/well in 96-well plates overnight. The cells were incubated with BCECF-AM (2 μM) in a 20 mM HEPES buffer (153 mM NaCl, 5 mM KCl, 5 mM glucose, pH 7.4) at 37 °C for 1 h. Then, the HeLa cells were incubated with each compound (6.25 μM) for 3 h. The fluorescence of BCECF-AM was measured using a multifunctional microplate reader (λ_{ex} = 485 nm, λ_{em} = 525 nm and 640 nm). The ratios of the

fluorescent intensity at 525 nm to that at 640 nm were calculated, and used to calculate the pH value of each compound based on the pH standard curve.

LysoSensor Green DND-189 assays

The experiments were conducted following the protocols reported in literatures. [14] HeLa cells were incubated on glass slide for 24 h. The cells were washed with PBS for three times and treated with each compounds at 37 °C for 4 h. Then the glass slide was washed with PBS and a solution of LysoSensor Green DND-189 (1 μM) in DMEM was added. After incubation for 0.5 h, the supernatant was removed and the cells growing on the glass slide were washed with PBS. Finally, the cells were washed with PBS buffer thrice and examined by fluorescence on a confocal microscope. Green fluorescence: λ_{ex} BP 470/40 nm, λ_{em} BP 525/50 nm. ImageJ software (Media Cybernetics) was used to calculate the intensity for each green fluorophore in each lysosome. The EC_{50} was obtained by fitting the fluorescent intensity of each compound relative to the control against the concentrations of each compound with GraphPad Prism 8 software.

Assays based on fluorescein and tetramethylrhodamine-labeled dextran (FRD)

The experiments were conducted following the protocols reported in literatures. [5, 15] In order to obtain the pH standard curve of FRD, HeLa cells were treated with FRD for 12 h and then treated with different pH calibration buffers (120 mM KCl, 20 mM NaCl, 1 mM $CaCl_2$, 1 mM $MgCl_2$, 10 μM nigericin, 10 μM valinomycin, 10 mM HEPES with the pH adjusted from 4 to 8) for 30 min. The cells were washed thrice with PBS prior to taking image from a confocal fluorescence microscope. Fluorescein and TMR were excited at 488 nm and 543 nm, respectively, and their corresponding emissions in the range of 500–550 nm and 590–700 nm were collected, respectively. The pH was measured by the intensity ratio of TMR (red) to fluorescein (green) in each lysosome. ImageJ software (Media Cybernetics) was used to calculate the intensity of each fluorophore in each lysosome and the red/green intensity ratio. The fluorescence intensity ratio was plotted against pH values.

Then, HeLa cells were treated with 0.2 mg/mL FRD for 12 h and then treated with each compound for another 12 h. The cells were washed thrice with PBS prior to taking image

from a confocal fluorescence microscope. Fluorescein and TMR were excited at 488 nm and 543 nm, respectively, and their corresponding emissions in the range of 500–550 nm and 590–700 nm were collected, respectively. ImageJ software (Media Cybernetics) was used to calculate the intensity of each red or green fluorophore in each lysosome. The pH values of each compound were obtained from the ratios of red to green fluorescent intensity based on the pH standard curve.

Magic Red Cathepsin assays

The experiments were conducted following the protocols reported in literatures. [5, 15] Cathepsin B activity was analyzed using Magic Red cathepsin detection kit-MR-$(RR)_2$ according to the manufacturer's instructions. Briefly, HeLa cells were incubated in confocal dishes for 24 h and then treated with each compound (6.25 μM) for 4 h. MR-$(RR)_2$ was added and incubation was carried out for 4 h. The cells were washed three times with PBS and subject to confocal imaging with a confocal microscope. λ_{ex} = 543 nm, λ_{em} = 630 ± 20 nm. ImageJ software (Media Cybernetics) was used to calculate the intensity for each red fluorophore in each lysosome, and the corresponding intensity ratios of red fluorescence relative to the control group were calculated.

MTT assays

The experiments were conducted following the protocols reported in literatures [16]. Specifically, HeLa cells were dispersed in a 96-well flat bottom tissue culture treated plates (Corning) at density of 5000 cells/well (per 100 μL) and incubated at 37 °C in a 5% CO_2 incubator for 24 h. Then, the cells were treated for 48 h with each compound at the concentration of 25 μM. A solution of MTT in PBS buffer (5 mg MTT/mL) was added to each well and incubation continued for an additional 4 h. Then, the MTT solution was removed and DMSO (100 μL) was added in each well to dissolve the formed formazan crystals. The absorbance at 570 nm was recorded in a microplate reader. For each condition, at least three independent experiments were performed and the mean value was taken. DMSO (1%) was used as a control. Cell viability was expressed as a percentage of control cells, and the data are reported as the mean value ± S.D.

Western blotting

The experiments were conducted following the protocols reported in literatures. [17] HeLa cells were cultured in a 6-well plate for 24 h, then the media containing compound **12** of varying concentrations (1.56, 6.25 and 25 μM) were added to the petri dishes. The cells were then homogenized with lysis buffer. The protein concentrations were detected using an enhanced BCA Protein Assay Kit (Beyotime, China), and their extracts were reconstituted within loading buffer (Beyotime, China) and inactivated for 5 min at 100 °C. Subsequently, proteins (20 μg) were fractionated by 10% SDS-PAGE, and transferred to PVDF membranes. Then, their levels were determined with the appropriate dilution of primary antibodies (Cell Signaling Technology, China), including LC3 and p62. The above primary antibodies were then incubated using HRP-conjugated secondary antibody (Cell Signaling Technology, China), and immunoreactive bands were visualized by a chemiluminescence reagent (NCM Biotech, China) and estimated through densitometry with a Biomolecular Imager (Azure Biosystems, Sapphire RGBNIR). Intensities of the blots were quantified with ImageJ.

References

1. W.-H. Chen and S. L. Regen, *J. Am. Chem. Soc.*, **2005**, 127, 6538-6539.
2. X.-H. Yu, C.-C. Peng, X.-X. Sun and W.-H. Chen, *Eur. J. Med. Chem.*, **2018**, 152, 115-125.
3. Z. Li, X.-H. Yu, Y. Chen, D.-Q. Yuan and W.-H. Chen, *J. Org. Chem.*, **2017**, 82, 13368-13375.
4. C.-C. Peng, M.-J. Zhang, X.-X. Sun, X.-J. Cai, Y. Chen and W.-H. Chen, *Org. Biomol. Chem.,* **2016**, 14, 8232-8236.
5. N. Busschaert, S. H. Park, K. H. Baek, Y. P. Choi, J. Park, E. N. W. Howe, J. R. Hiscock, L. E. Karagiannidis, I. Marques, V. Felix, W. Namkung, J. L. Sessler, P. A. Gale and I. Shin, *Nat. Chem.*, **2017**, 9, 667-675.
6. W. Van Rossom, D. J. Asby, A. Tavassoli and P. A. Gale, *Org. Biomol. Chem.*, **2016**, 14, 2645-2650.
7. T. Saha, M. S. Hossain, D. Saha, M. Lahiri and P. Talukdar, *J. Am. Chem. Soc.*, **2016**, 138, 7558-7567.

8. S. H. Park, S. H. Park, E. N. W. Howe, J. Y. Hyun, L. J. Chen, I. Huang, G. Vargas-Zuniga, N. Busschaert, P. A. Gale, J. L. Sessler and I. Shin, *Chem*, **2019**, 5, 1-20.
9. E. Hernando, V. Soto-Cerrato, S. Cortes-Arroyo, R. Perez-Tomasv and R. Quesada, *Org. Biomol. Chem.*, **2014**, 12, 1771-1778.
10. N. Busschaert, M. Wenzel, M. E. Light, P. Iglesias-Hernandez, R. Perez-Tomas and P. A. Gale, *J. Am. Chem. Soc.*, **2011**, 133, 14136-14148.
11. V. Soto-Cerrato, P. Manuel-Manresa, E. Hernando, S. Calabuig-Farinas, A. Martinez-Romero, V. Fernandez-Duenas, K. Sahlholm, T. Knopfel, M. Garcia-Valverde, A. M. Rodilla, E. Jantus-Lewintre, R. Farras, F. Ciruela, R. Perez-Tomas and R. Quesada, *J. Am. Chem. Soc.*, **2015**, 137, 15892-15898.
12. A. M. Rodilla, L. Korrodi-Gregorio, E. Hernando, P. Manuel-Manresa, R. Quesada, R. Perez-Tomas and V. Soto-Cerrato, *Biochem. Pharmacol.*, **2017**, 126, 23-33.
13. P. Franck, N. Petitipain, M. Cherlet, M. Dardennes, F. Maachi, B. Schutz, L. Poisson and P. Nabet, *J. Biotechnol.*, **1996**, 46, 187-195.
14. X.-Q. Hong, X.-Y. He, K. Y. Tam and W.-H. Chen, *Bioorg. Med. Chem. Lett.*, **2020**, 30, 127461.
15. M.-H. Chen, Y. Zheng, X.-J. Cai, H. Zhang, F.-X. Wang, C.-P. Tan, W.-H. Chen, L.-N. Ji and Z.-W. Mao, *Chem. Sci.*, **2019**, 10, 3315-3323.
16. X.-H. Yu, X.-Q. Hong and W.-H. Chen, *Org. Biomol. Chem.*, **2019**, 17, 1558-1571.
17. C.-J. Wu, J.-Q. Wu, Y. Hu, S. Pu, Y. Lin, Z. Zeng, J. Hu and W.-H. Chen, *Eur. J. Med. Chem.*, **2021**, 223, 113629.

2. Structural characterizations

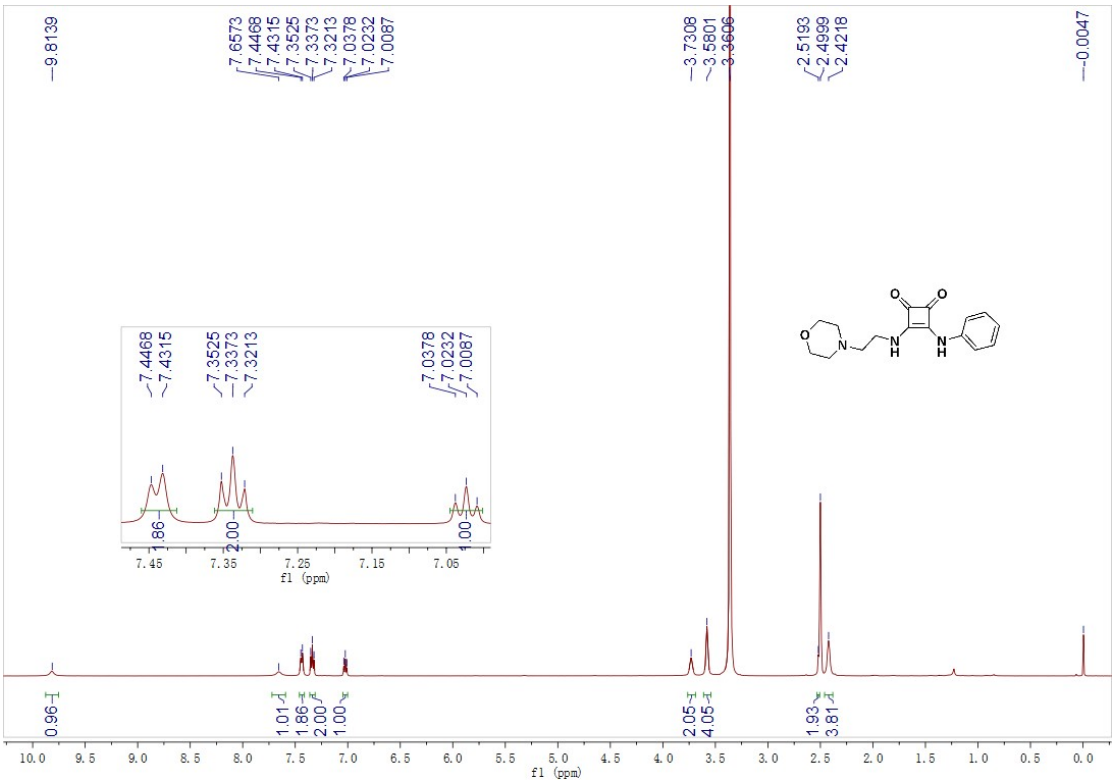

Fig. S1. ^{1}H NMR (500 MHz, DMSO-d_6) of compound **1**

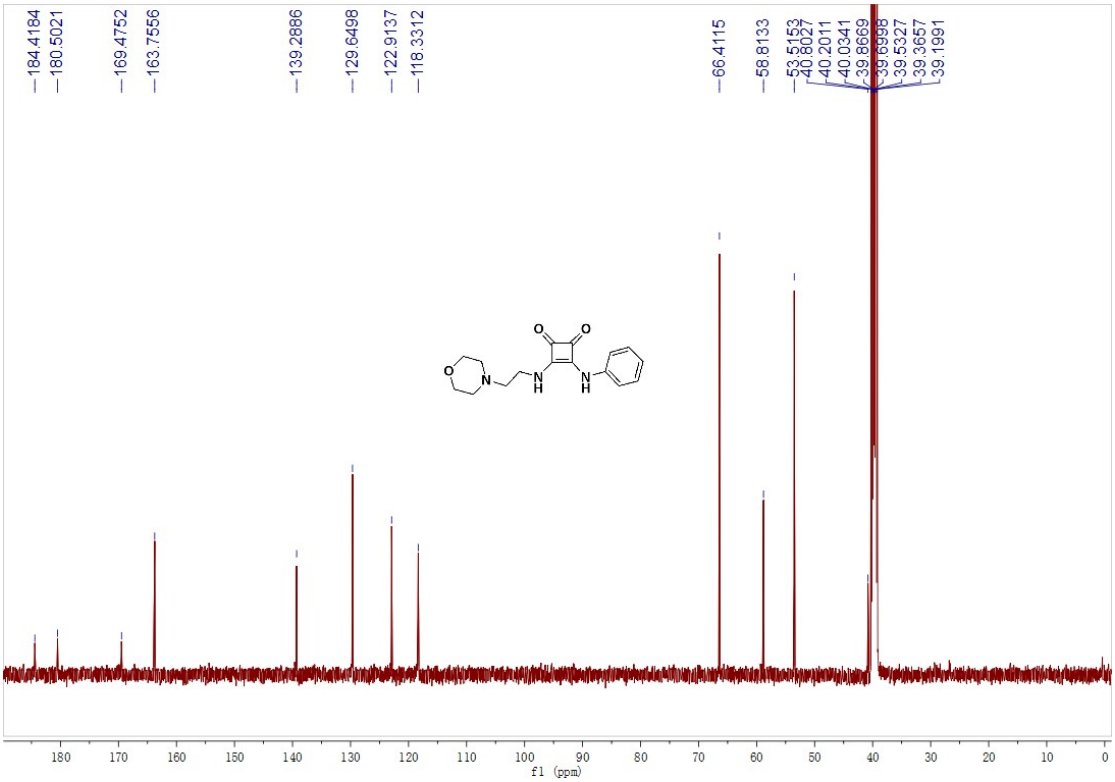

Fig. S2. ^{13}C NMR (125 MHz, DMSO-d_6) of compound **1**

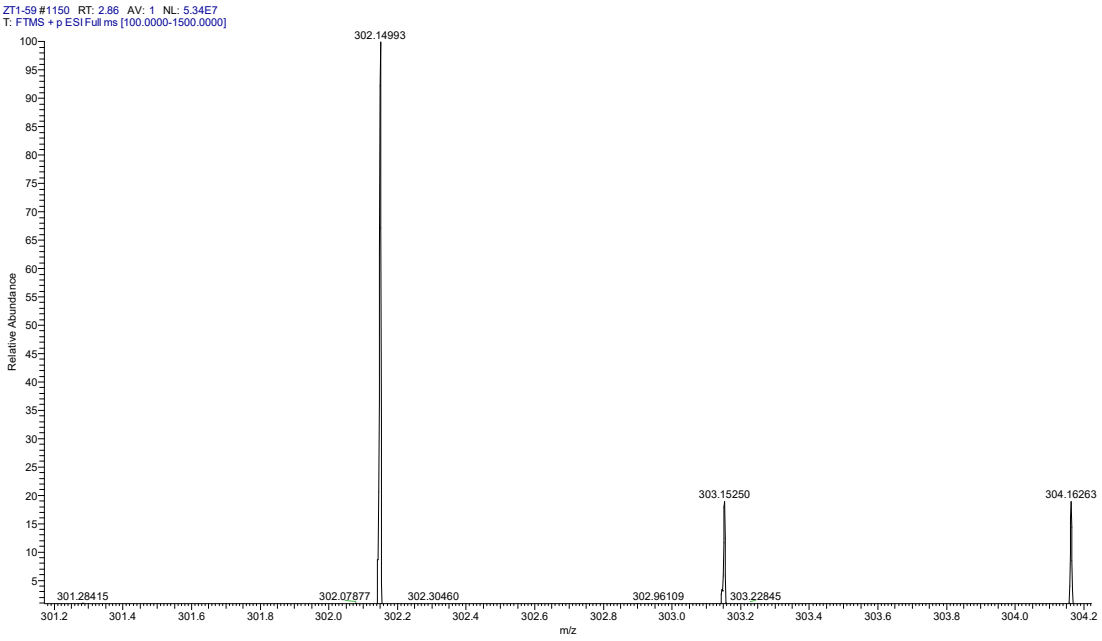

Fig. S3. HR-ESI-MS of compound **1**

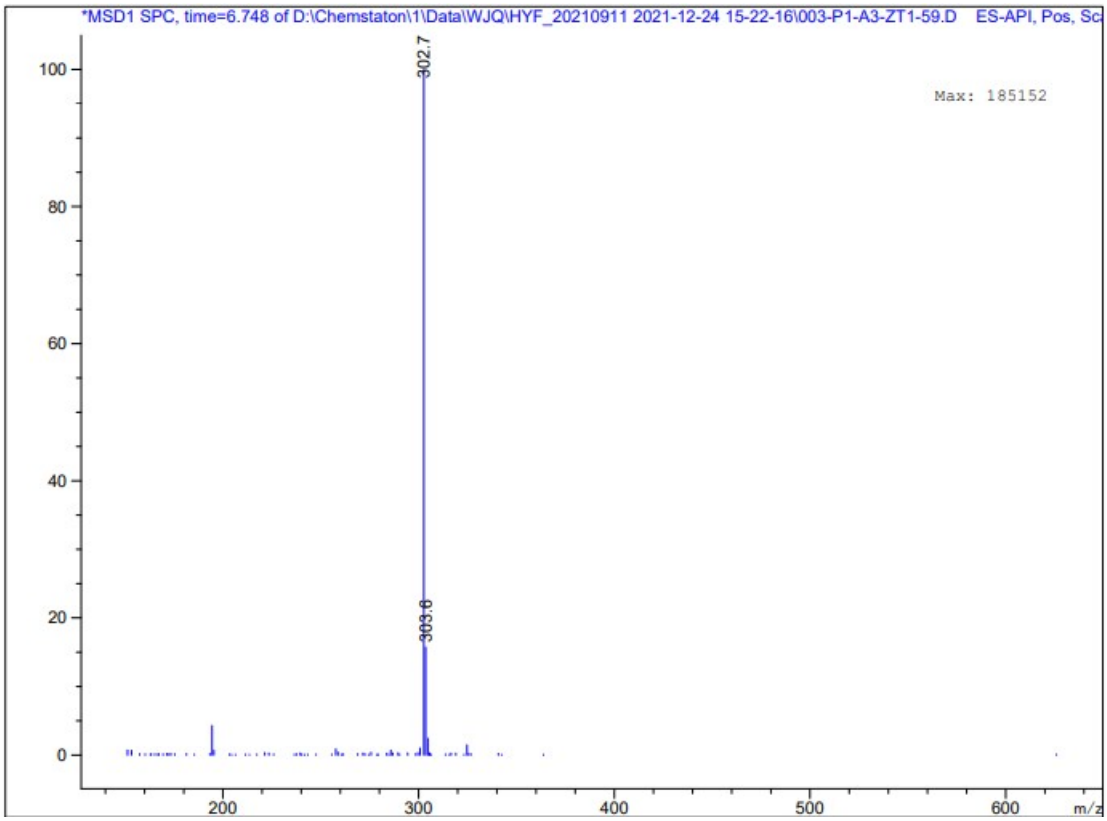

Fig. S4. LR-ESI-MS of compound **1**

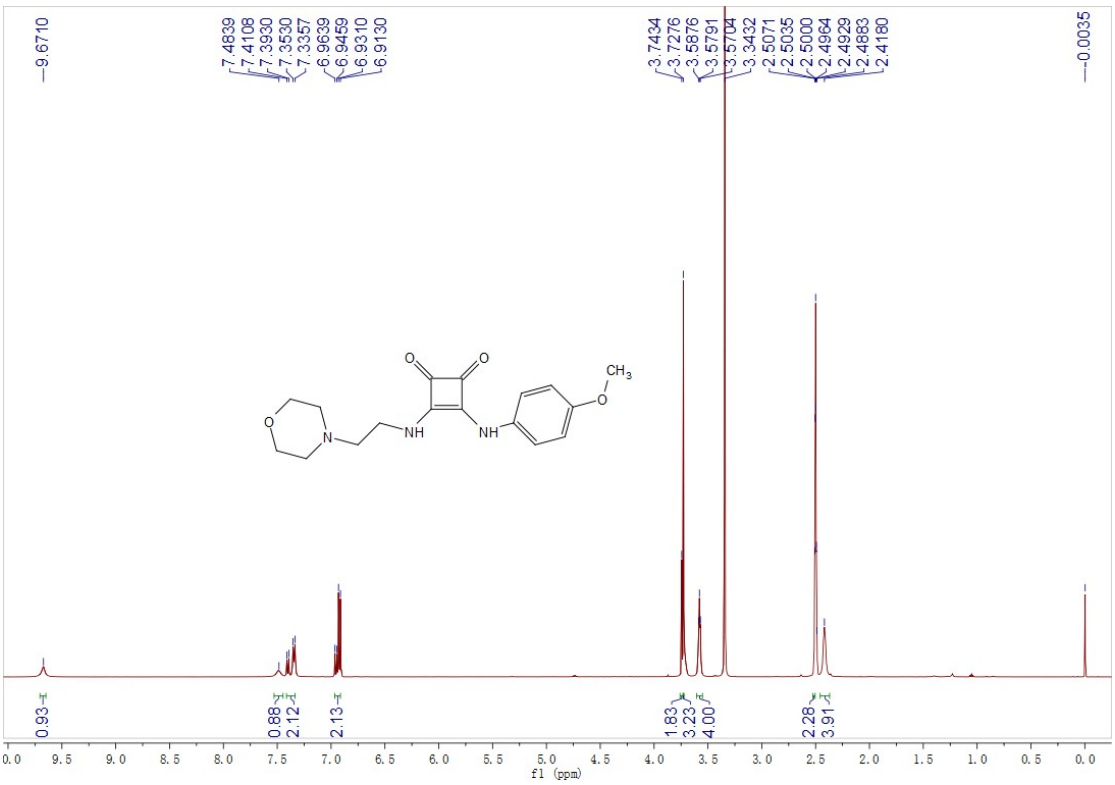

Fig. S5. ^{1}H NMR (500 MHz, DMSO-d_6) of compound **2**

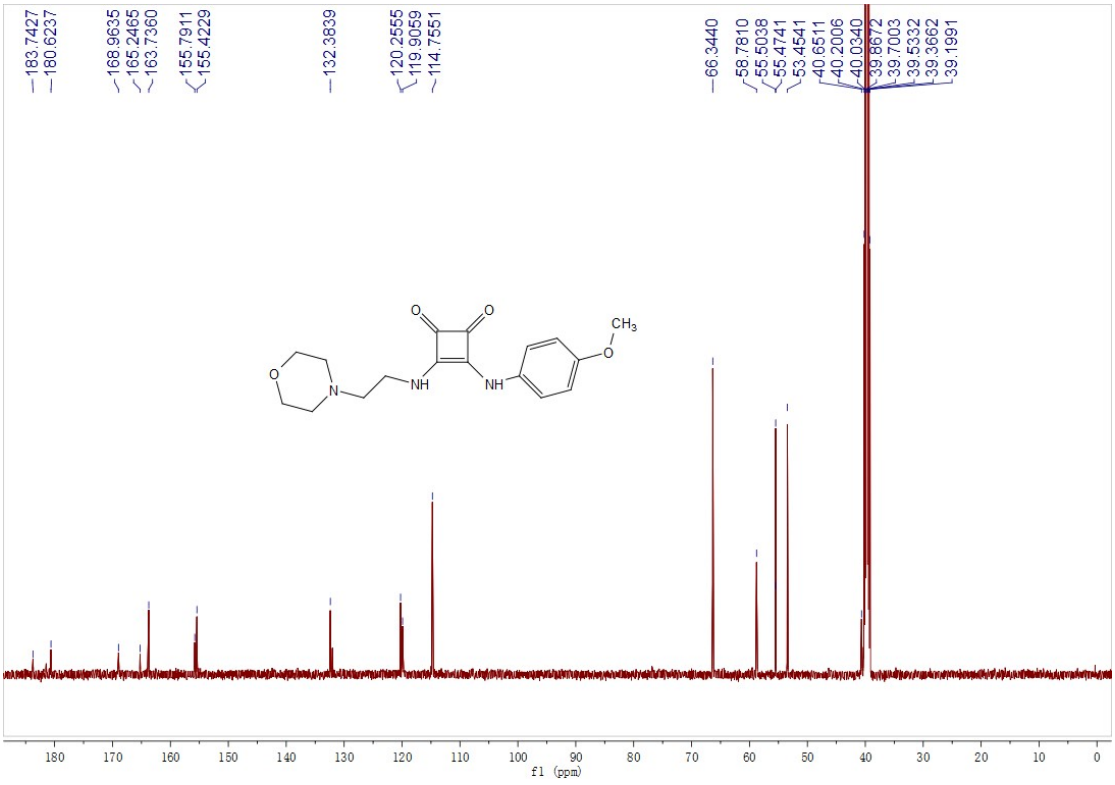

Fig. S6. ^{13}C NMR (125 MHz, DMSO-d_6) of compound **2**

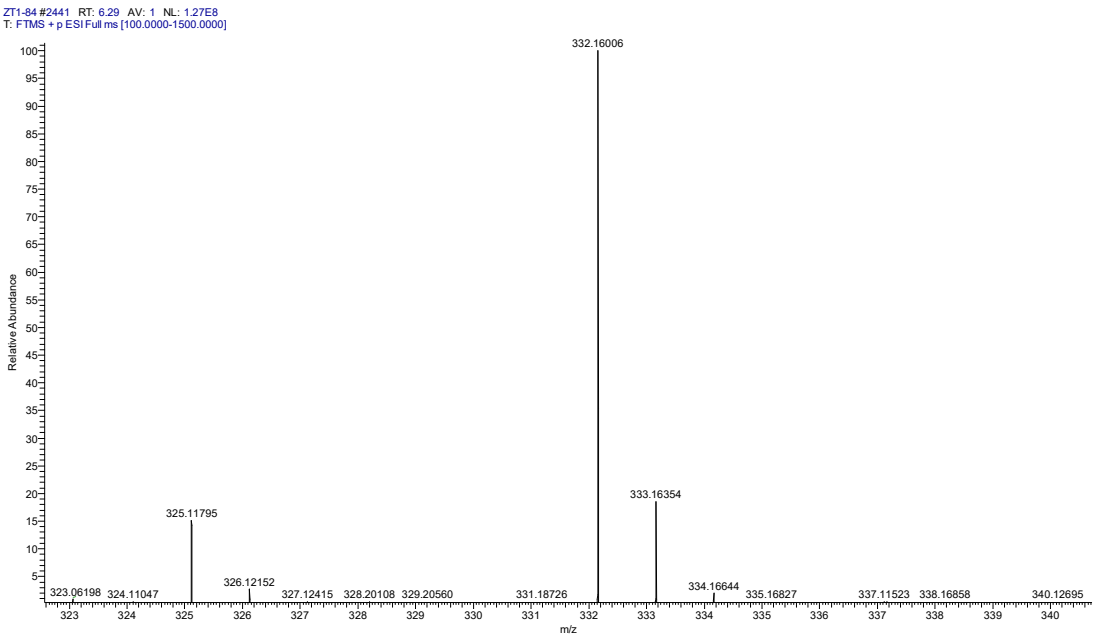

Fig. S7. HR-ESI-MS of compound **2**

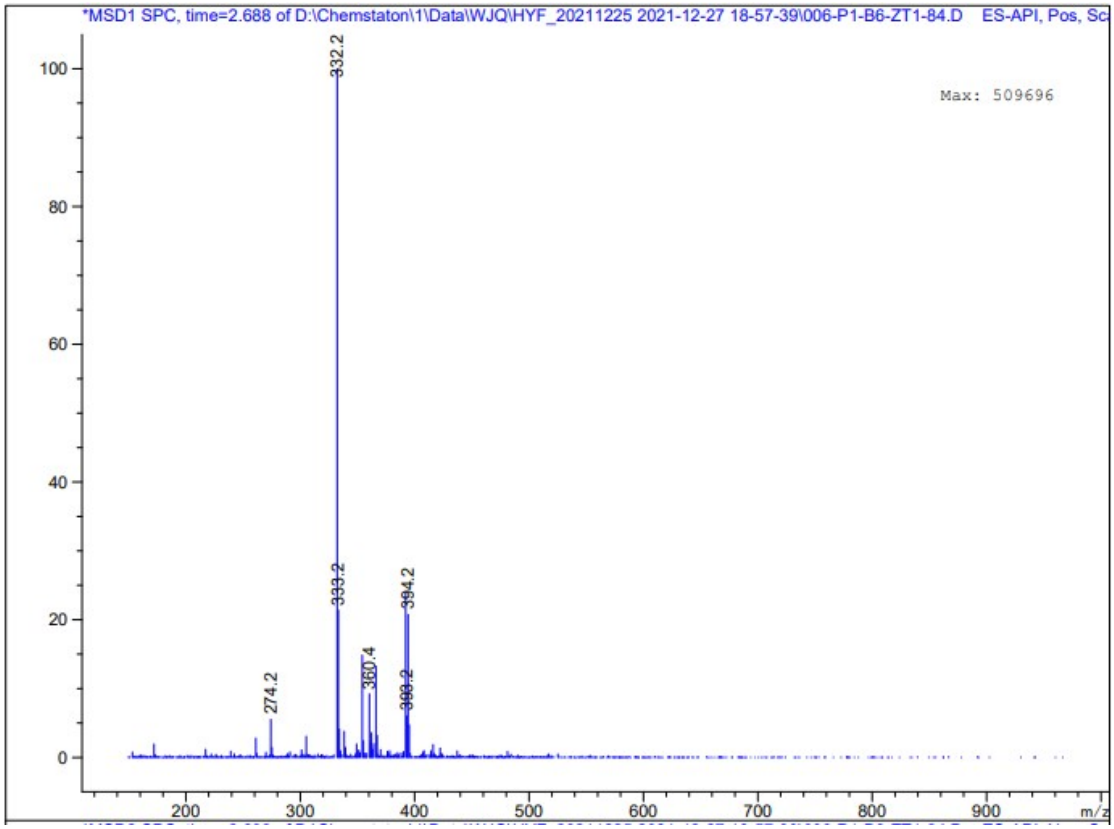

Fig. S8. LR-ESI-MS of compound **2**

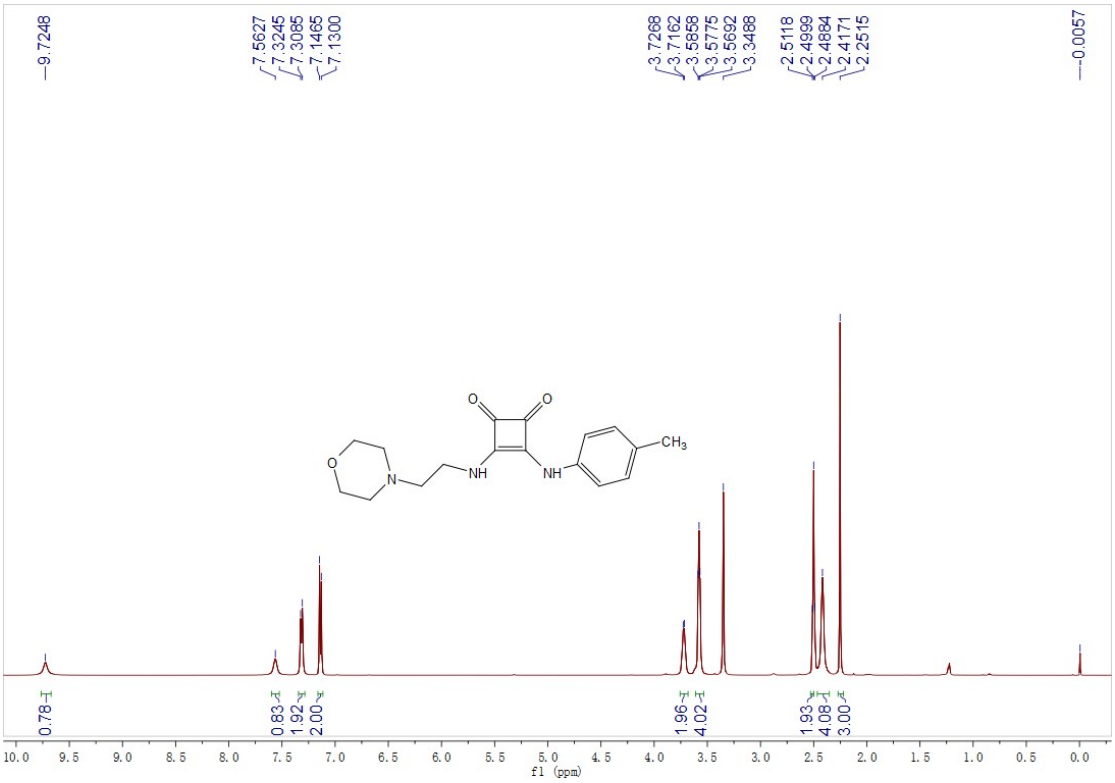

Fig. S9. ^{1}H NMR (500 MHz, DMSO-d_6) of compound **3**

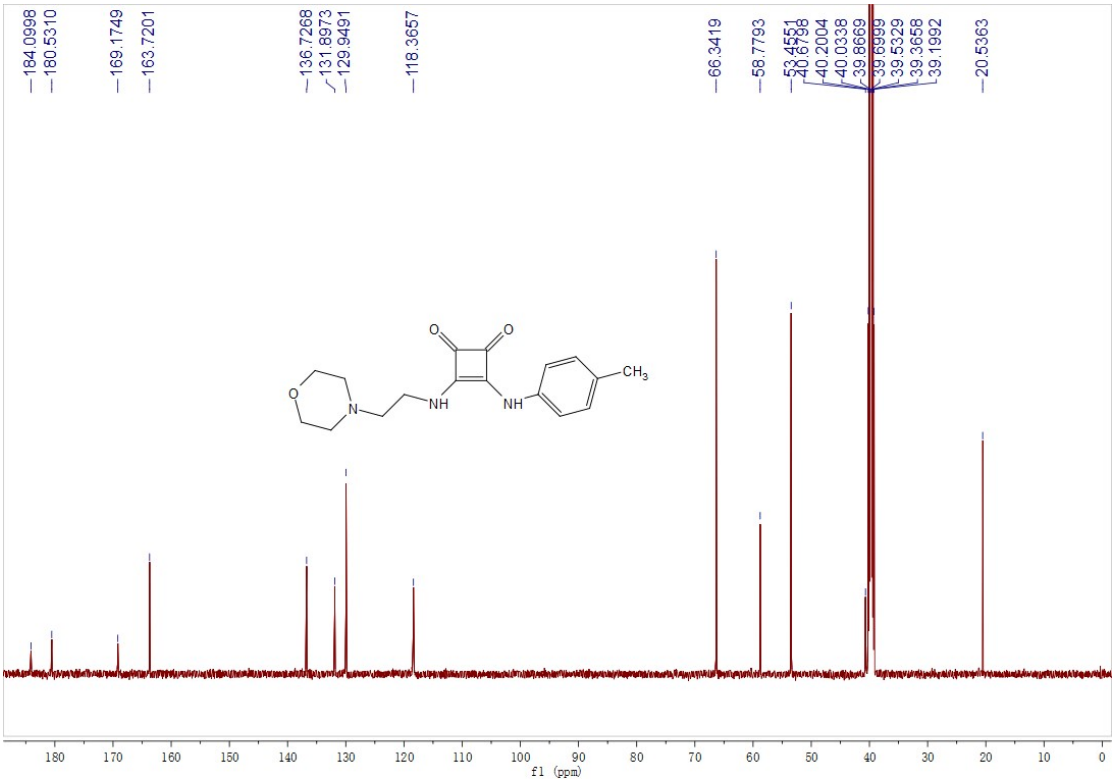

Fig. S10. ^{13}C NMR (125 MHz, DMSO-d_6) of compound **3**

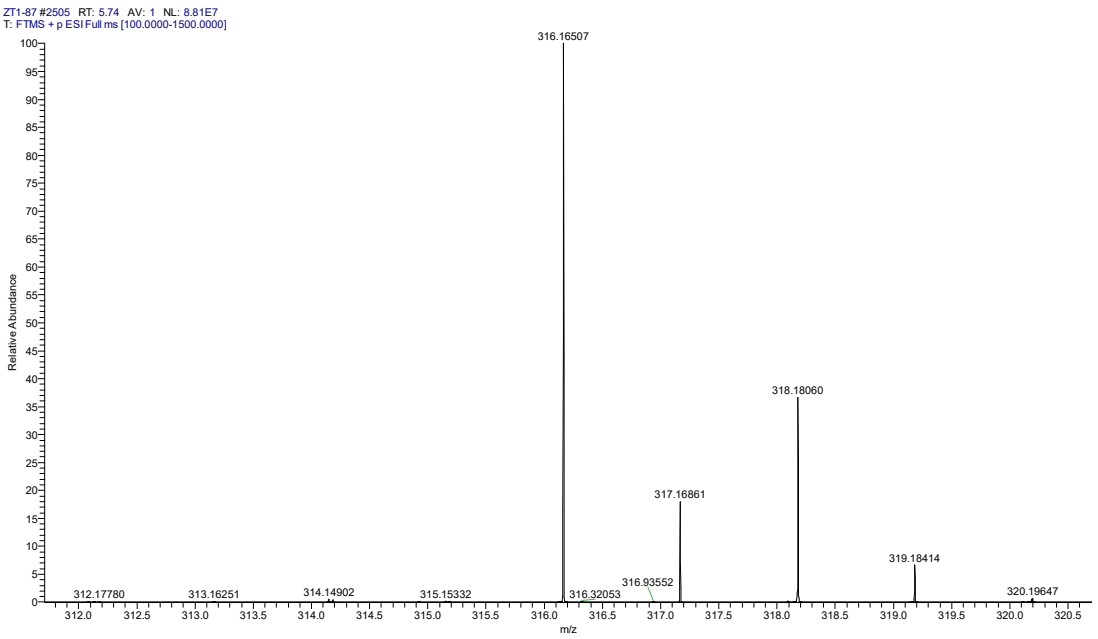

Fig. S11. HR-ESI-MS of compound **3**

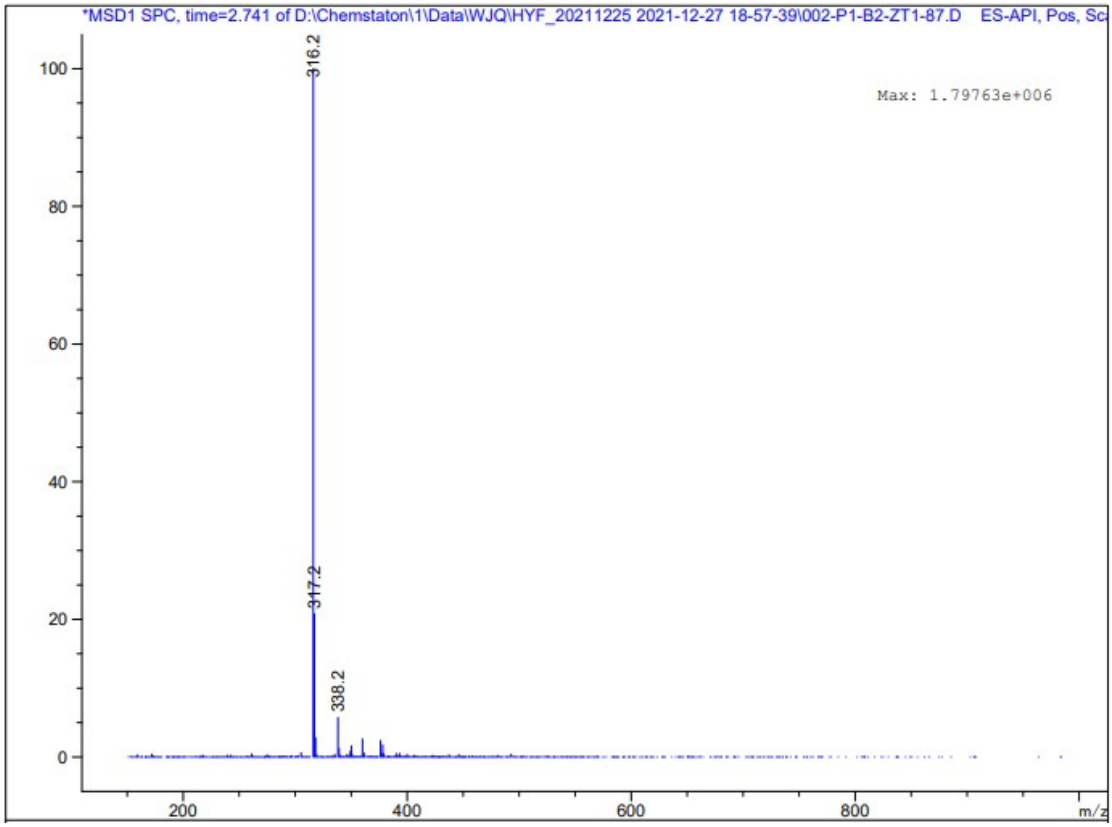

Fig. S12. LR-ESI-MS of compound **3**

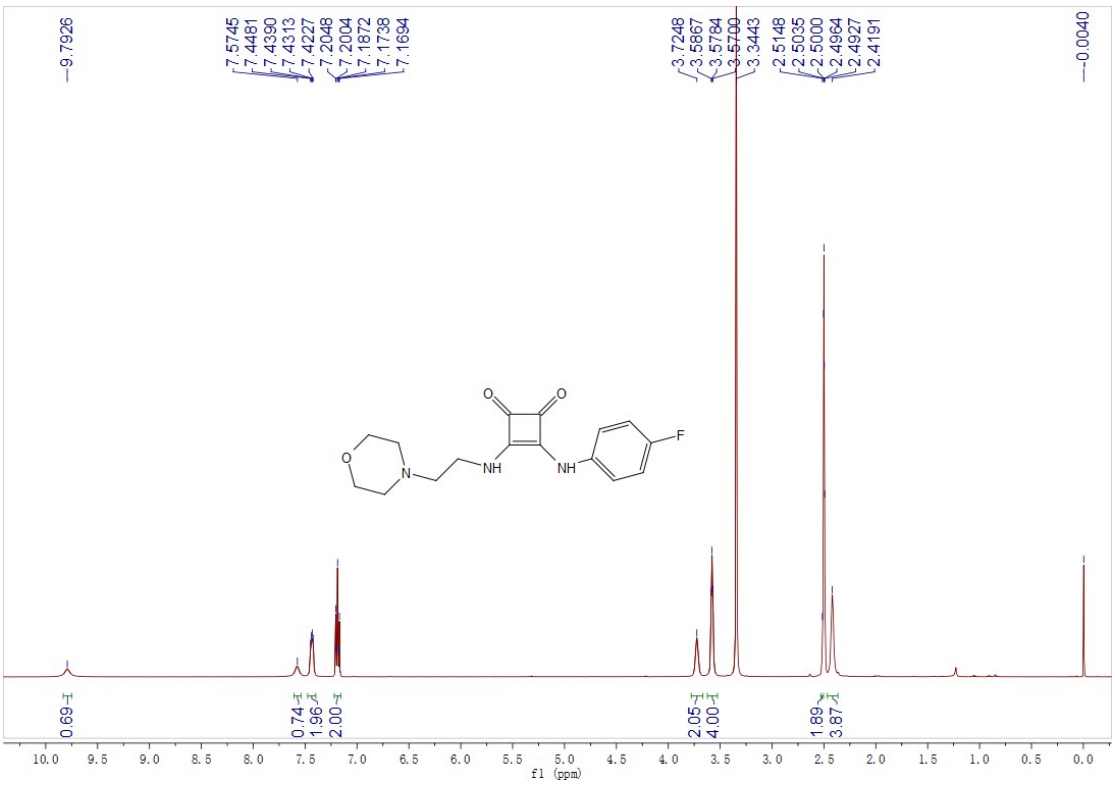

Fig. S13. ^{1}H NMR (500 MHz, DMSO-d_6) of compound **4**

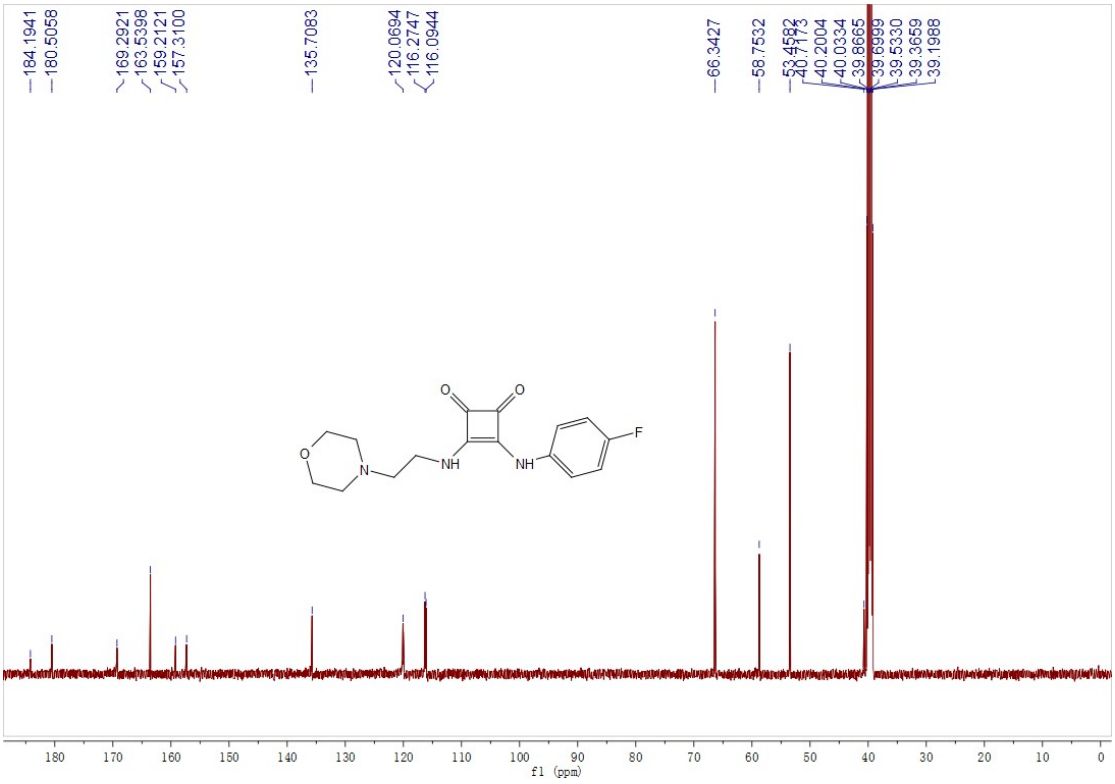

Fig. S14. ^{13}C NMR (125 MHz, DMSO-d_6) of compound **4**

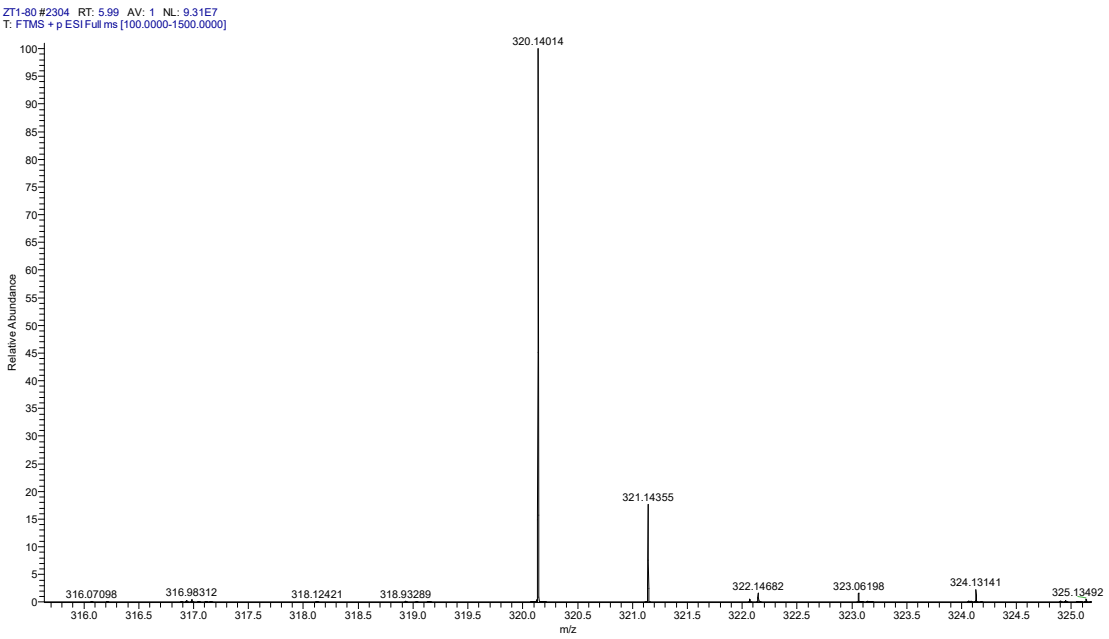

Fig. S15. HR-ESI-MS of compound **4**

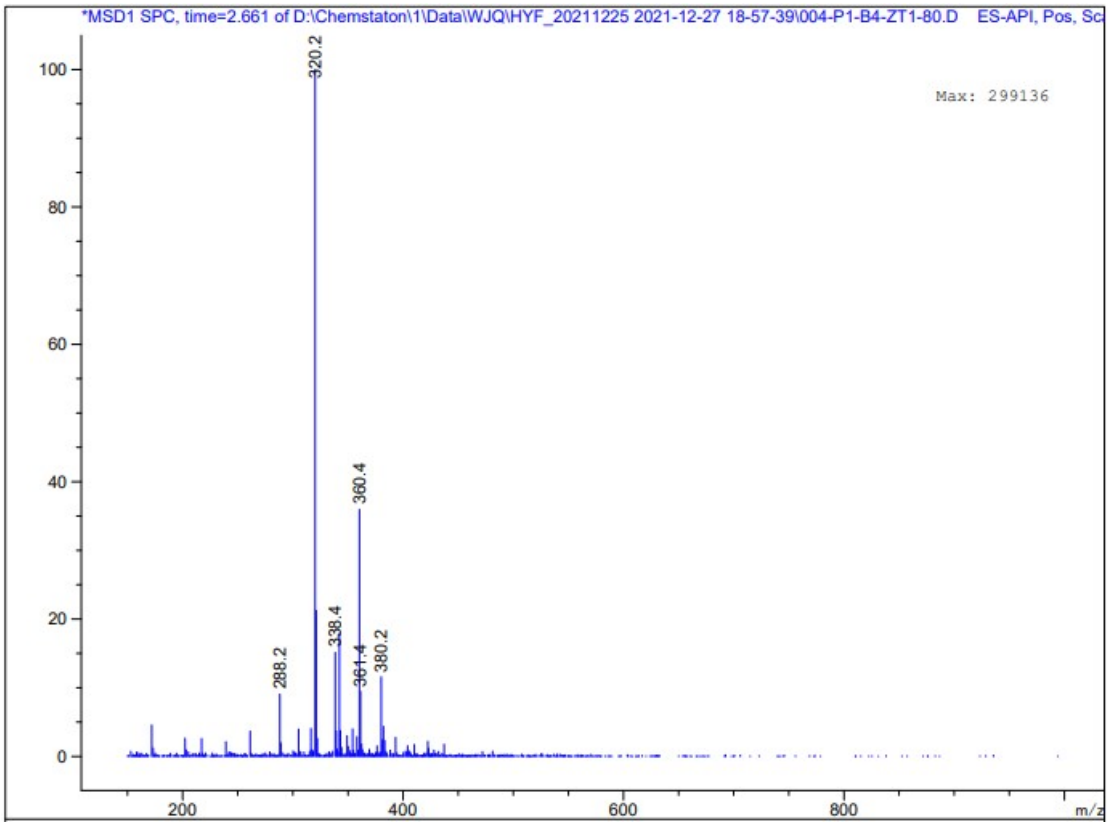

Fig. S16. LR-ESI-MS of compound **4**

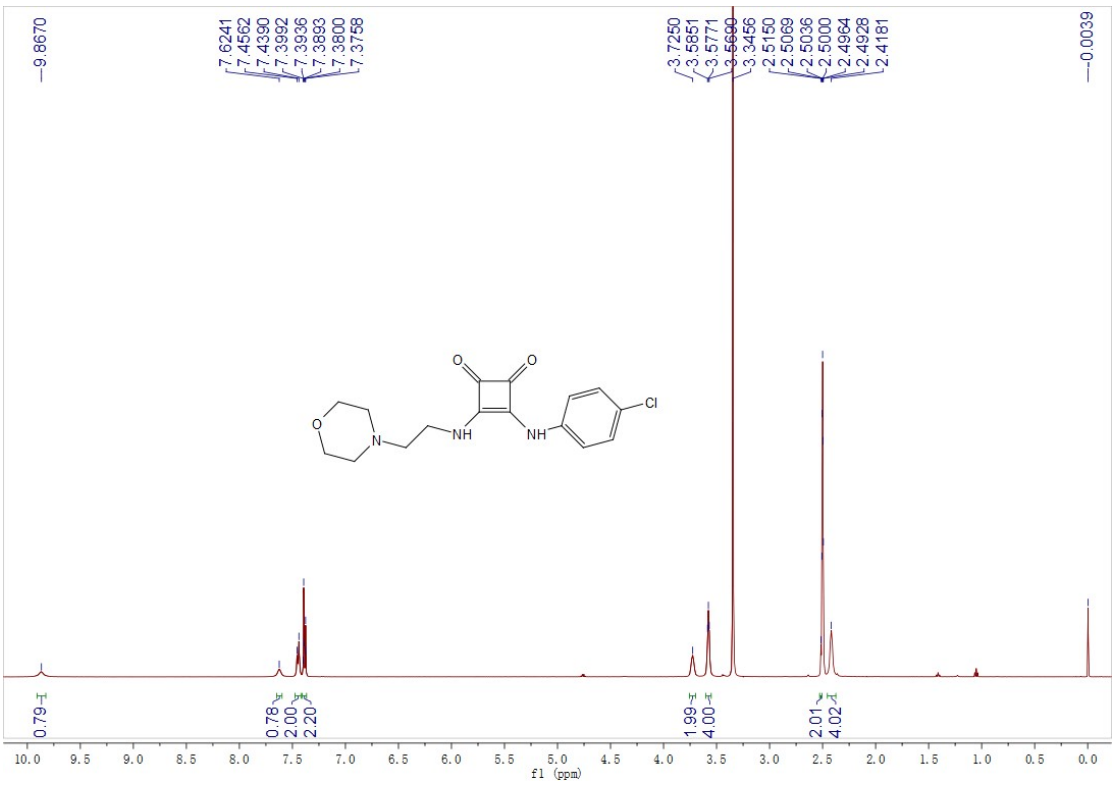

Fig. S17. ^{1}H NMR (500 MHz, DMSO-d_6) of compound **5**

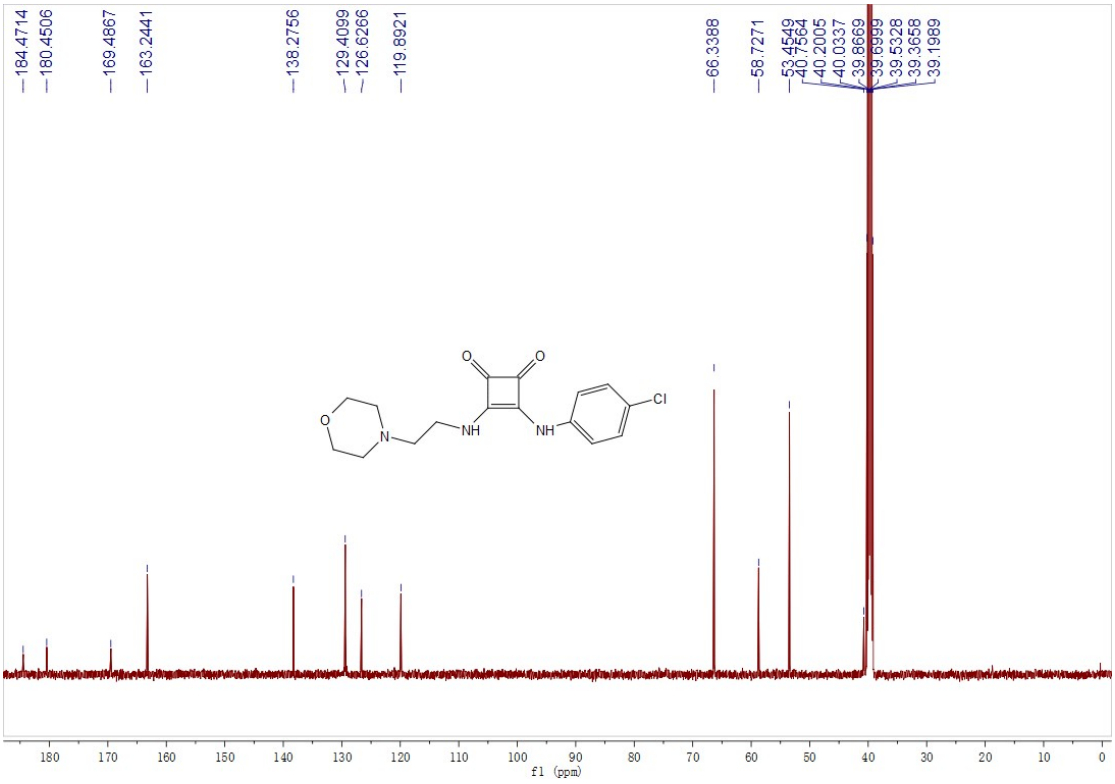

Fig. S18. ^{13}C NMR (125 MHz, DMSO-d_6) of compound **5**

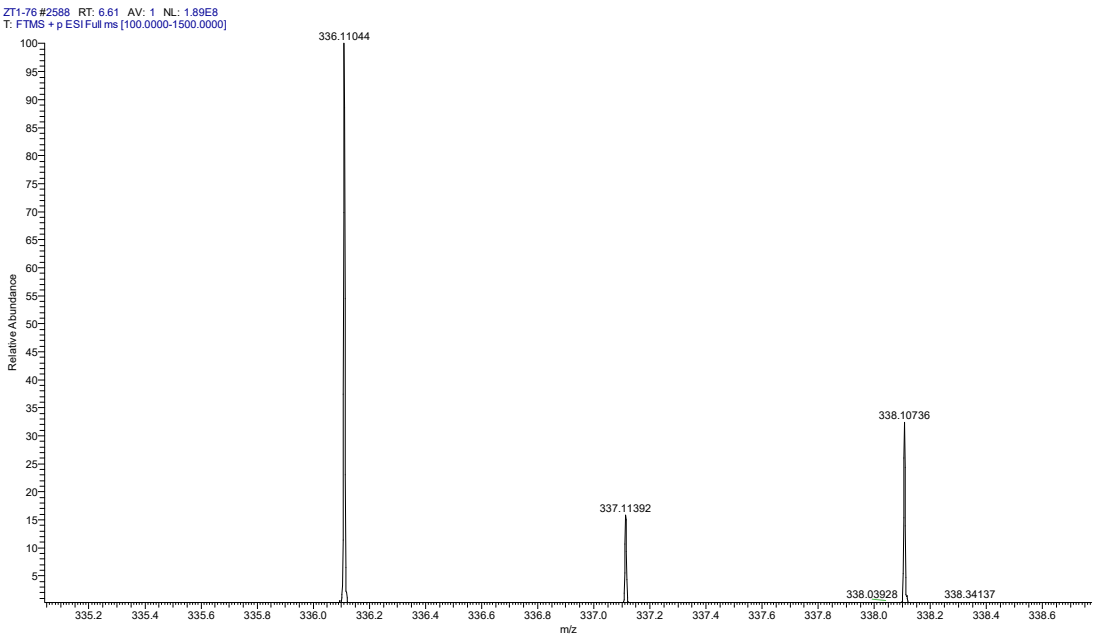

Fig. S19. HR-ESI-MS of compound **5**

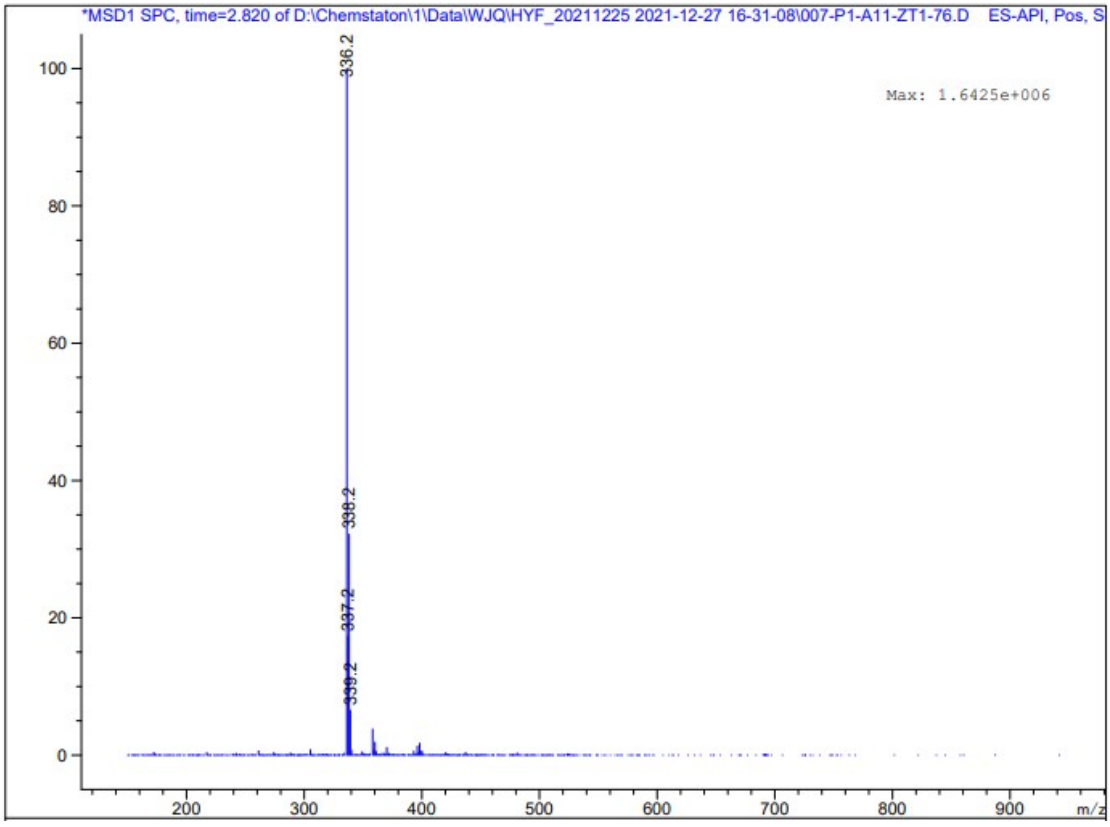

Fig. S20. LR-ESI-MS of compound **5**

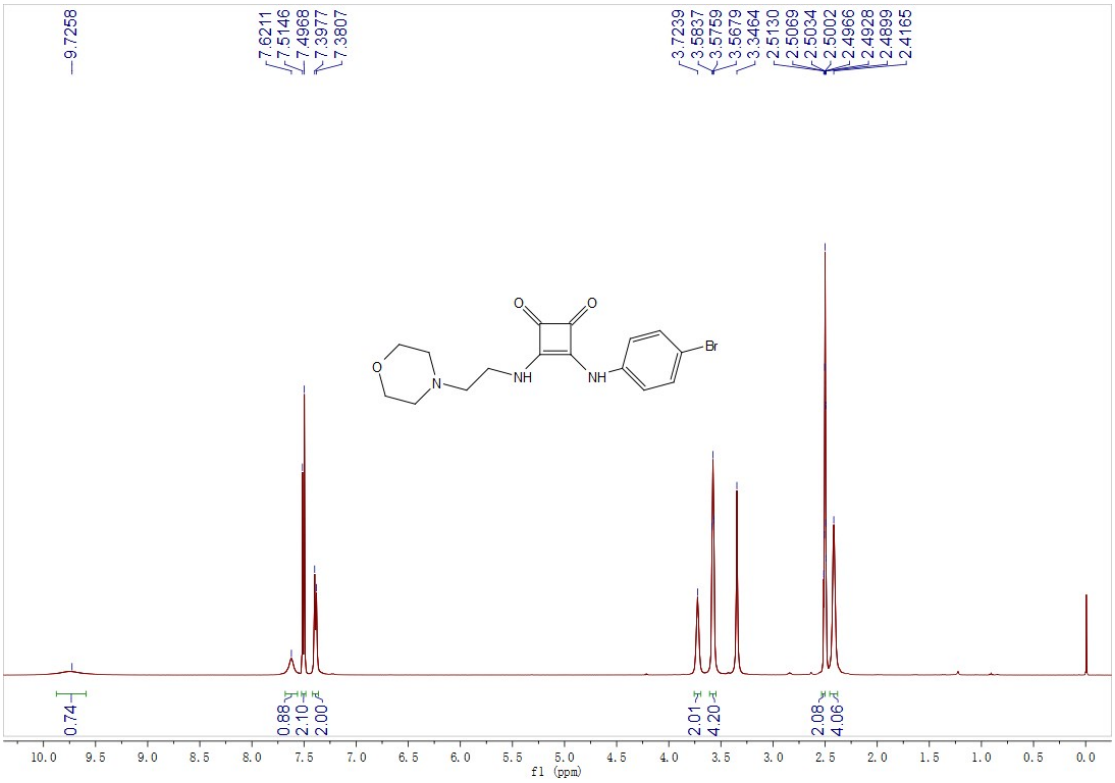

Fig. S21. ^{1}H NMR (500 MHz, DMSO-d_6) of compound **6**

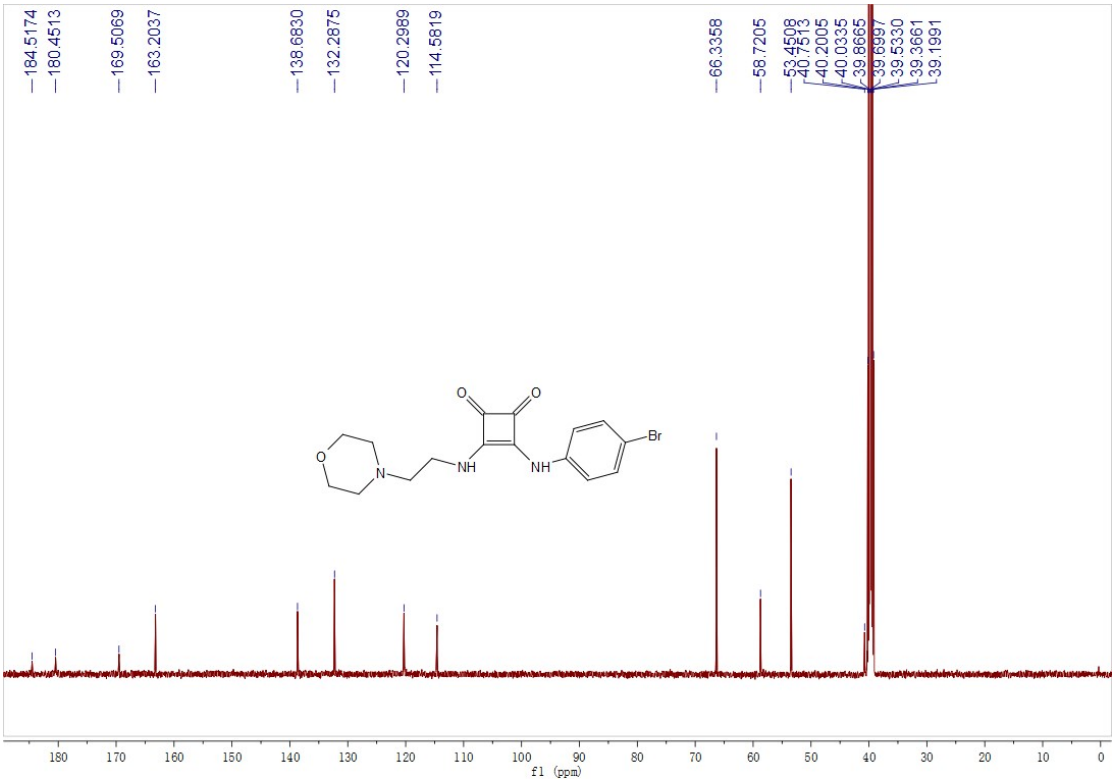

Fig. S22. ^{13}C NMR (125 MHz, DMSO-d_6) of compound **6**

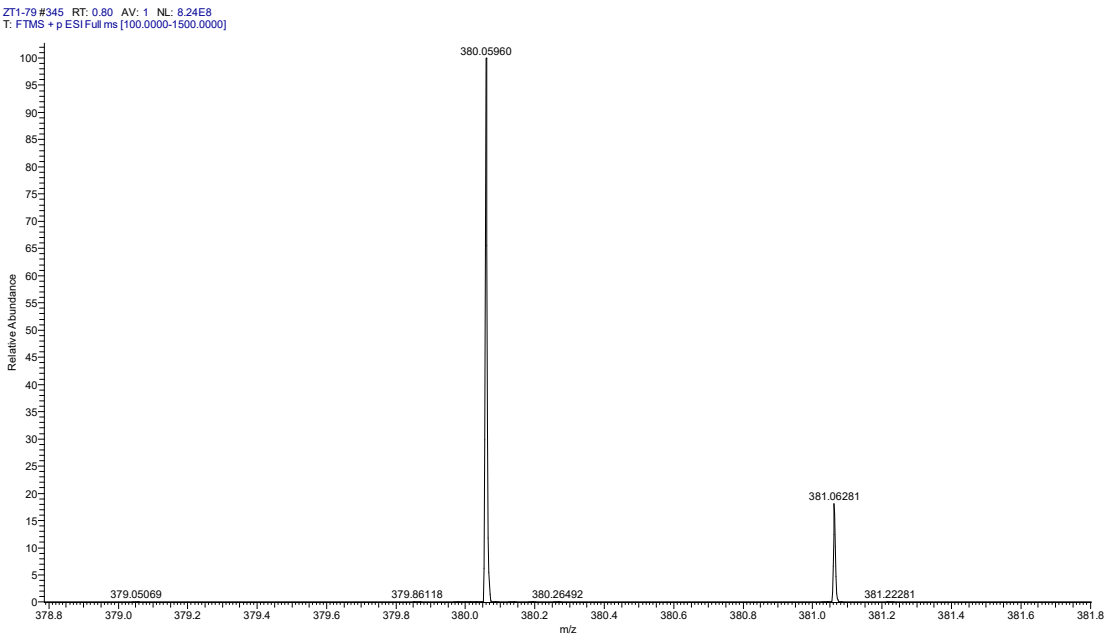

Fig. S23. HR-ESI-MS of compound **6**

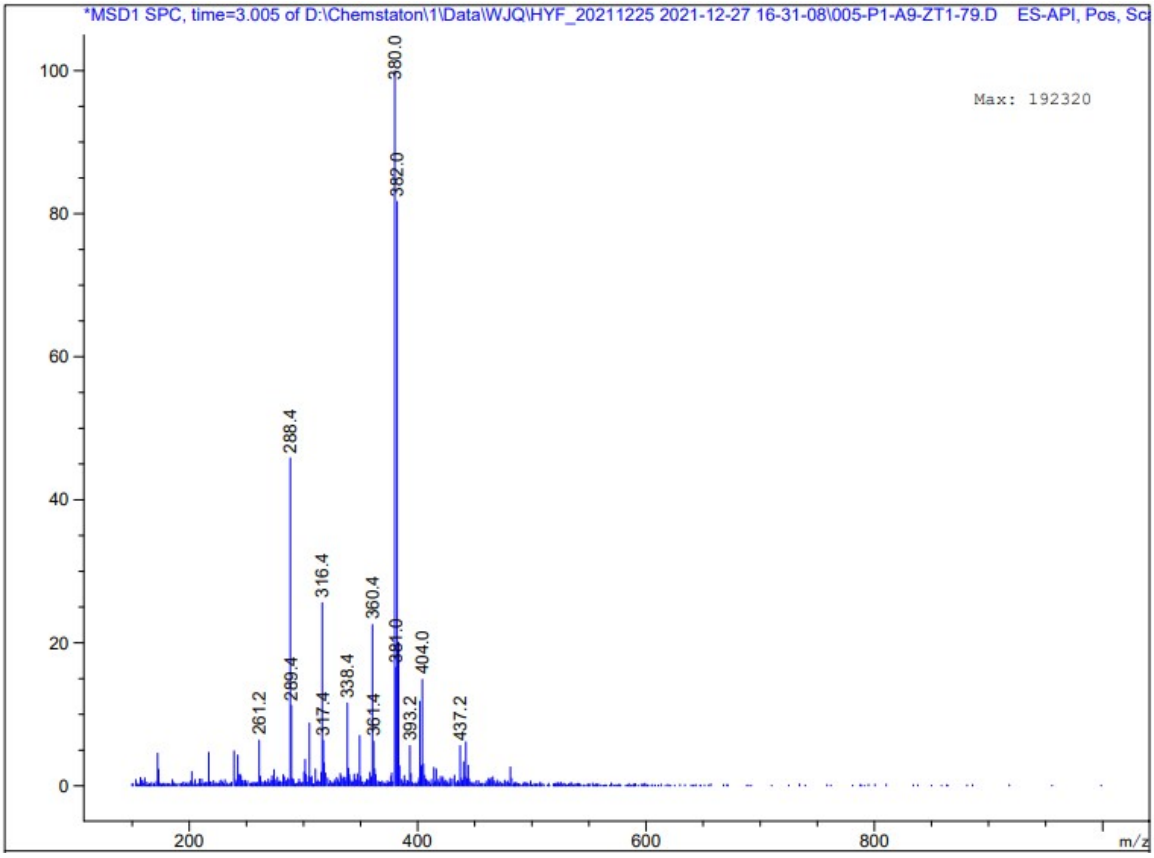

Fig. S24. LR-ESI-MS of compound **6**

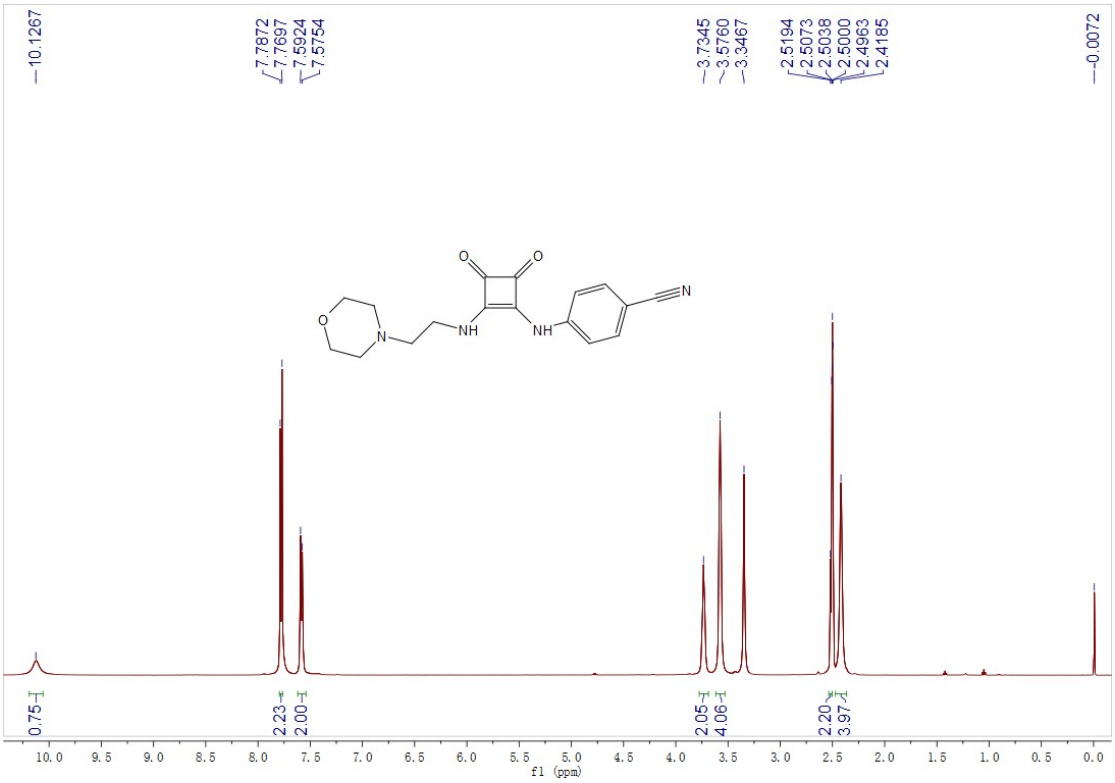

Fig. S25. ^{1}H NMR (500 MHz, DMSO-d_6) of compound **7**

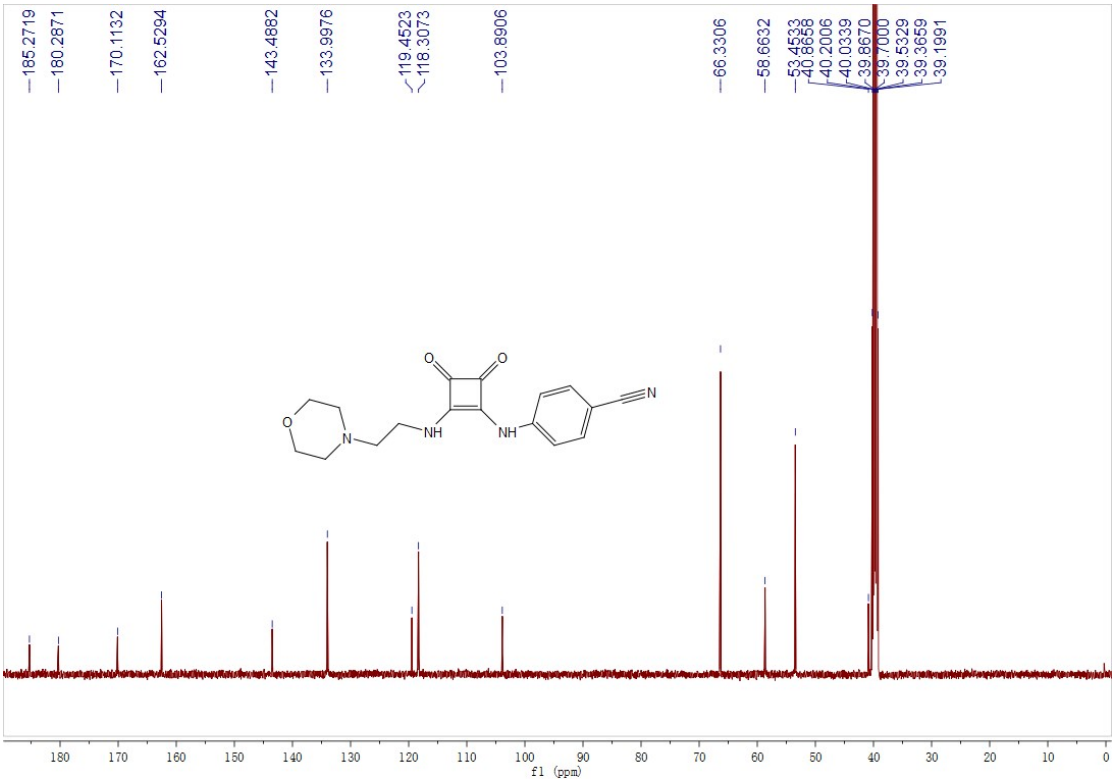

Fig. S26. ^{13}C NMR (125 MHz, DMSO-d_6) of compound **7**

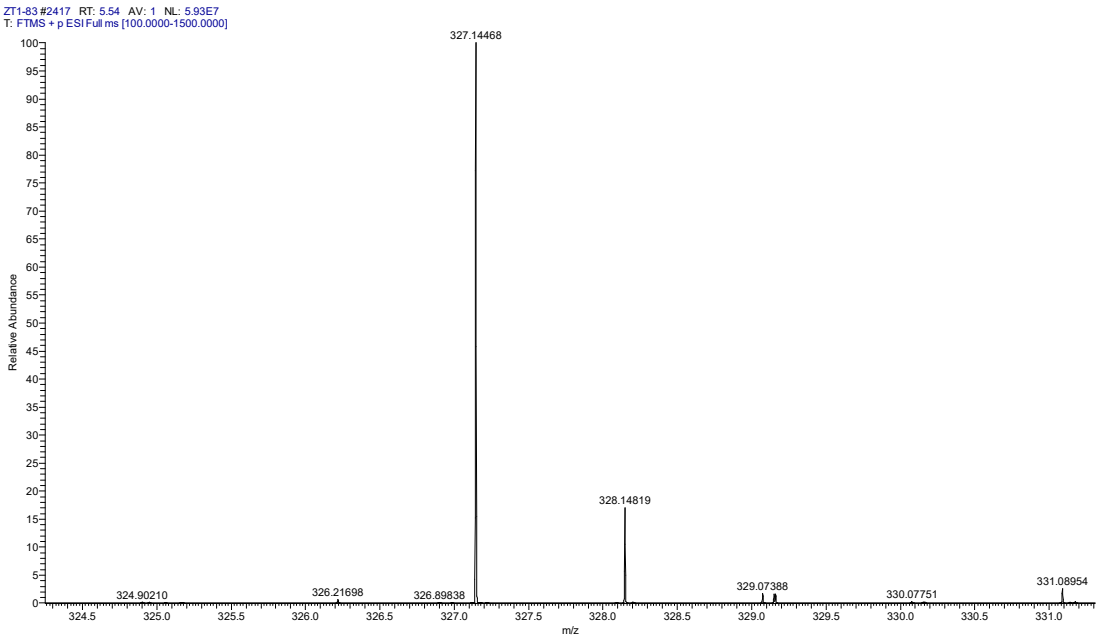

Fig. S27. HR-ESI-MS of compound **7**

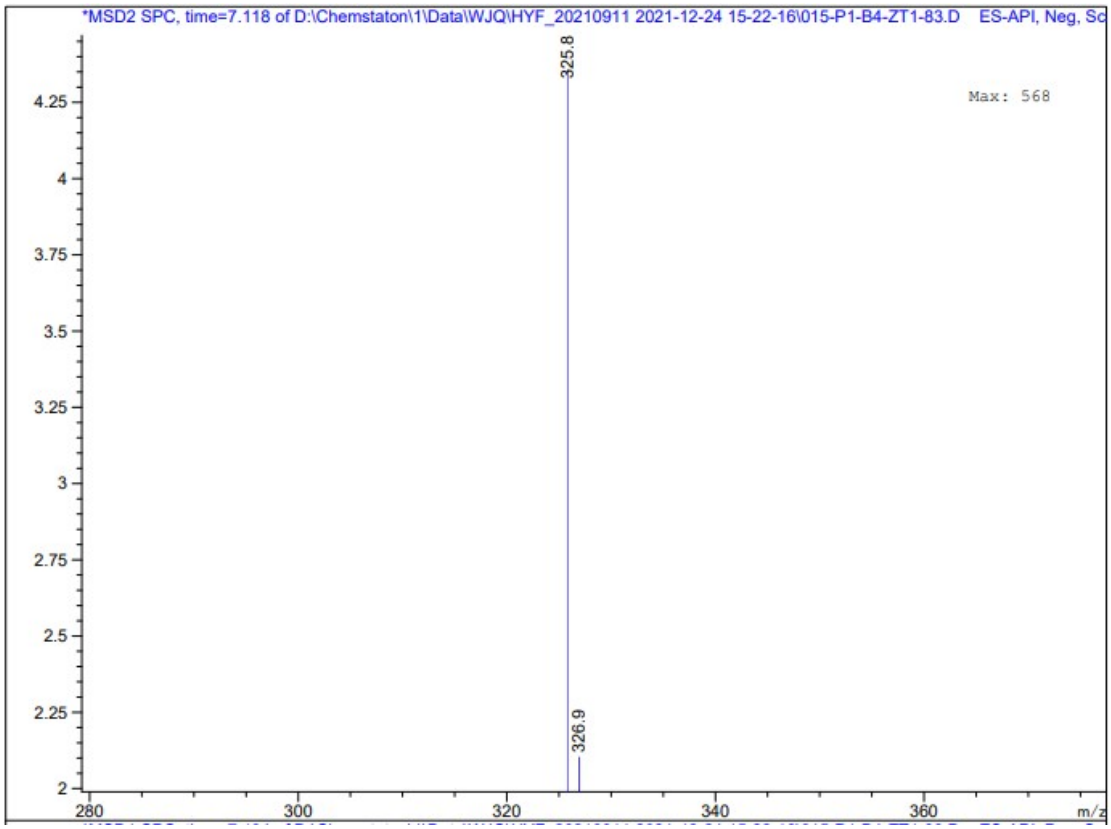

Fig. S28. Negative LR-ESI-MS of compound **7**

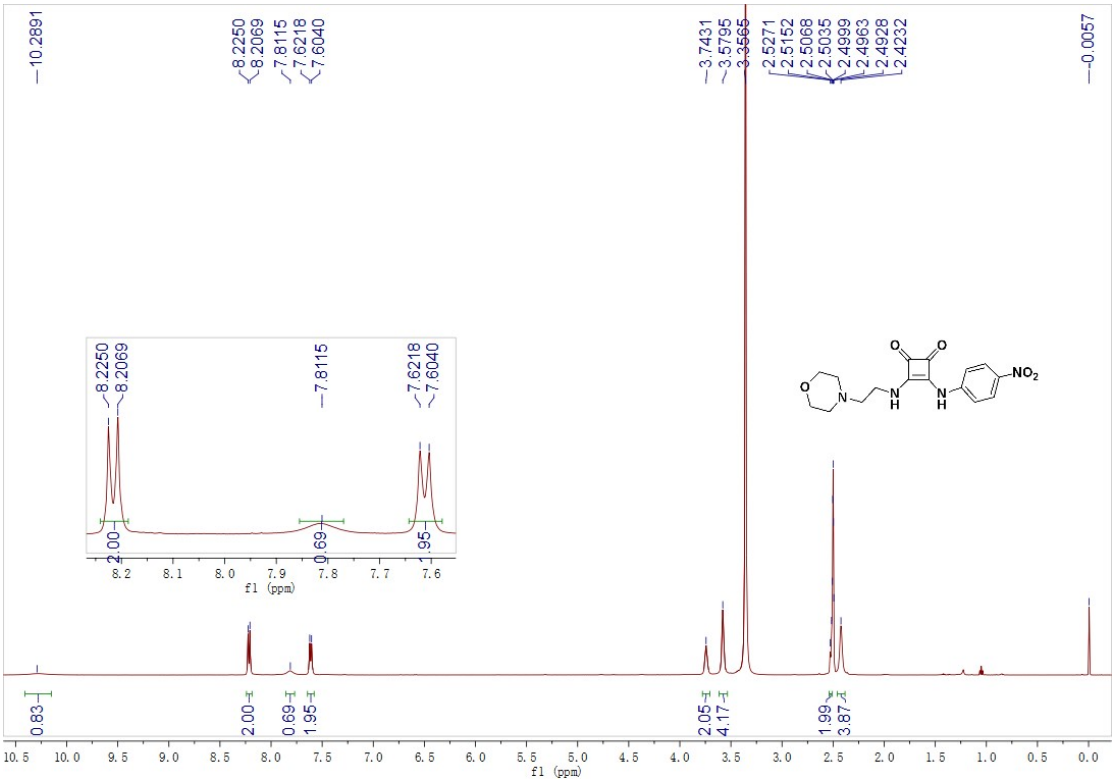

Fig. S29. ^{1}H NMR (500 MHz, DMSO-d_6) of compound **8**

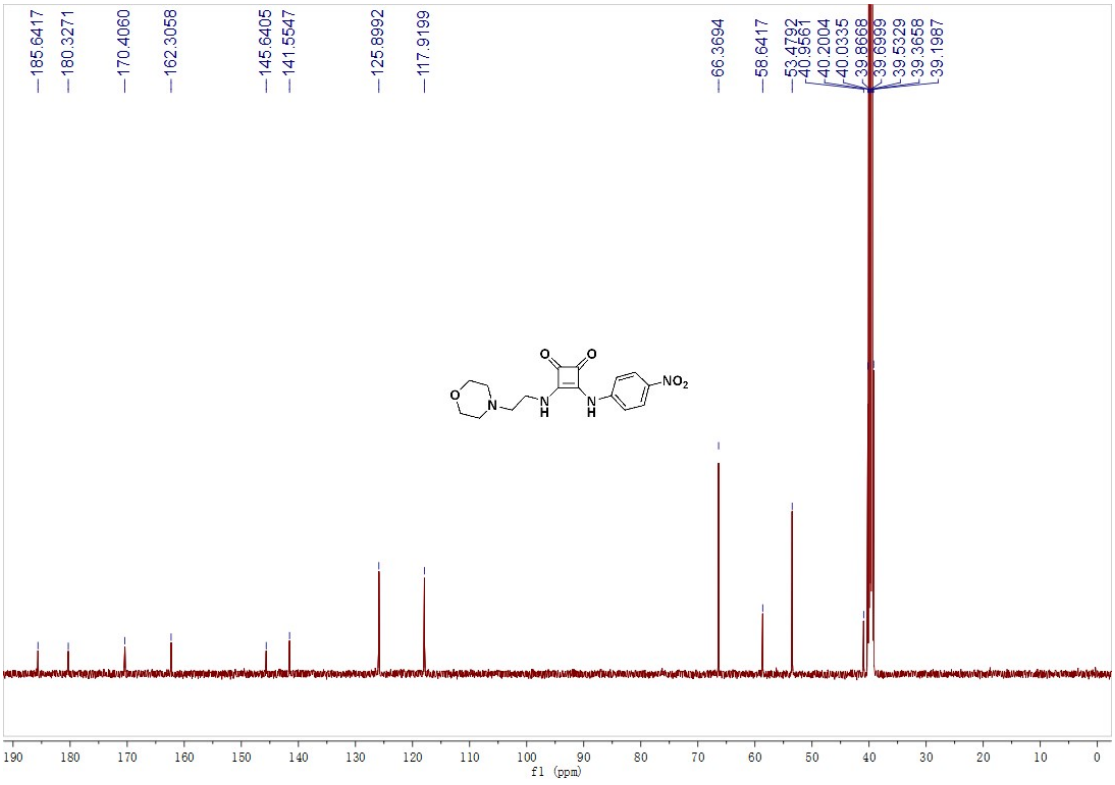

Fig. S30. ^{13}C NMR (125 MHz, DMSO-d_6) of compound **8**

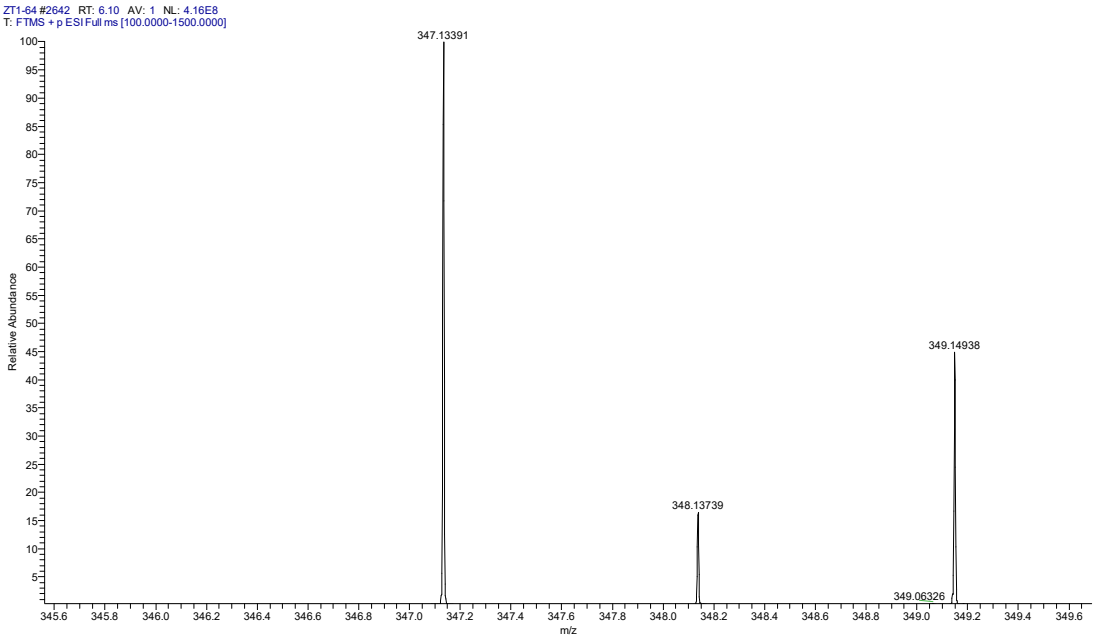

Fig. S31. HR-ESI-MS of compound **8**

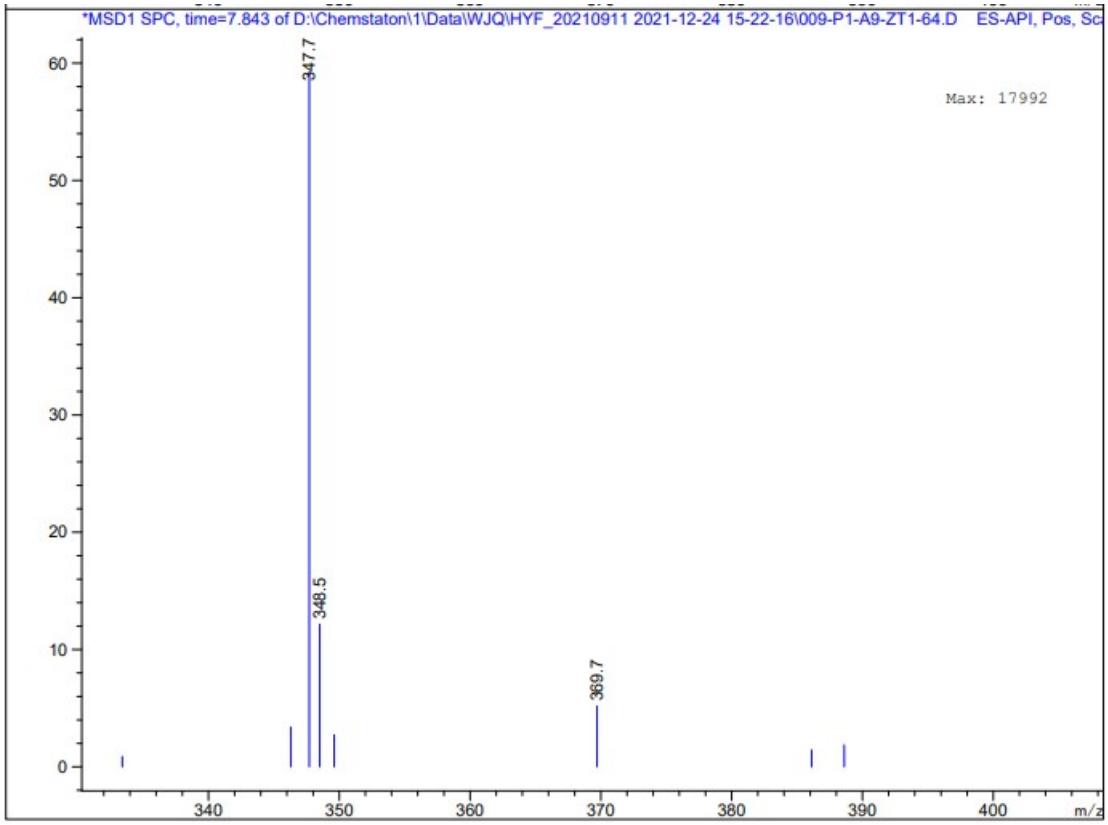

Fig. S32. LR-ESI-MS of compound **8**

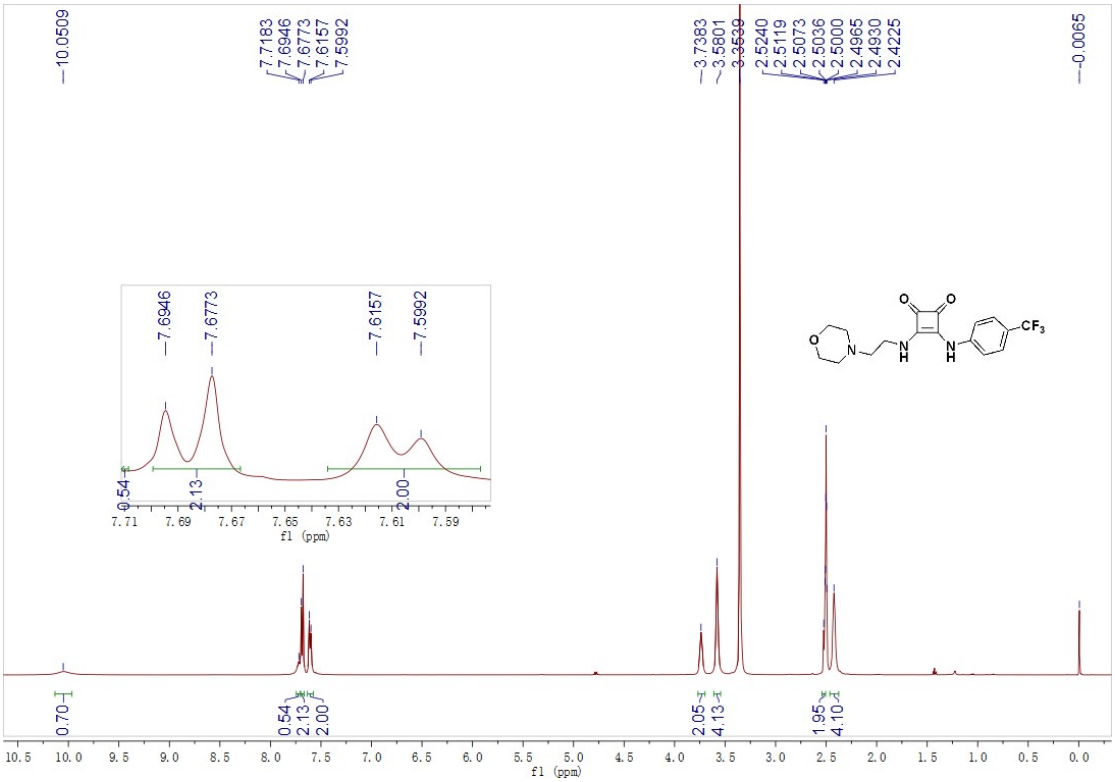

Fig. S33. ^{1}H NMR (500 MHz, DMSO-d_6) of compound **9**

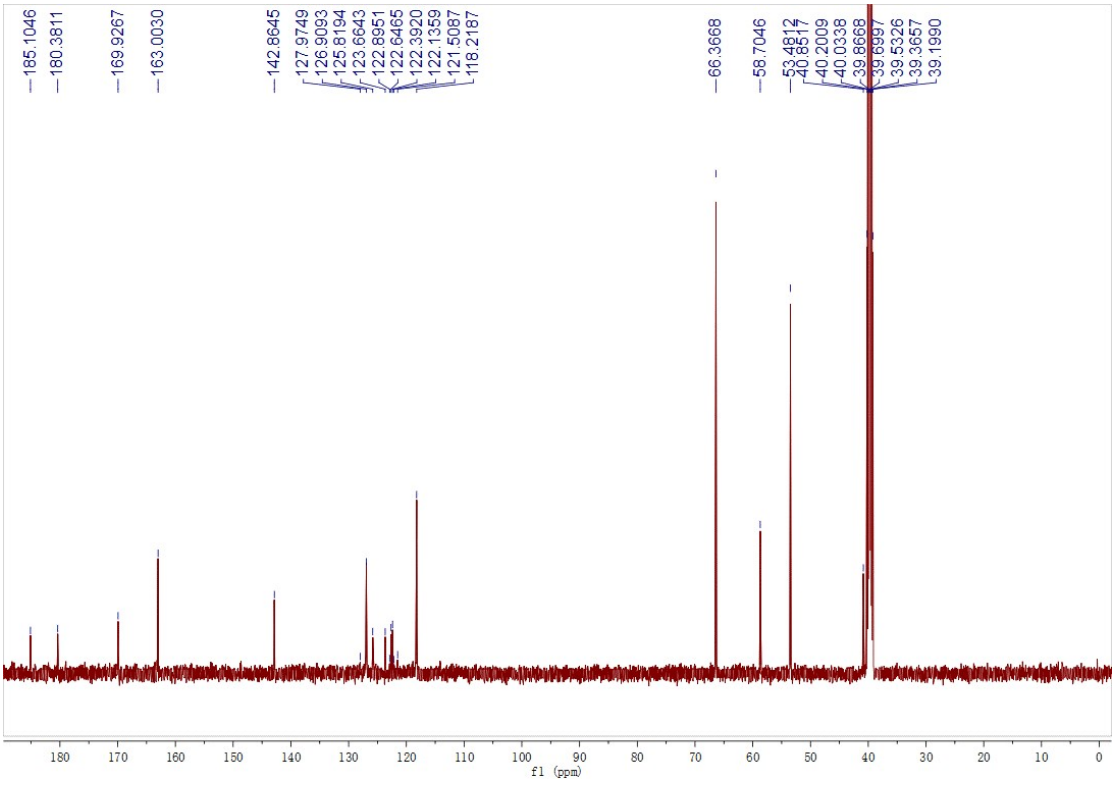

Fig. S34. ^{13}C NMR (125 MHz, DMSO-d_6) of compound **9**

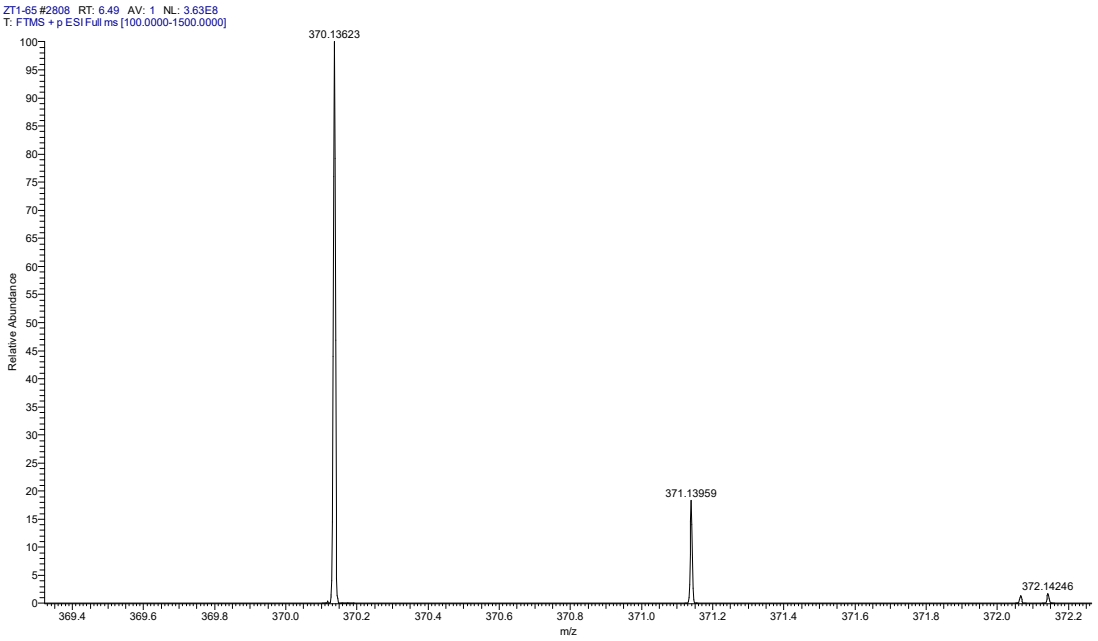

Fig. S35. HR-ESI-MS of compound **9**

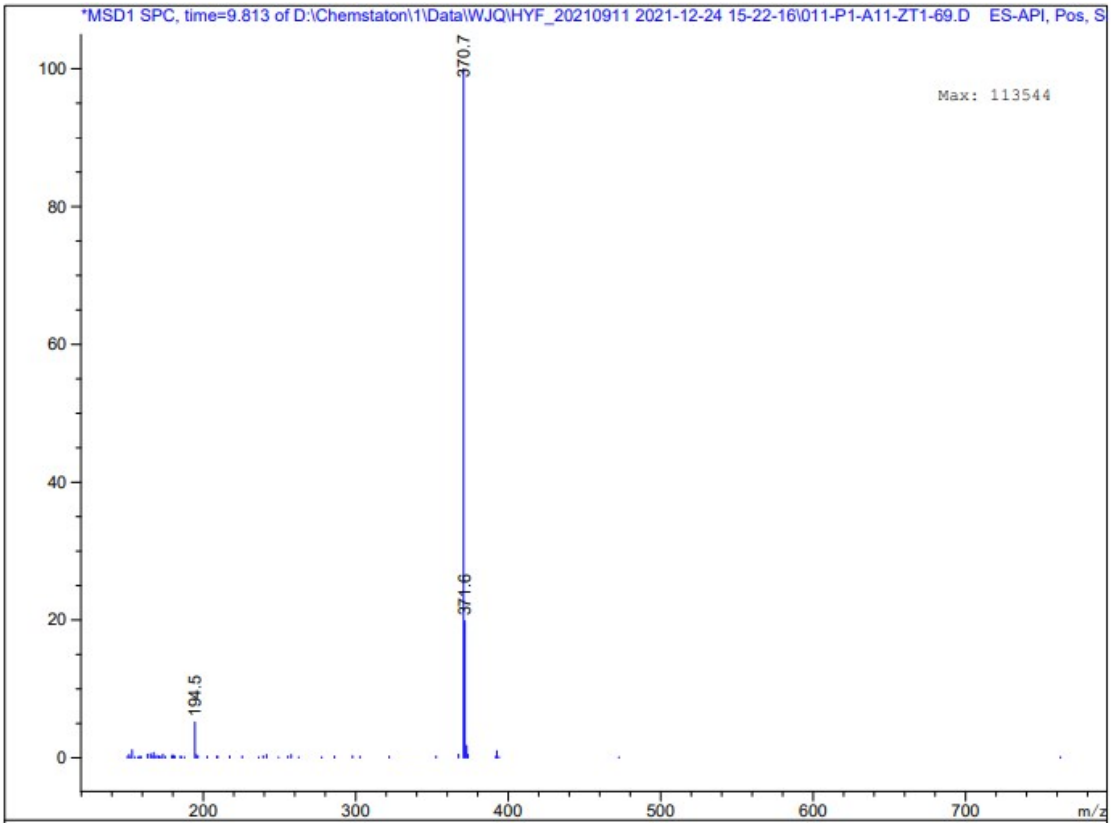

Fig. S36. LR-ESI-MS of compound **9**

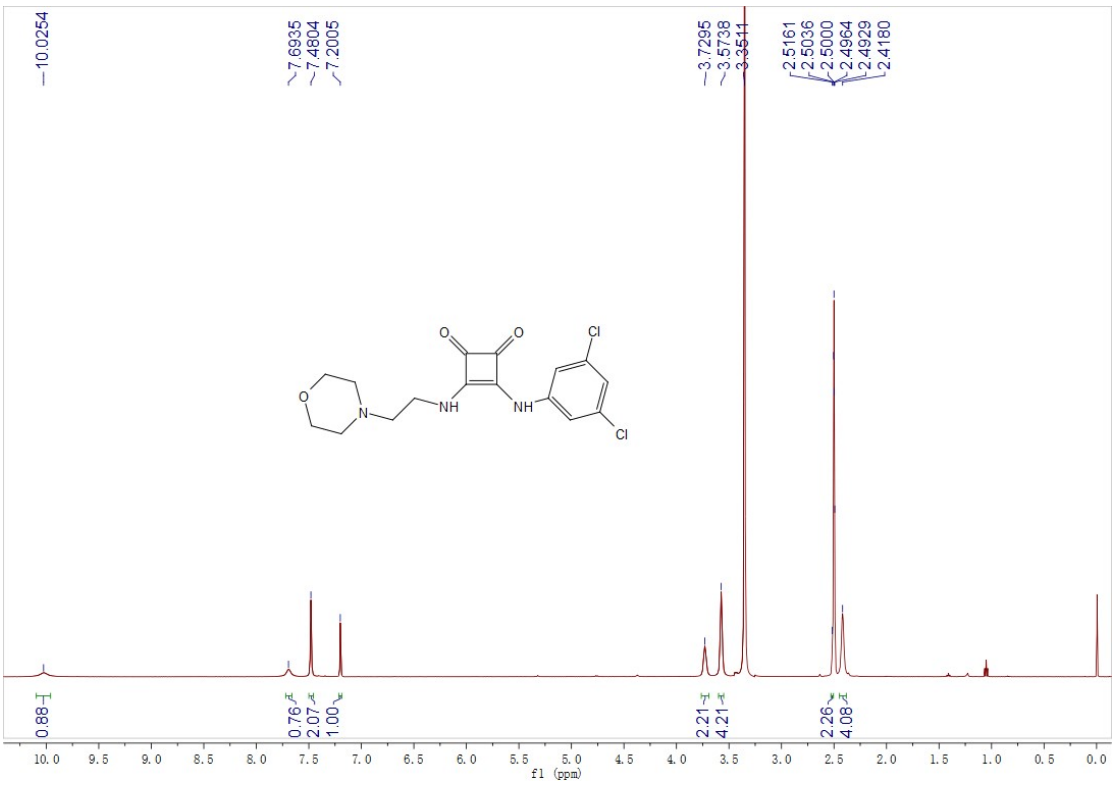

Fig. S37. ^{1}H NMR (500 MHz, DMSO-d_6) of compound **10**

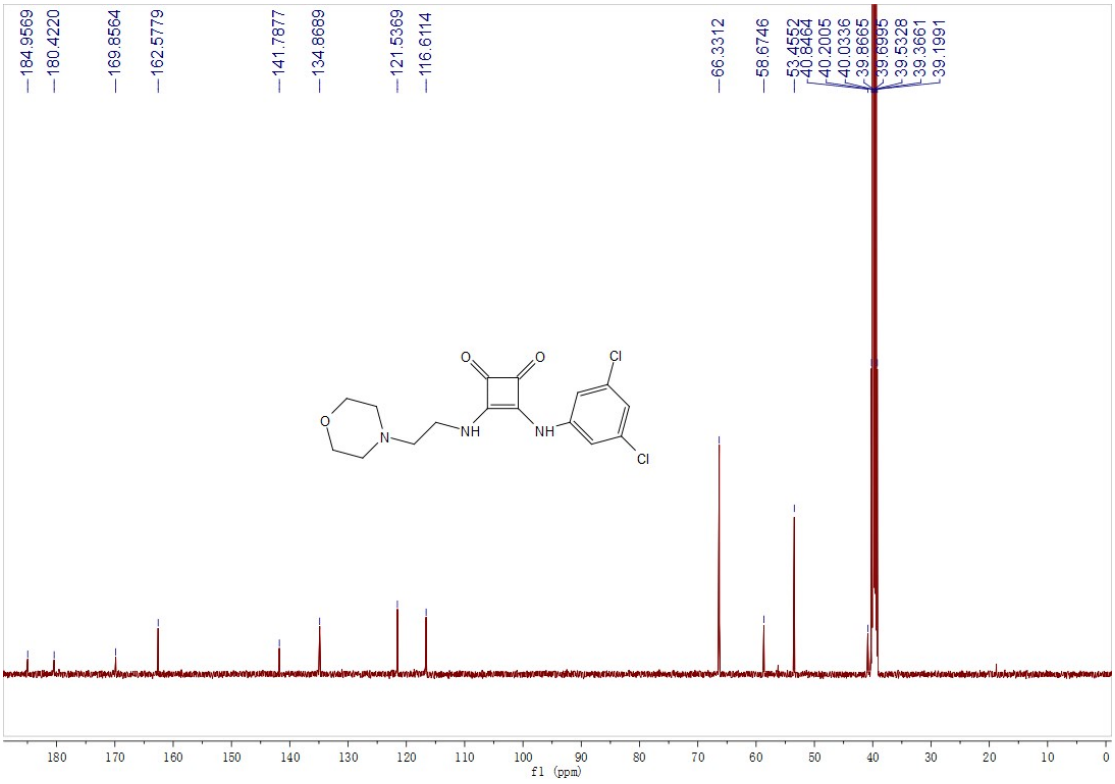

Fig. S38. ^{13}C NMR (125 MHz, DMSO-d_6) of compound **10**

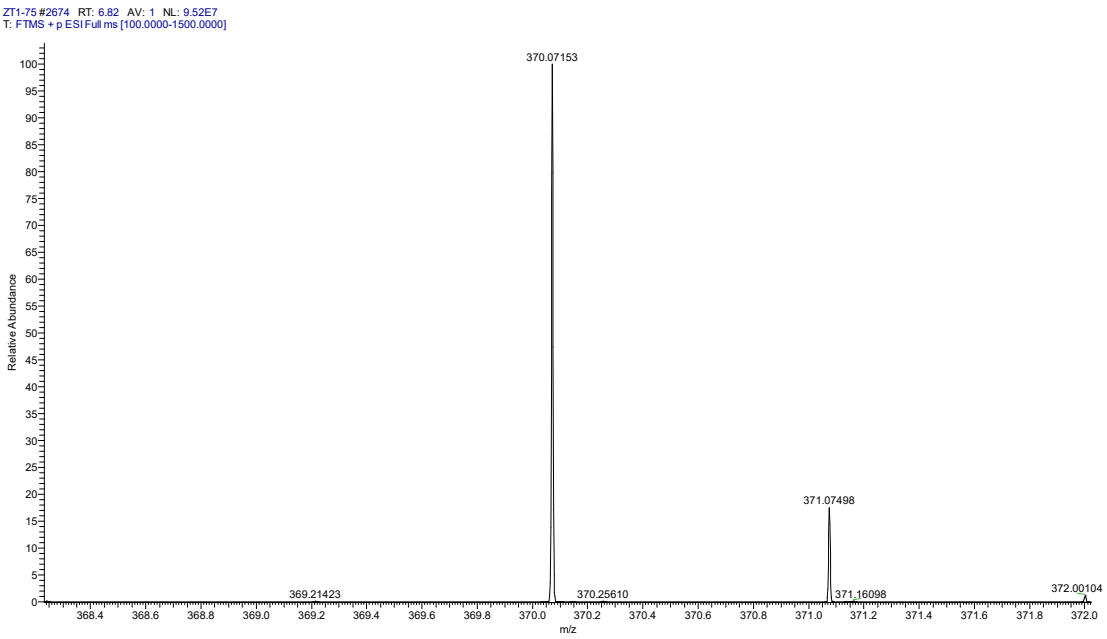

Fig. S39. HR-ESI-MS of compound **10**

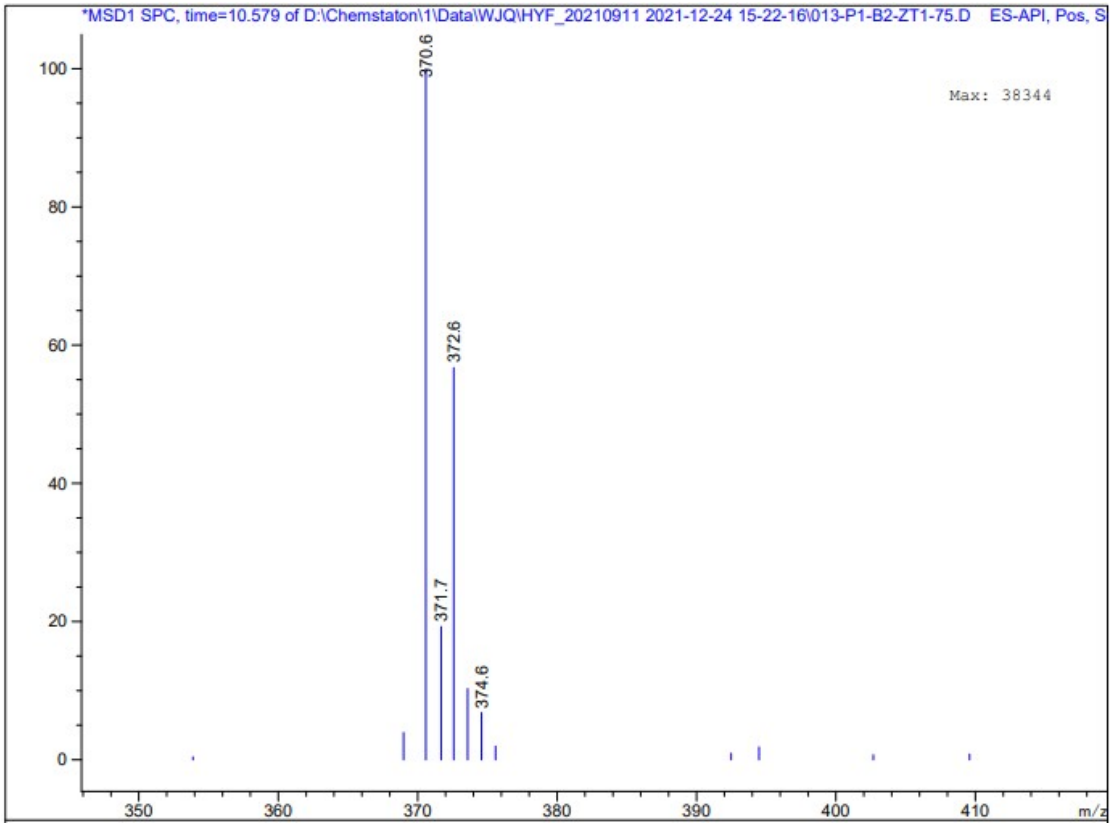

Fig. S40. LR-ESI-MS of compound **10**

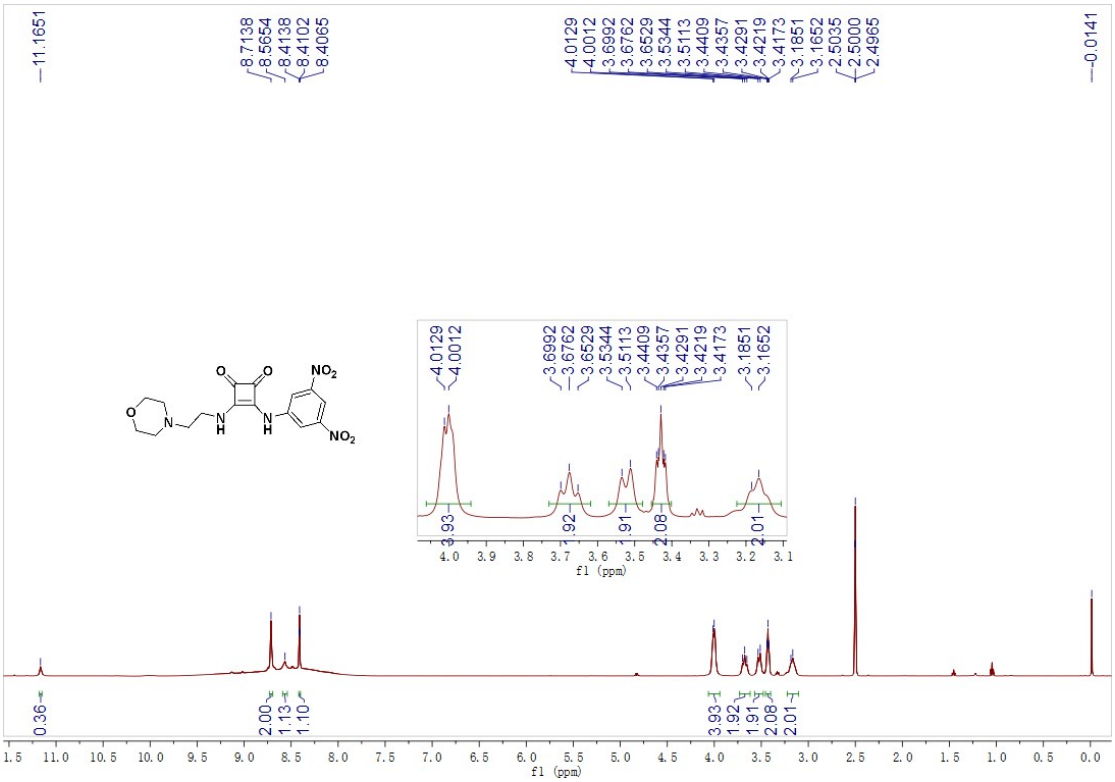

Fig. S41. ^{1}H NMR (500 MHz, DMSO-d_6) of compound **11**

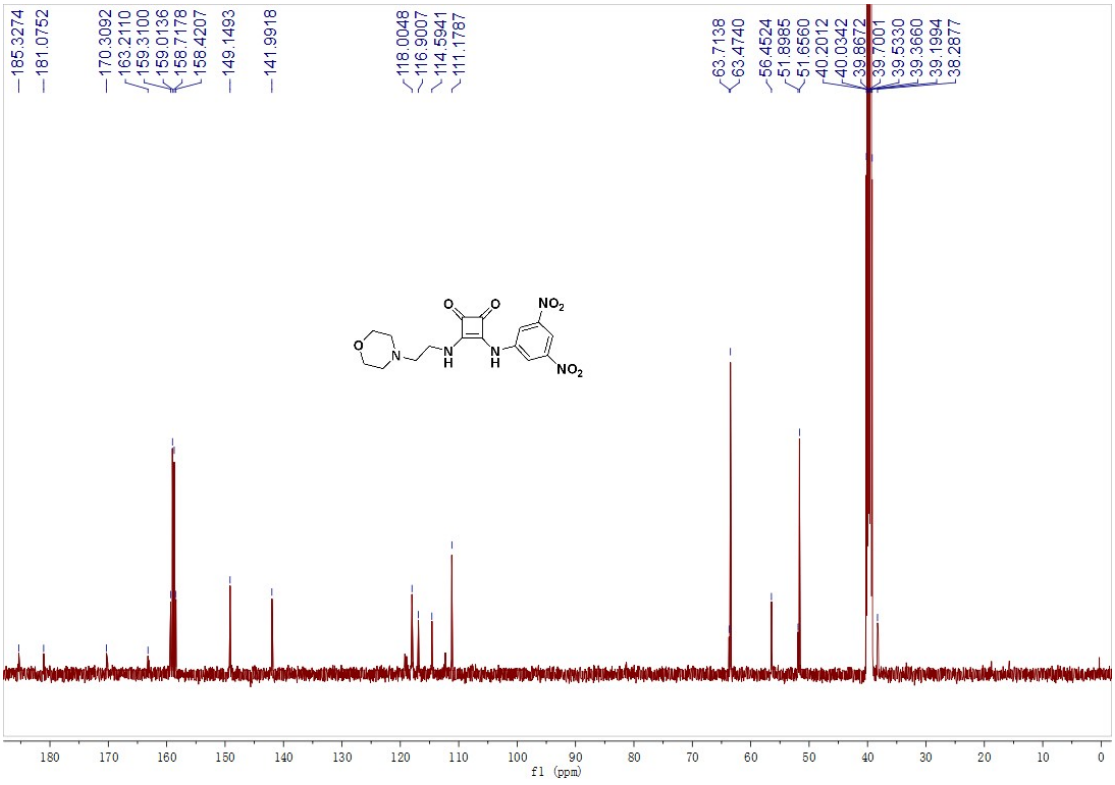

Fig. S42. ^{13}C NMR (125 MHz, DMSO-d_6-TFA-d, 19/1, *v/v*) of compound **11**

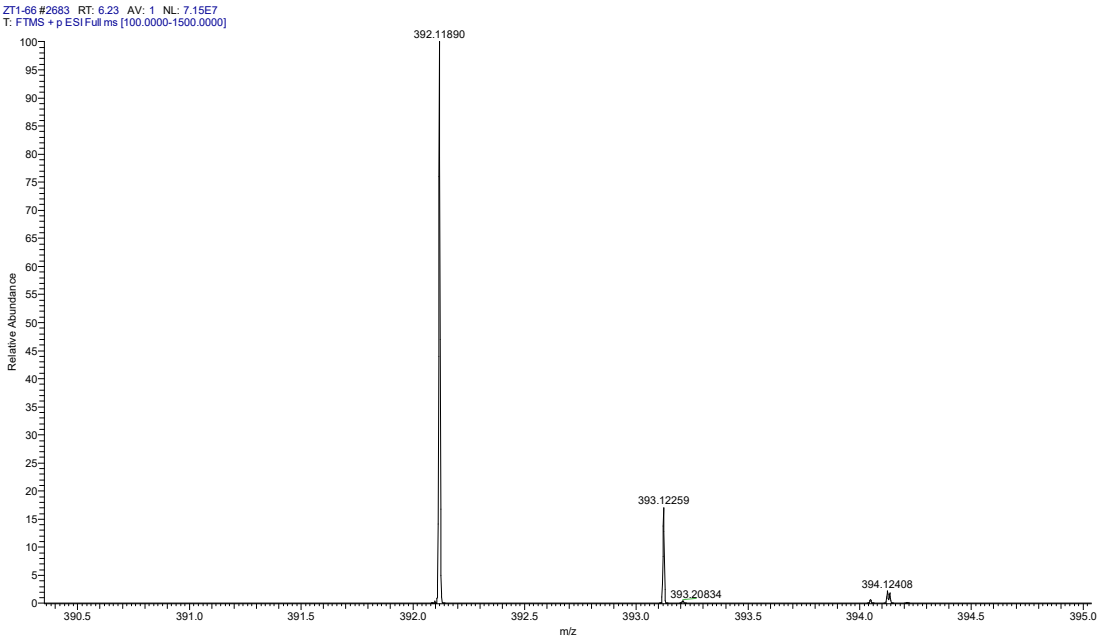

Fig. S43. HR-ESI-MS of compound **11**

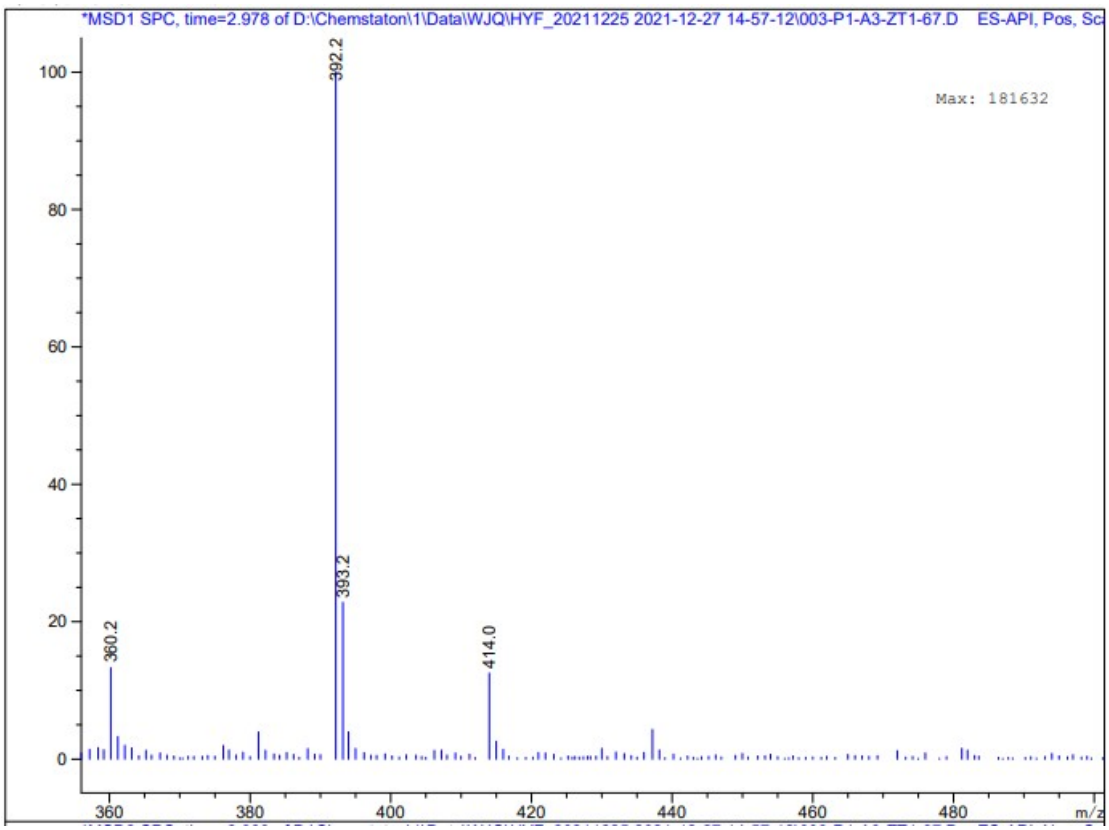

Fig. S44. LR-ESI-MS of compound **11**

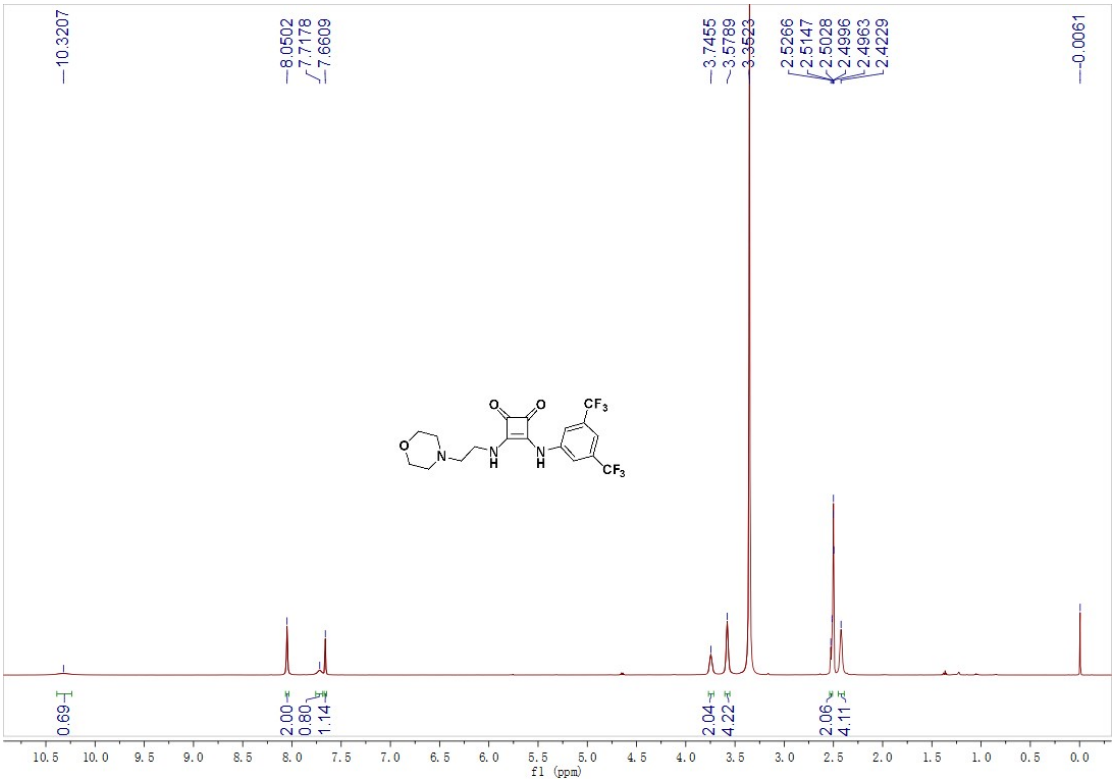

Fig. S45. ^{1}H NMR (500 MHz, DMSO-d_6) of compound **12**

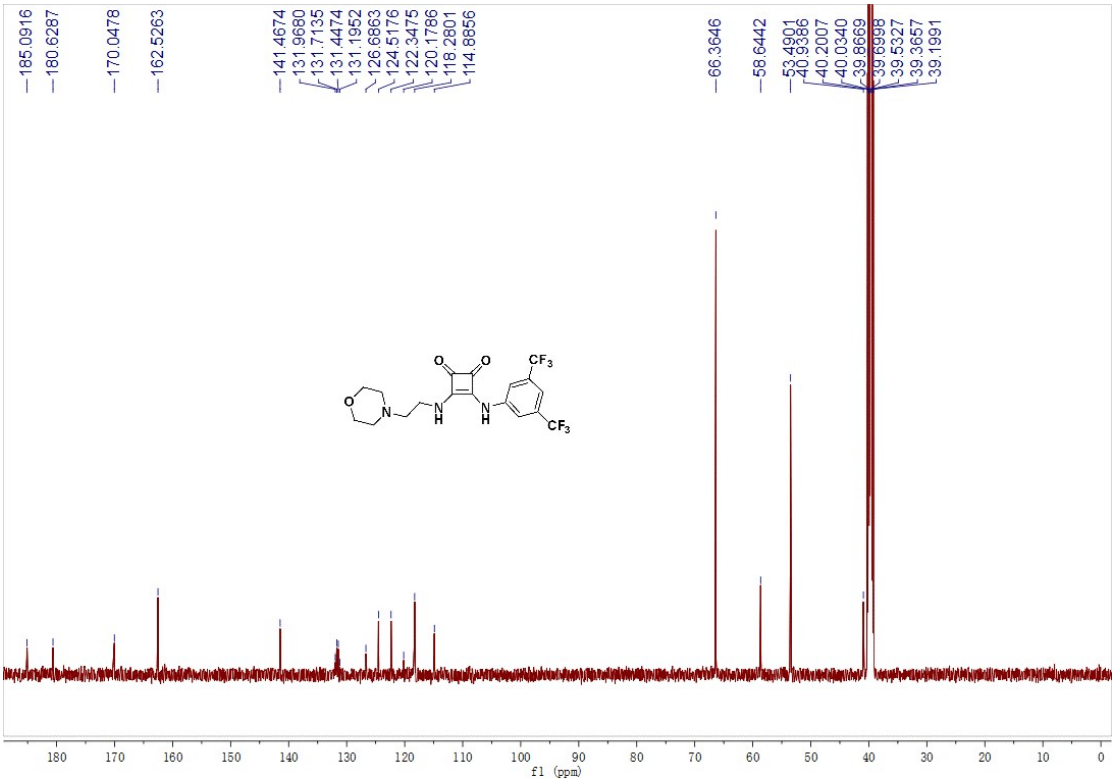

Fig. S46. ^{13}C NMR (125 MHz, DMSO-d_6) of compound **12**

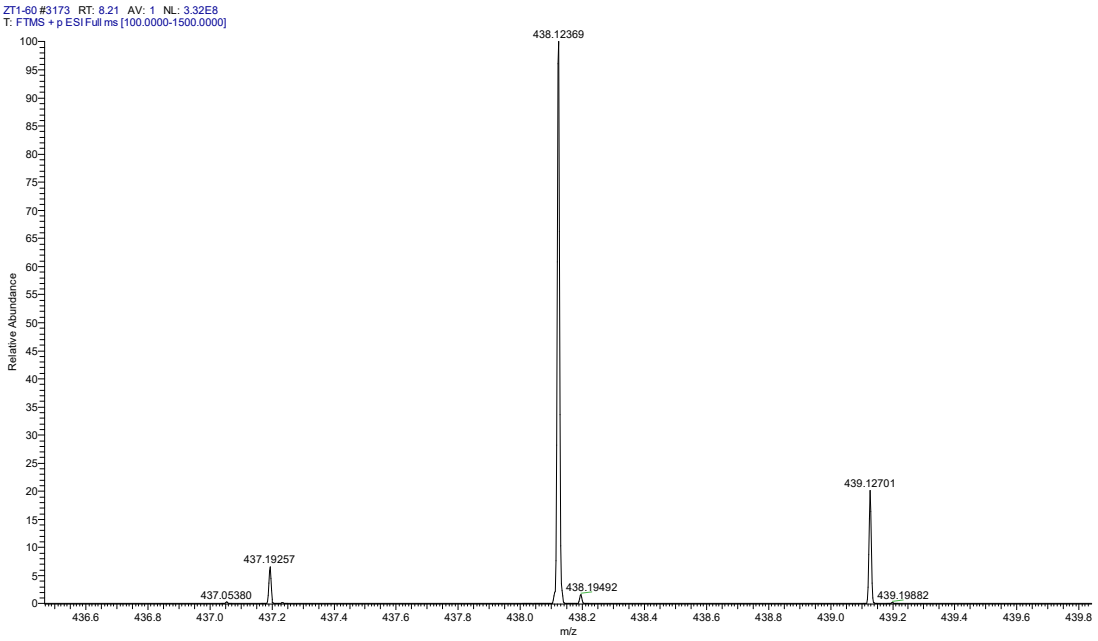

Fig. S47. HR-ESI-MS of compound **12**

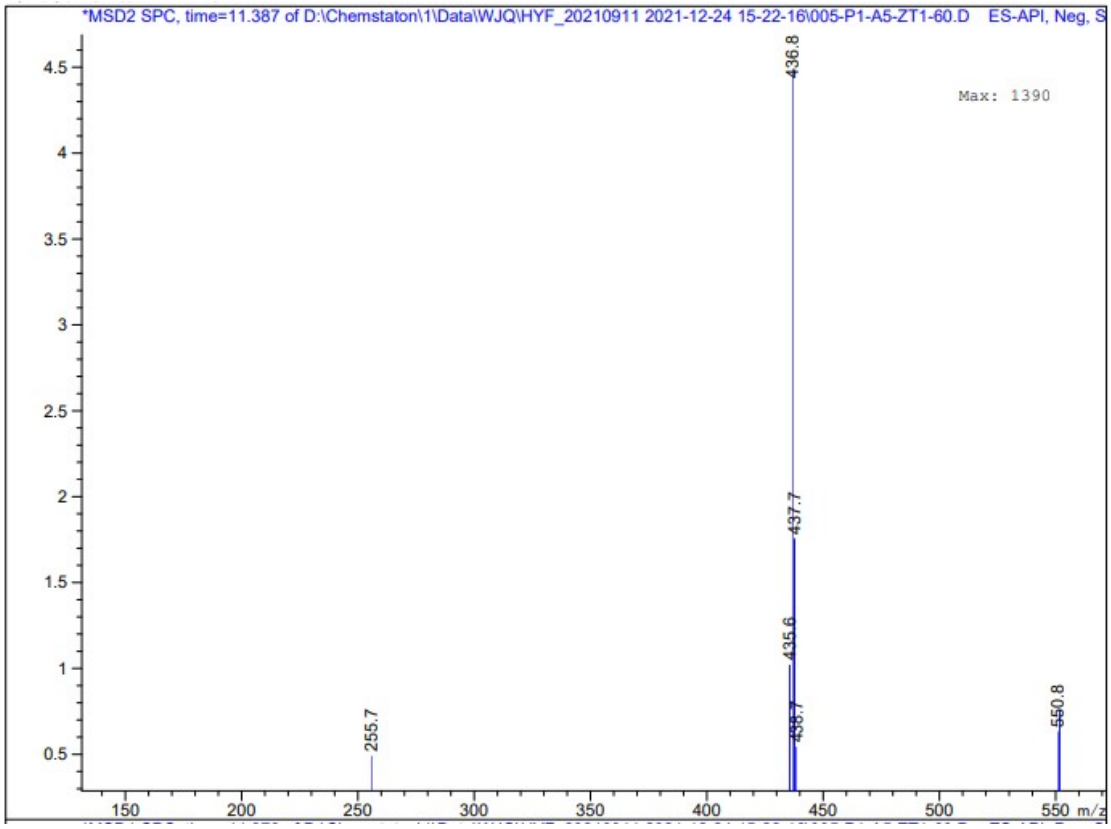

Fig. S48. Negative LR-ESI-MS of compound **12**

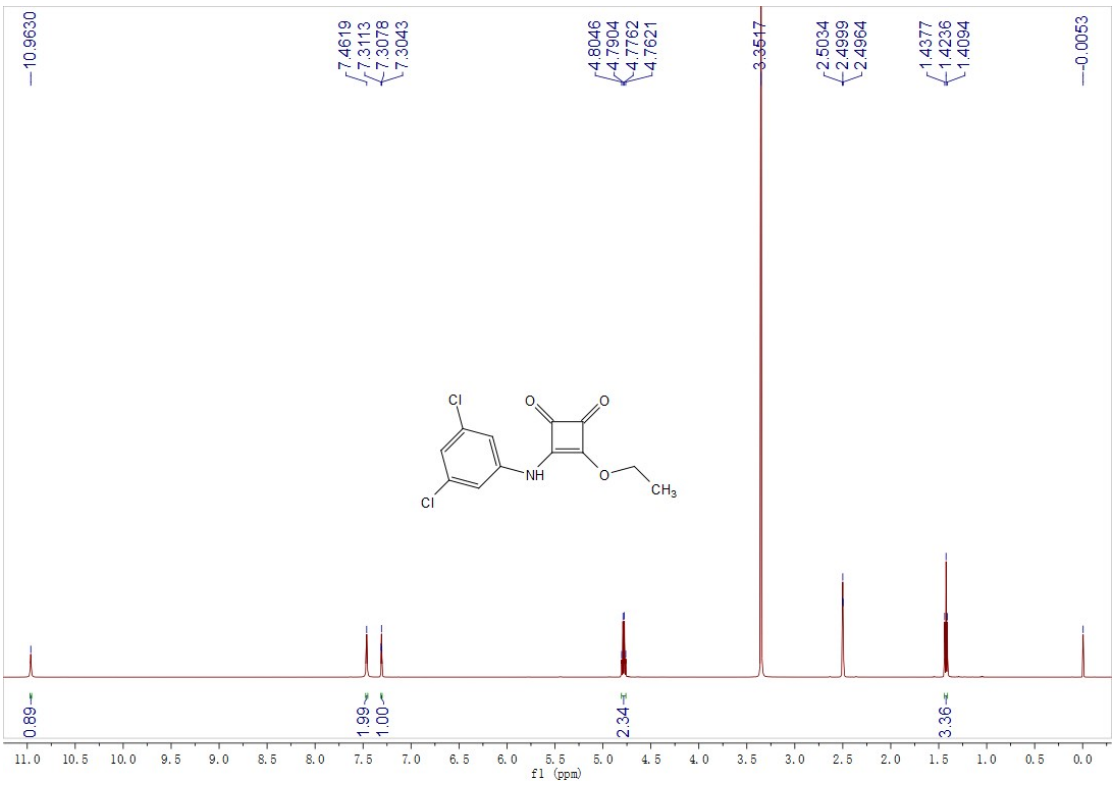

Fig. S49. ^{1}H NMR (500 MHz, DMSO-d_6) of compound **22**

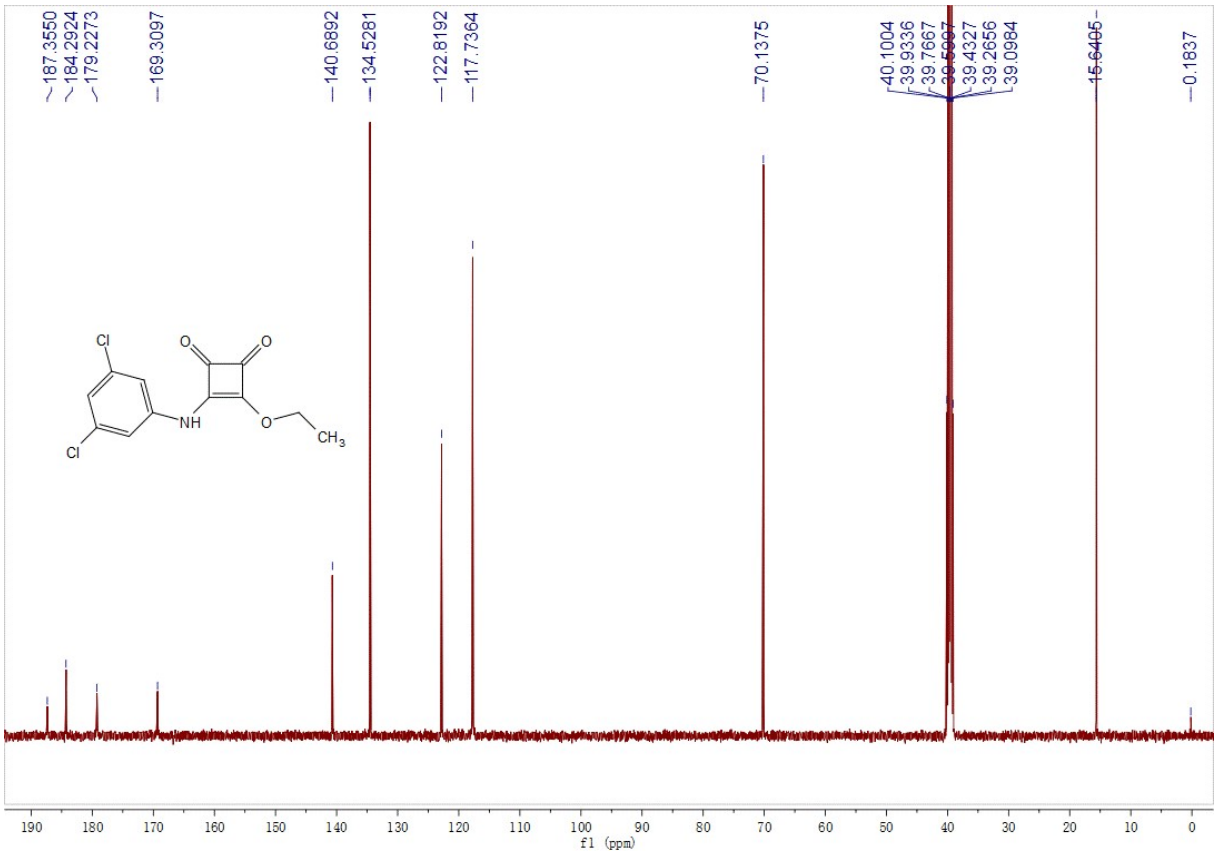

Fig. S50. ^{13}C NMR (125 MHz, DMSO-d_6) of compound **22**

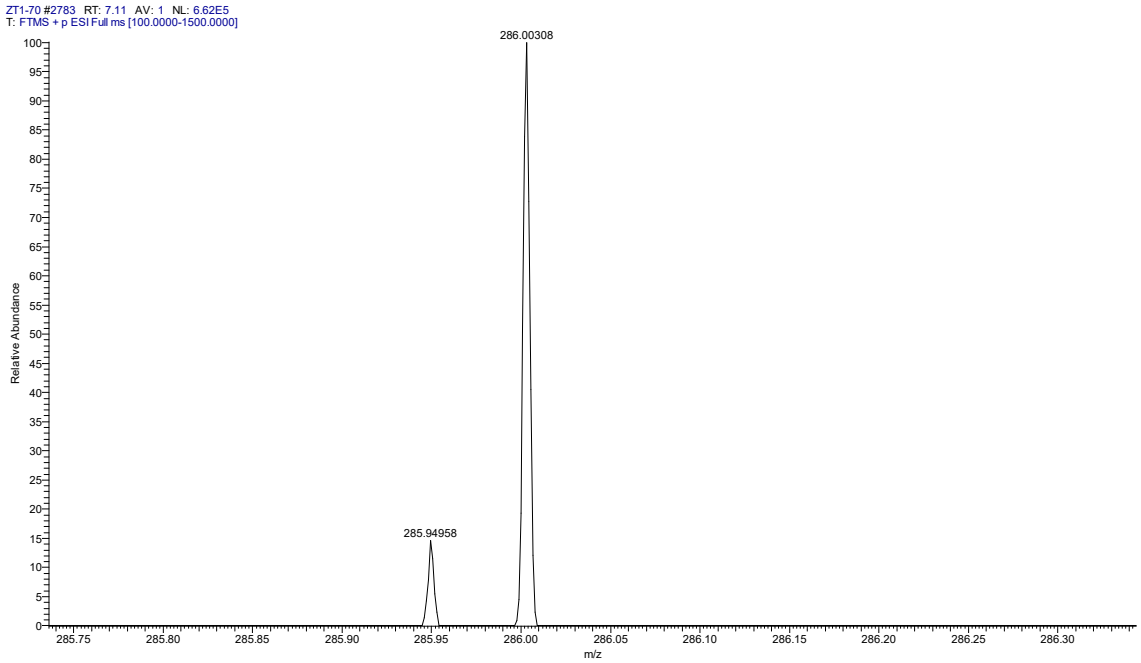

Fig. S51. HR-ESI-MS of compound **22**

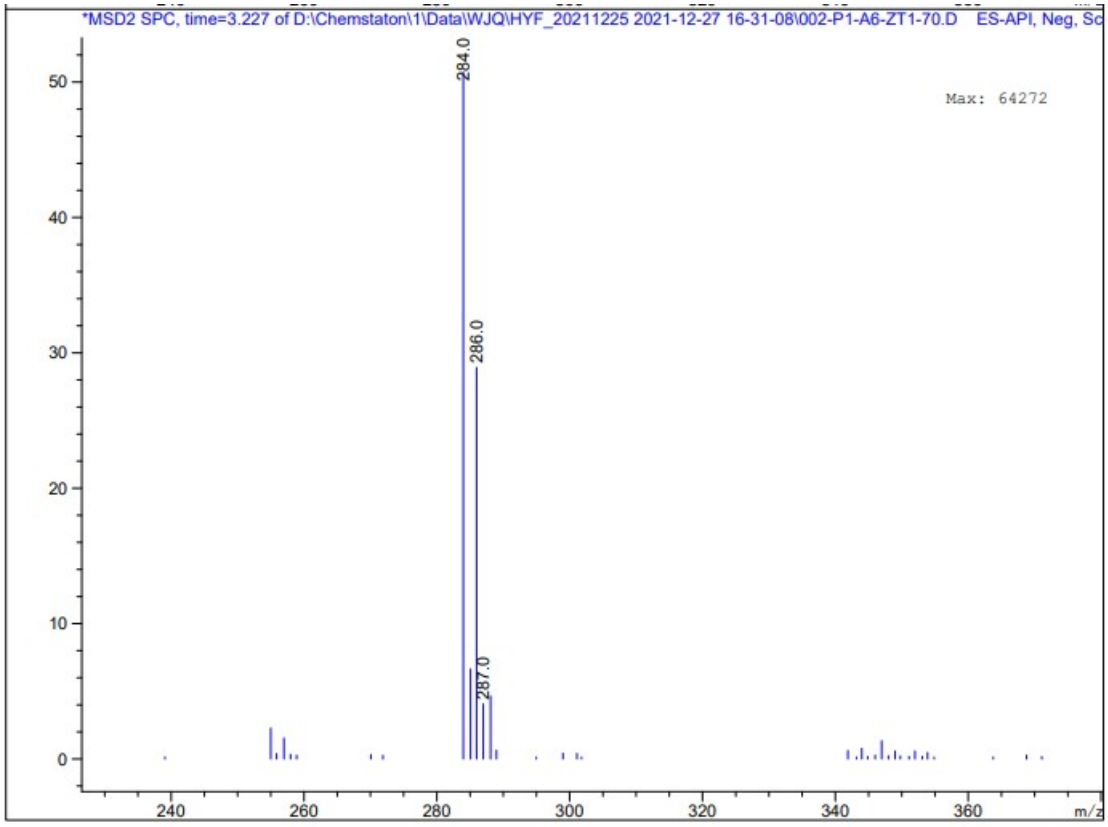

Fig. S52. Negative LR-ESI-MS of compound **22**

3. Anion transport

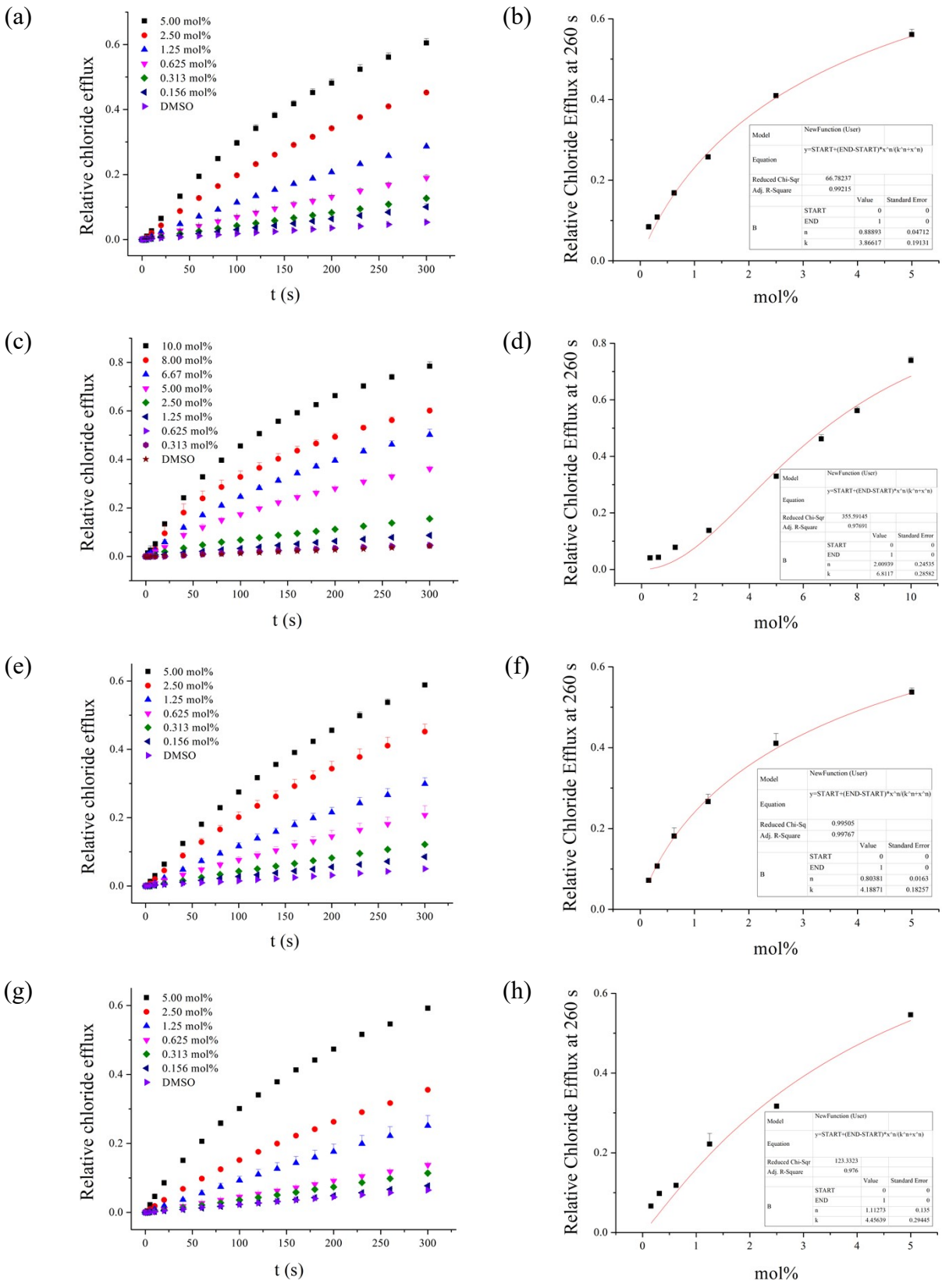

Fig. 53. (a, c, e, g) Relative chloride efflux out of EYPC liposomes (100 nm, extrusion) enhanced by compounds **8** (a), **10** (c), **11** (e) and **12** (g) of varying concentrations, respectively; (b, d, f, h) Hill plots of

the relative chloride efflux at 260 s against the mol% concentrations of compounds **8** (b), **10** (d), **11** (f) and **12** (h), respectively. Intravesicular conditions: 500 mM NaCl in 25 mM HEPES buffer (pH 7.0); and extravesicular conditions: 500 mM $NaNO_3$ in 25 mM HEPES buffer (pH 7.0).

4. Size distribution and integrity of vesicles

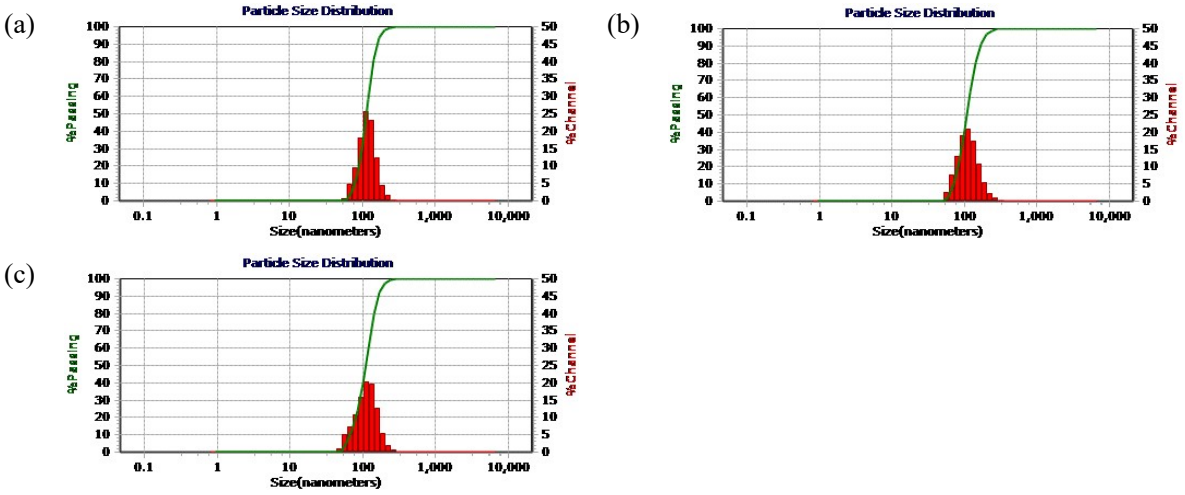

Fig. S54. Effect of compound **12** (5 mol%) on liposome particle size. (a, b) Blank and DMSO controls; (c) Treatment with of 5 mol% of compound **12**. Each particle size distribution graph is the average of three tests on the same liposome batch. Test conditions: 500 mM NaCl in 25 mM HEPES buffer (pH 7.0) for internal liposomes; and 500 mM $NaNO_3$ in 25 mM HEPES buffer (pH 7.0) for external liposomes.

Table S1. Size distribution of vesicles after the addition of 5 mol% of compound **12**

Compound	Diameters /nm
untreated	117.2±30.8
DMSO	113.2±36.3
12	113.3±37.9

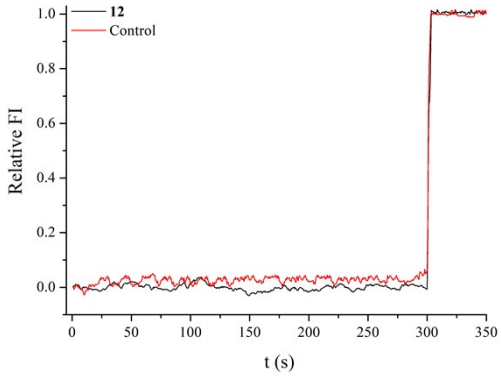

Fig. S55. (b) Relative fluorescence intensity of calcein against time (s) treated by compound **12** (5 mol%), under the conditions of an intravesicular 100 mM calcein and 50 mM NaCl solution in 25 mM HEPES buffer (pH 7.0) and extravesicular 50 mM NaCl in 25 mM HEPES buffer (pH 7.0).

5. AO staining

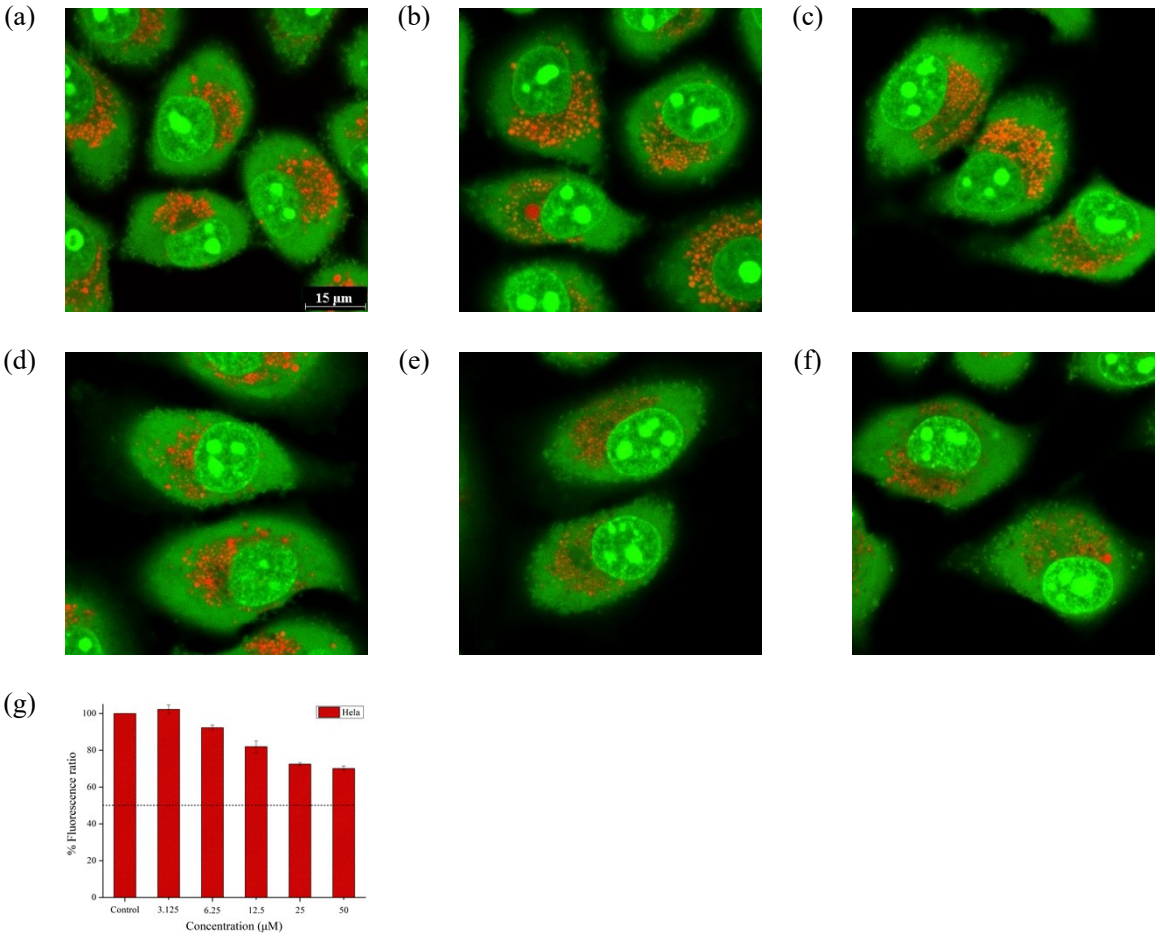

Fig. S56. AO staining of (a) untreated HeLa cells and (b-f) HeLa cells treated with compound **1** at the concentrations of (b) 3.125 μM; (c) 6.25 μM; (d) 12.5 μM; (e) 25 μM and (f) 50 μM for 3 h, respectively. Green fluorescence: λ_{ex} BP 470/40 nm, λ_{em} BP 525/50 nm; Red fluorescence: λ_{ex} BP 546/12 nm, λ_{em} BP 575-640 nm. (g) Graph of the AO fluorescence against the concentrations of compound **1**.

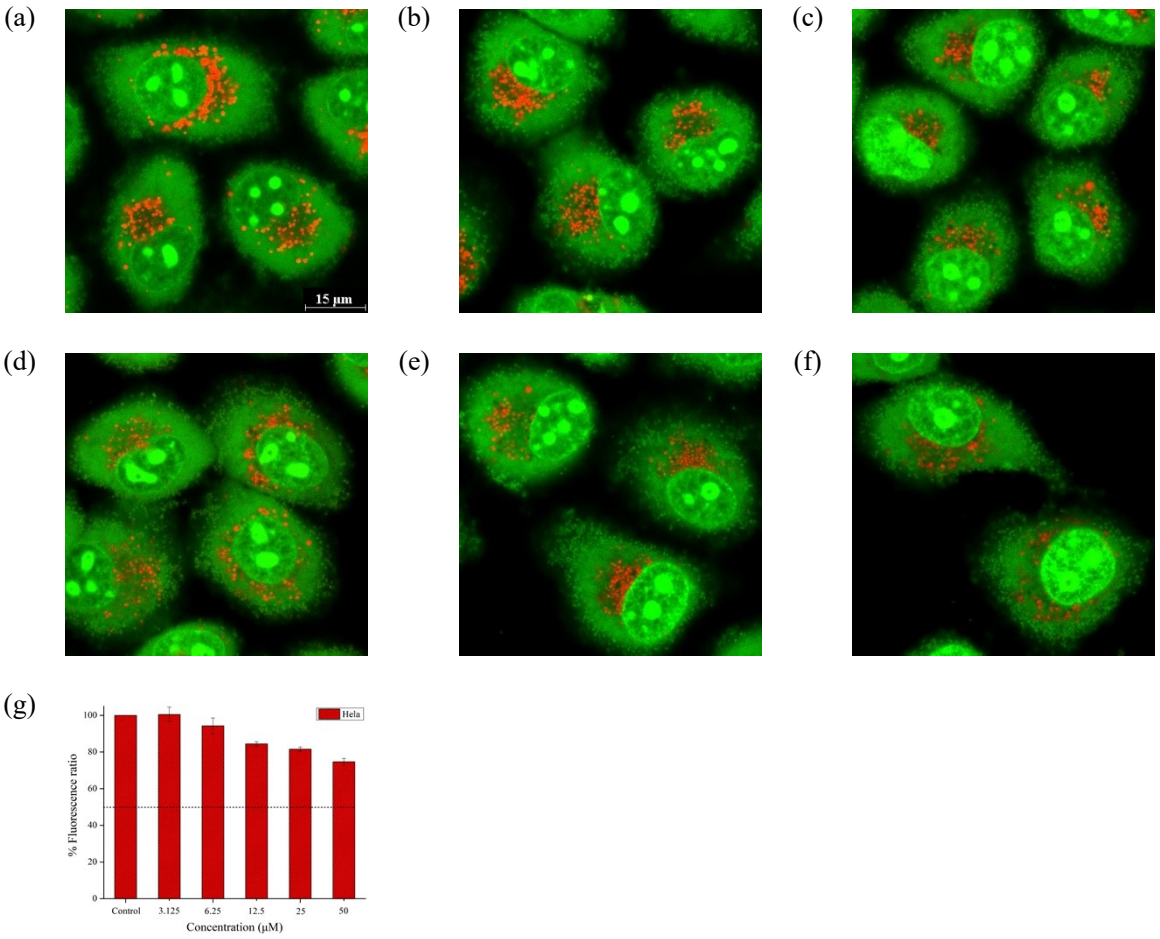

Fig. S57. AO staining of (a) untreated HeLa cells and (b-f) HeLa cells treated with compound **2** at the concentrations of (b) 3.125 μM; (c) 6.25 μM; (d) 12.5 μM; (e) 25 μM and (f) 50 μM for 3 h, respectively. Green fluorescence: λ_{ex} BP 470/40 nm, λ_{em} BP 525/50 nm; Red fluorescence: λ_{ex} BP 546/12 nm, λ_{em} BP 575-640 nm. (g) Graph of the AO fluorescence against the concentrations of compound **2**.

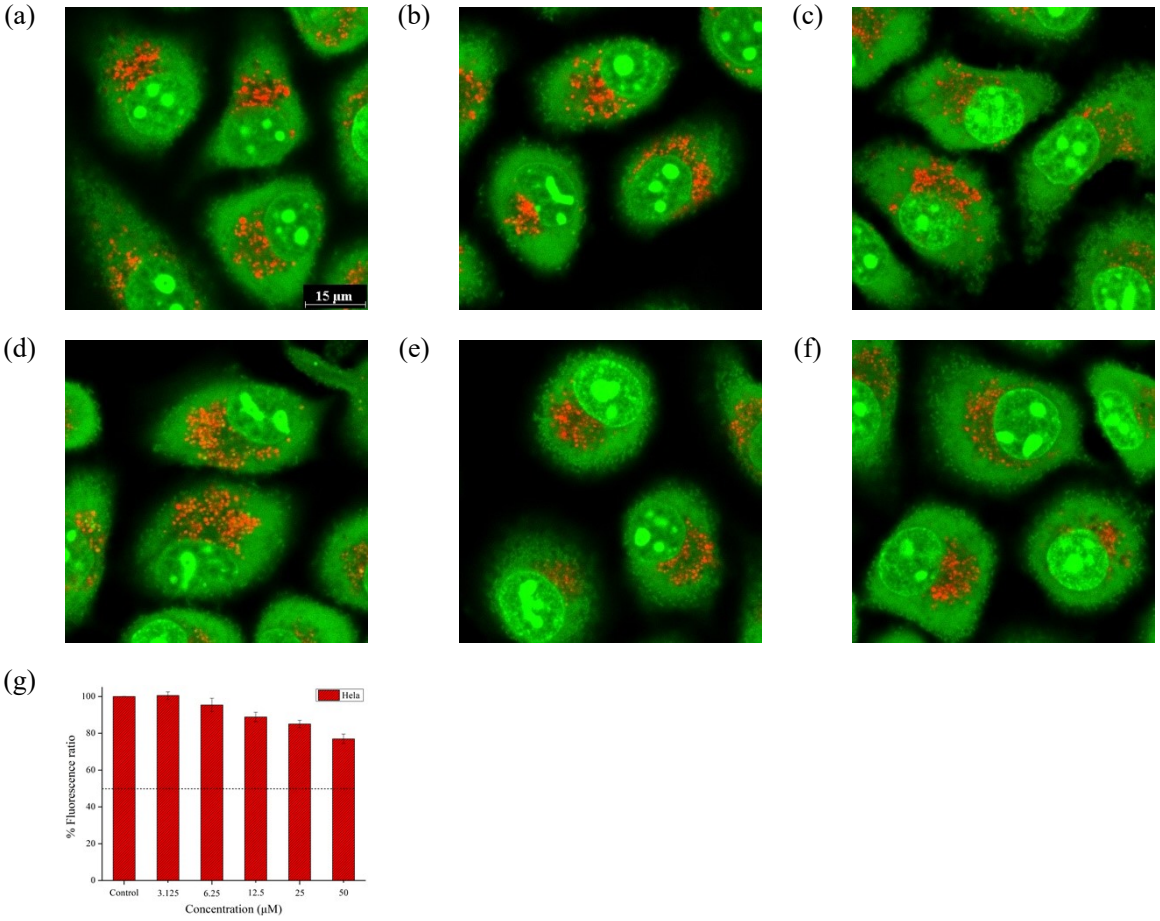

Fig. S58. AO staining of (a) untreated HeLa cells and (b-f) HeLa cells treated with compound **3** at the concentrations of (b) 3.125 μM; (c) 6.25 μM; (d) 12.5 μM; (e) 25 μM and (f) 50 μM for 3 h, respectively. Green fluorescence: λ_{ex} BP 470/40 nm, λ_{em} BP 525/50 nm; Red fluorescence: λ_{ex} BP 546/12 nm, λ_{em} BP 575-640 nm. (g) Graph of the AO fluorescence against the concentrations of compound **3**.

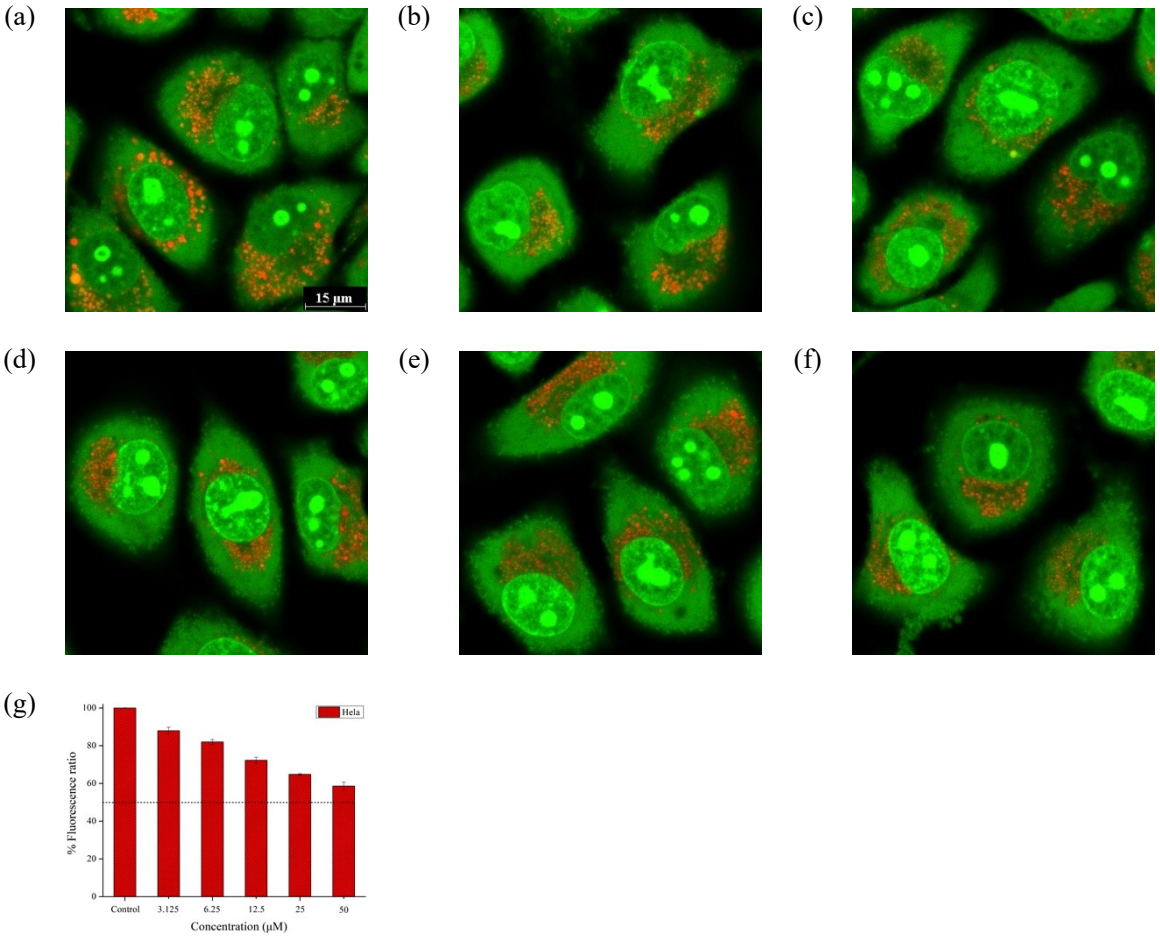

Fig. 59. AO staining of (a) untreated HeLa cells and (b-f) HeLa cells treated with compound **4** at the concentrations of (b) 3.125 μM; (c) 6.25 μM; (d) 12.5 μM; (e) 25 μM and (f) 50 μM for 3 h, respectively. Green fluorescence: λ_{ex} BP 470/40 nm, λ_{em} BP 525/50 nm; Red fluorescence: λ_{ex} BP 546/12 nm, λ_{em} BP 575-640 nm. (g) Graph of the AO fluorescence against the concentrations of compound **4**.

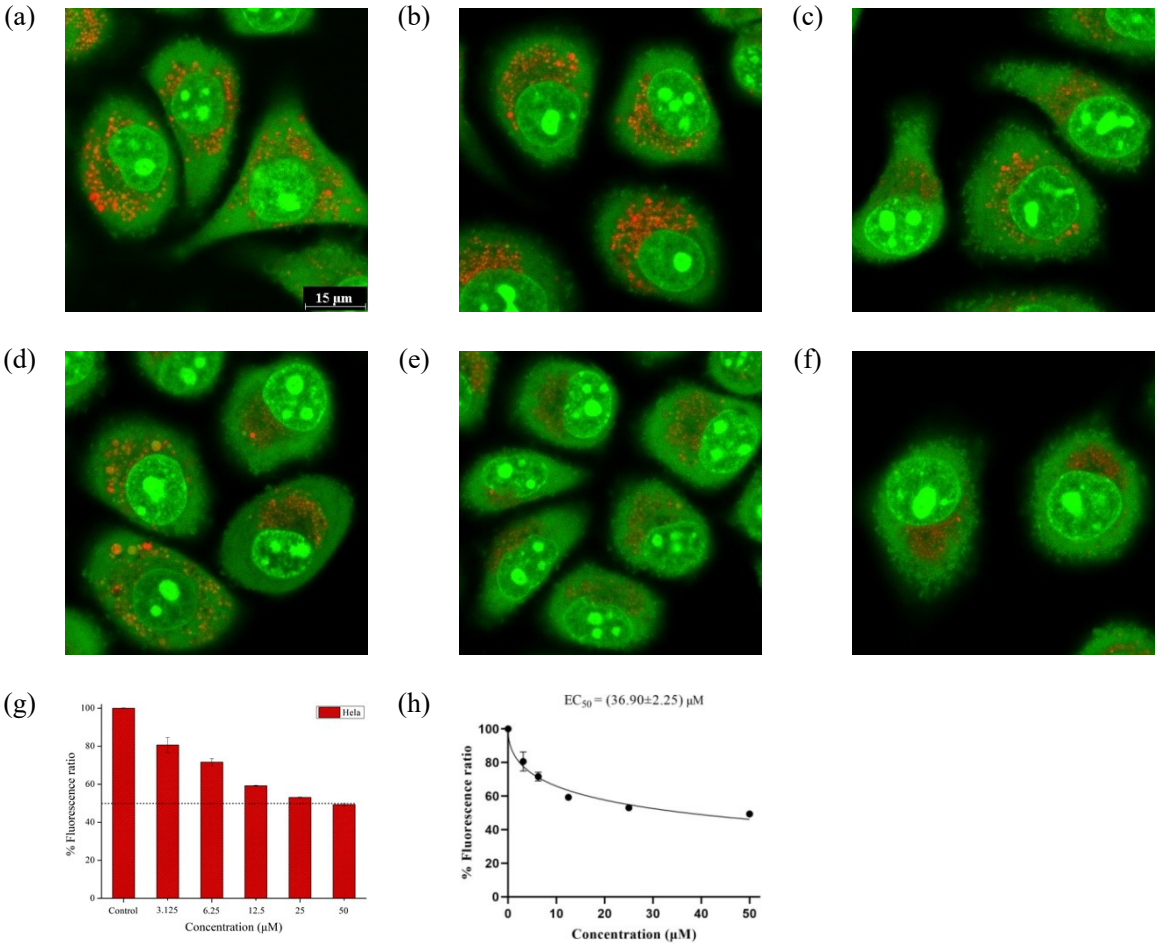

Fig. S60. AO staining of (a) untreated HeLa cells and (b-f) HeLa cells treated with compound **5** at the concentrations of (b) 3.125 μM; (c) 6.25 μM; (d) 12.5 μM; (e) 25 μM and (f) 50 μM for 3 h, respectively. Green fluorescence: λ_{ex} BP 470/40 nm, λ_{em} BP 525/50 nm; Red fluorescence: λ_{ex} BP 546/12 nm, λ_{em} BP 575-640 nm. (g) Graph of the AO fluorescence against the concentrations of compound **5**. (h) Curve fitting of the AO fluorescence against the concentrations of compound **5**.

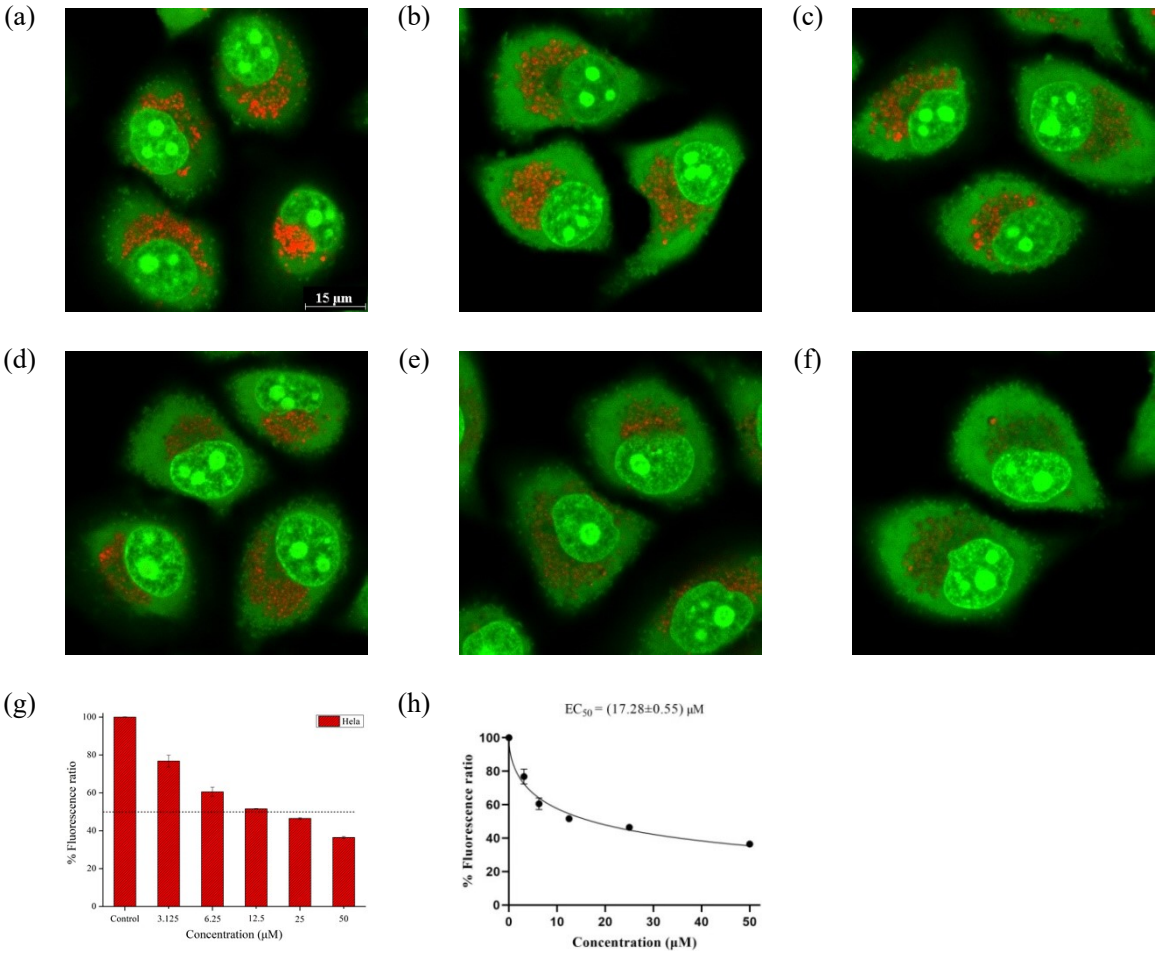

Fig. S61. AO staining of (a) untreated HeLa cells and (b-f) HeLa cells treated with compound **6** at the concentrations of (b) 3.125 μM; (c) 6.25 μM; (d) 12.5 μM; (e) 25 μM and (f) 50 μM for 3 h, respectively. Green fluorescence: λ_{ex} BP 470/40 nm, λ_{em} BP 525/50 nm; Red fluorescence: λ_{ex} BP 546/12 nm, λ_{em} BP 575-640 nm. (g) Graph of the AO fluorescence against the concentrations of compound **6**. (h) Curve fitting of the AO fluorescence against the concentrations of compound **6**.

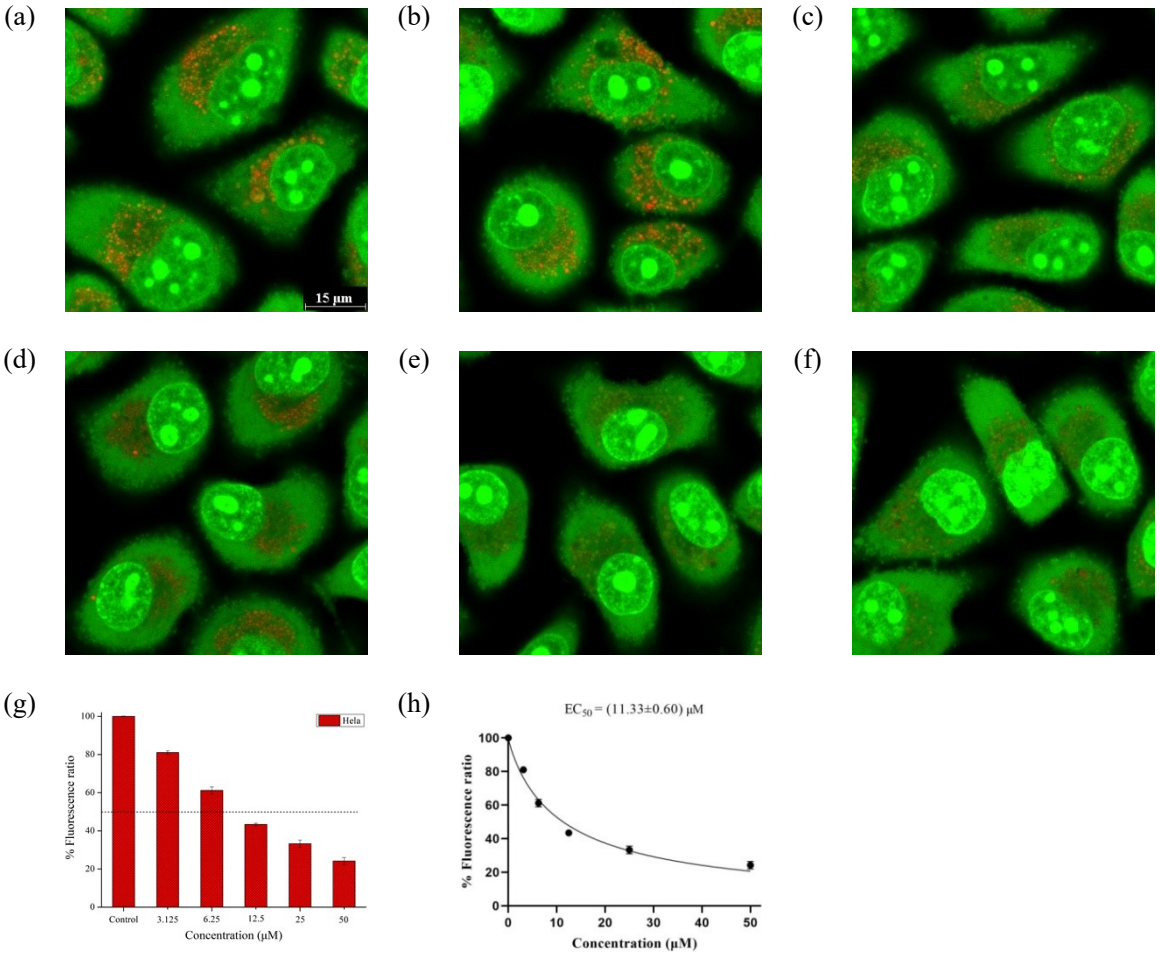

Fig. S62. AO staining of (a) untreated HeLa cells and (b-f) HeLa cells treated with compound **7** at the concentrations of (b) 3.125 μM; (c) 6.25 μM; (d) 12.5 μM; (e) 25 μM and (f) 50 μM for 3 h, respectively. Green fluorescence: λ_{ex} BP 470/40 nm, λ_{em} BP 525/50 nm; Red fluorescence: λ_{ex} BP 546/12 nm, λ_{em} BP 575-640 nm. (g) Graph of the AO fluorescence against the concentrations of compound **7**. (h) Curve fitting of the AO fluorescence against the concentrations of compound **7**.

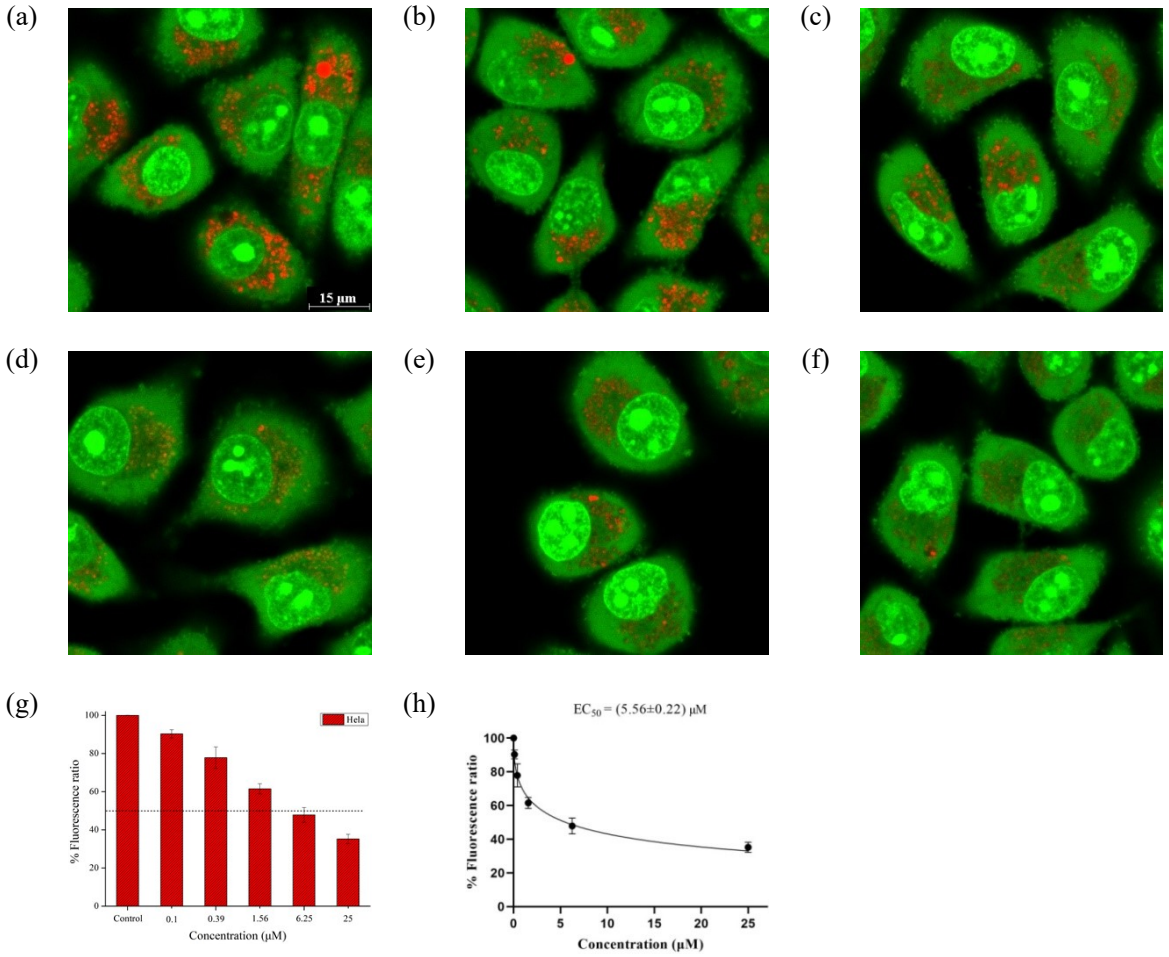

Fig. S63. AO staining of (a) untreated HeLa cells and (b-f) HeLa cells treated with compound **8** at the concentrations of (b) 0.10 μM; (c) 0.39 μM; (d) 1.56 μM; (e) 6.25 μM and (f) 25 μM for 3 h, respectively. Green fluorescence: λ_{ex} BP 470/40 nm, λ_{em} BP 525/50 nm; Red fluorescence: λ_{ex} BP 546/12 nm, λ_{em} BP 575-640 nm. (g) Graph of the AO fluorescence against the concentrations of compound **8**. (h) Curve fitting of the AO fluorescence against the concentrations of compound **8**.

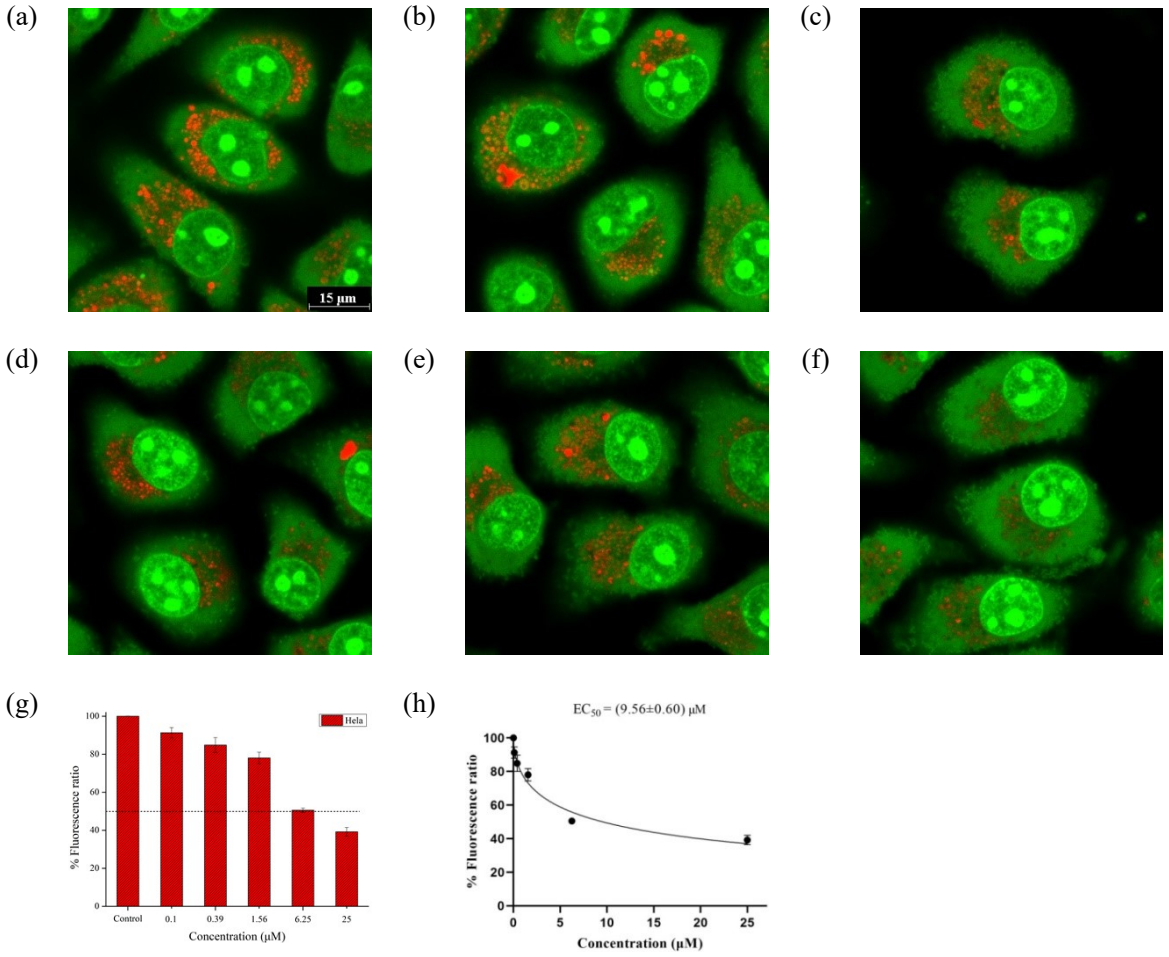

Fig. S64. AO staining of (a) untreated HeLa cells and (b-f) HeLa cells treated with compound **9** at the concentrations of (b) 0.10 μM; (c) 0.39 μM; (d) 1.56 μM; (e) 6.25 μM and (f) 25 μM for 3 h, respectively. Green fluorescence: λ_{ex} BP 470/40 nm, λ_{em} BP 525/50 nm; Red fluorescence: λ_{ex} BP 546/12 nm, λ_{em} BP 575-640 nm. (g) Graph of the AO fluorescence against the concentrations of compound **9**. (h) Curve fitting of the AO fluorescence against the concentrations of compound **9**.

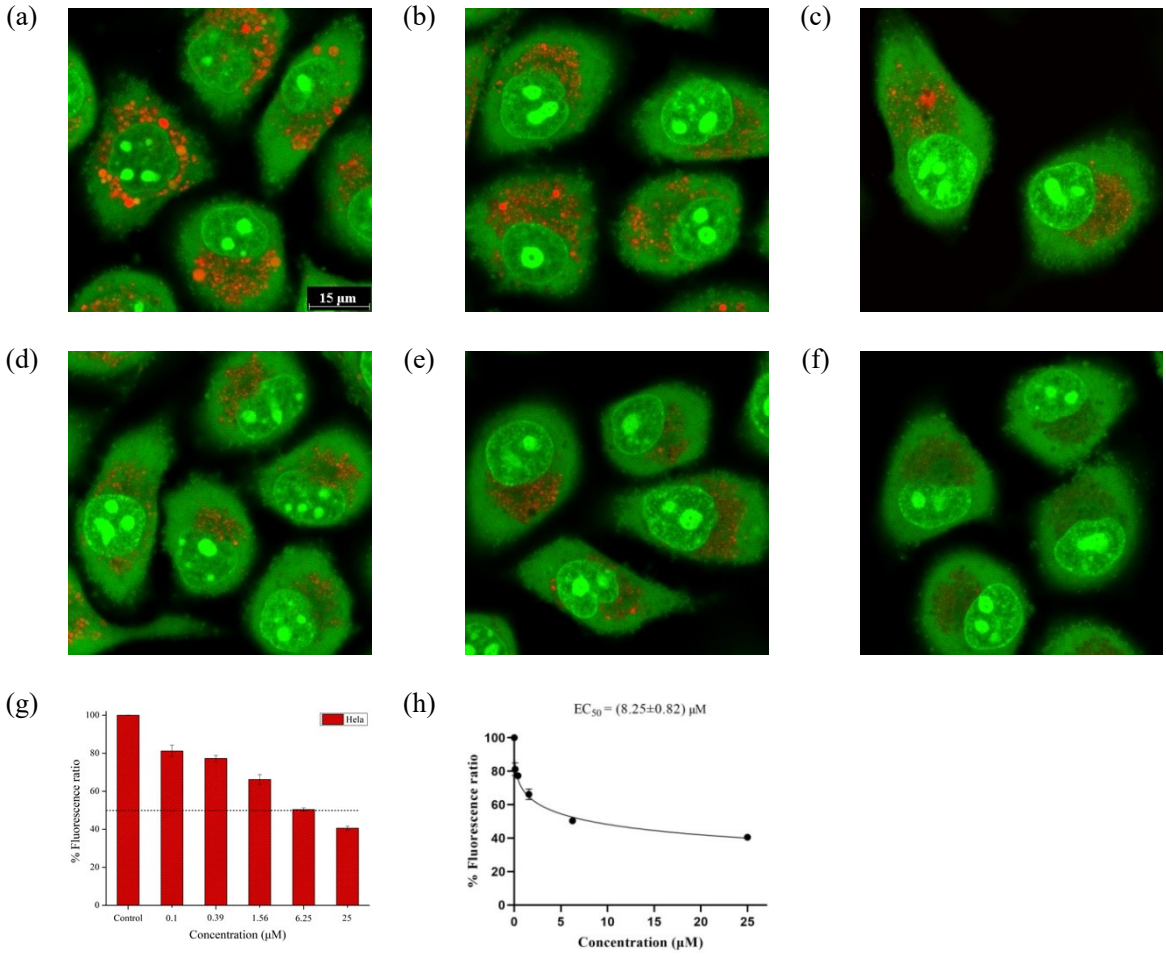

Fig. S65. AO staining of (a) untreated HeLa cells and (b-f) HeLa cells treated with compound **10** at the concentrations of (b) 0.10 μM; (c) 0.39 μM; (d) 1.56 μM; (e) 6.25 μM and (f) 25 μM for 3 h, respectively. Green fluorescence: λ_{ex} BP 470/40 nm, λ_{em} BP 525/50 nm; Red fluorescence: λ_{ex} BP 546/12 nm, λ_{em} BP 575-640 nm. (g) Graph of the AO fluorescence against the concentrations of compound **10**. (h) Curve fitting of the AO fluorescence against the concentrations of compound **10**.

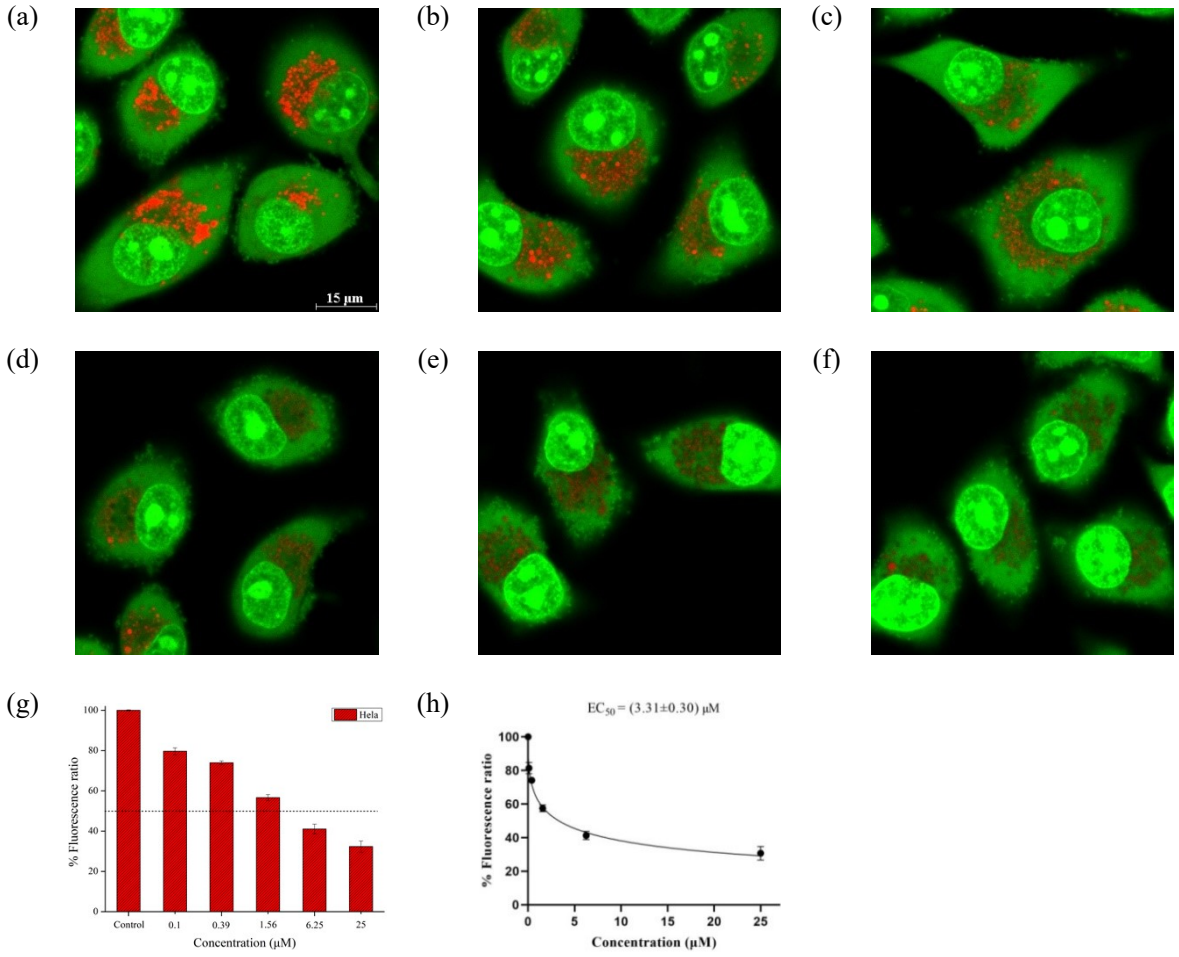

Fig. S66. AO staining of (a) untreated HeLa cells and (b-f) HeLa cells treated with compound **11** at the concentrations of (b) 0.10 μM; (c) 0.39 μM; (d) 1.56 μM; (e) 6.25 μM and (f) 25 μM for 3 h, respectively. Green fluorescence: λ_{ex} BP 470/40 nm, λ_{em} BP 525/50 nm; Red fluorescence: λ_{ex} BP 546/12 nm, λ_{em} BP 575-640 nm. (g) Graph of the AO fluorescence against the concentrations of compound **11**. (h) Curve fitting of the AO fluorescence against the concentrations of compound **11**.

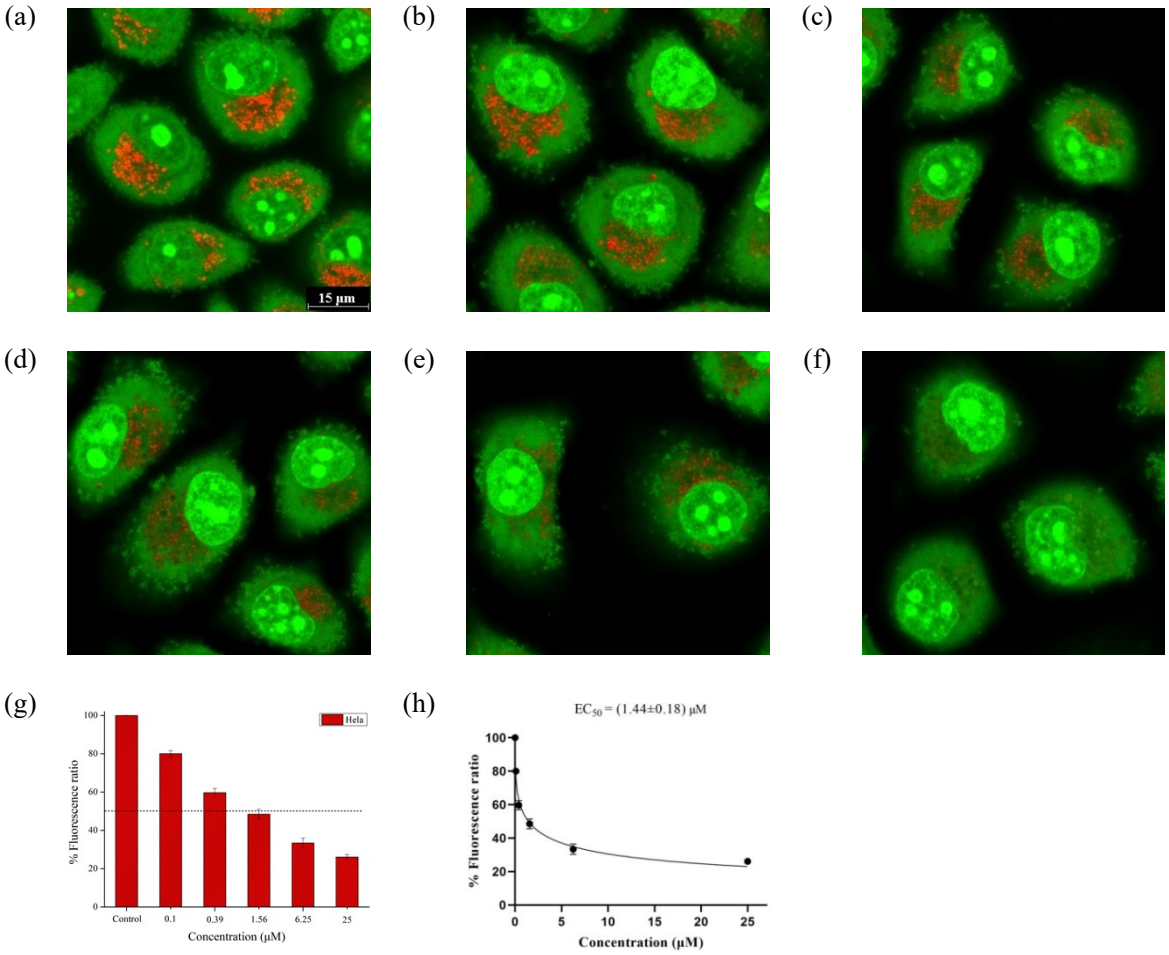

Fig. S67. AO staining of (a) untreated HeLa cells and (b-f) HeLa cells treated with chloroquine phosphate at the concentrations of (b) 0.10 μM; (c) 0.39 μM; (d) 1.56 μM; (e) 6.25 μM and (f) 25 μM for 3 h, respectively. Green fluorescence: λ_{ex} BP 470/40 nm, λ_{em} BP 525/50 nm; Red fluorescence: λ_{ex} BP 546/12 nm, λ_{em} BP 575-640 nm. (g) Graph of the AO fluorescence against the concentrations of chloroquine phosphate. (h) Curve fitting of the AO fluorescence against the concentrations of chloroquine phosphate.

6. LysoSensor Green DND-189 staining

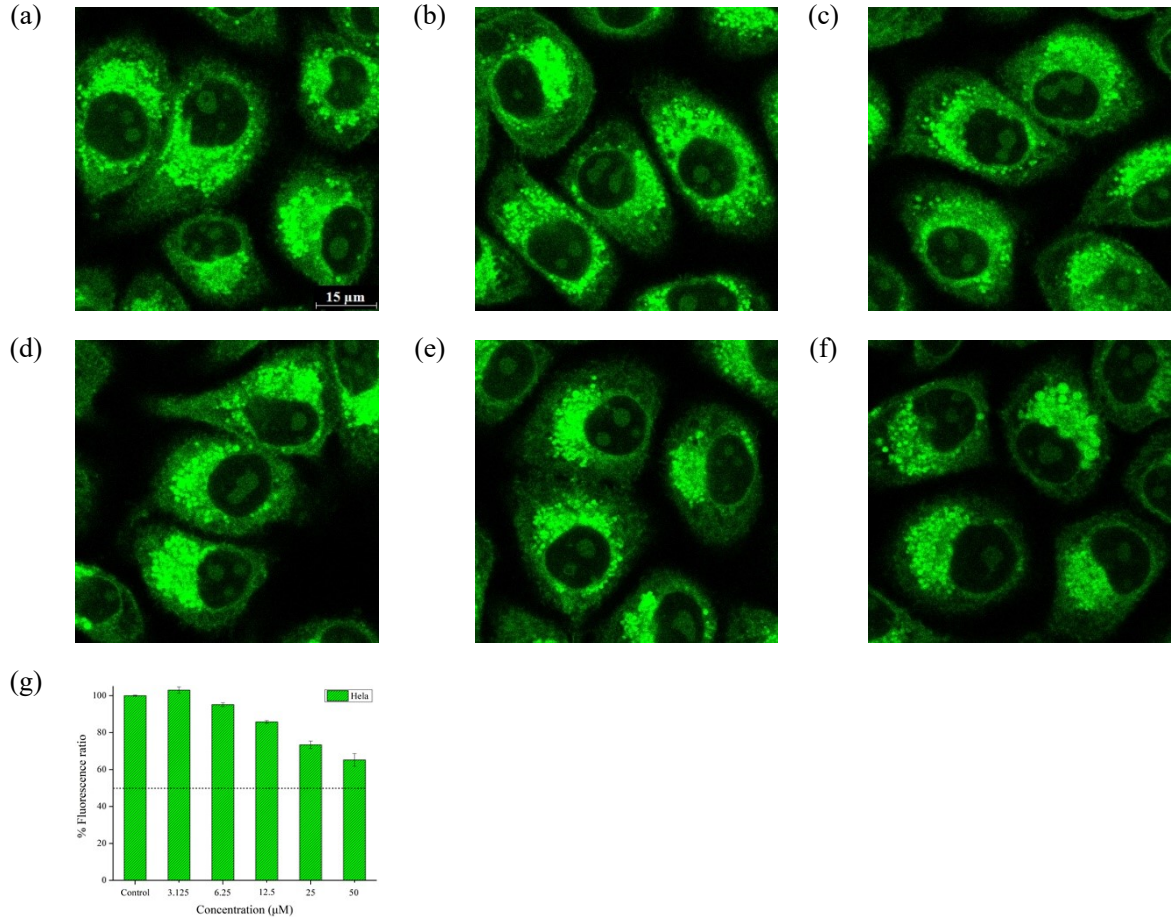

Fig. S68. (a-f) LysoSensor Green DND-189 (1.0 μM, 1 h) staining of (a) untreated HeLa cells and (b-f) HeLa cells treated with compound **1** at the concentrations of (b) 3.125 μM; (c) 6.25 μM; (d) 12.5 μM; (e) 25 μM and (f) 50 μM for 4 h, respectively. Green fluorescence: λ_{ex} BP 470/40 nm, λ_{em} BP 525/50 nm. (g) Graph of the LysoSensor Green DND-189 fluorescence against the concentrations of compound **1**.

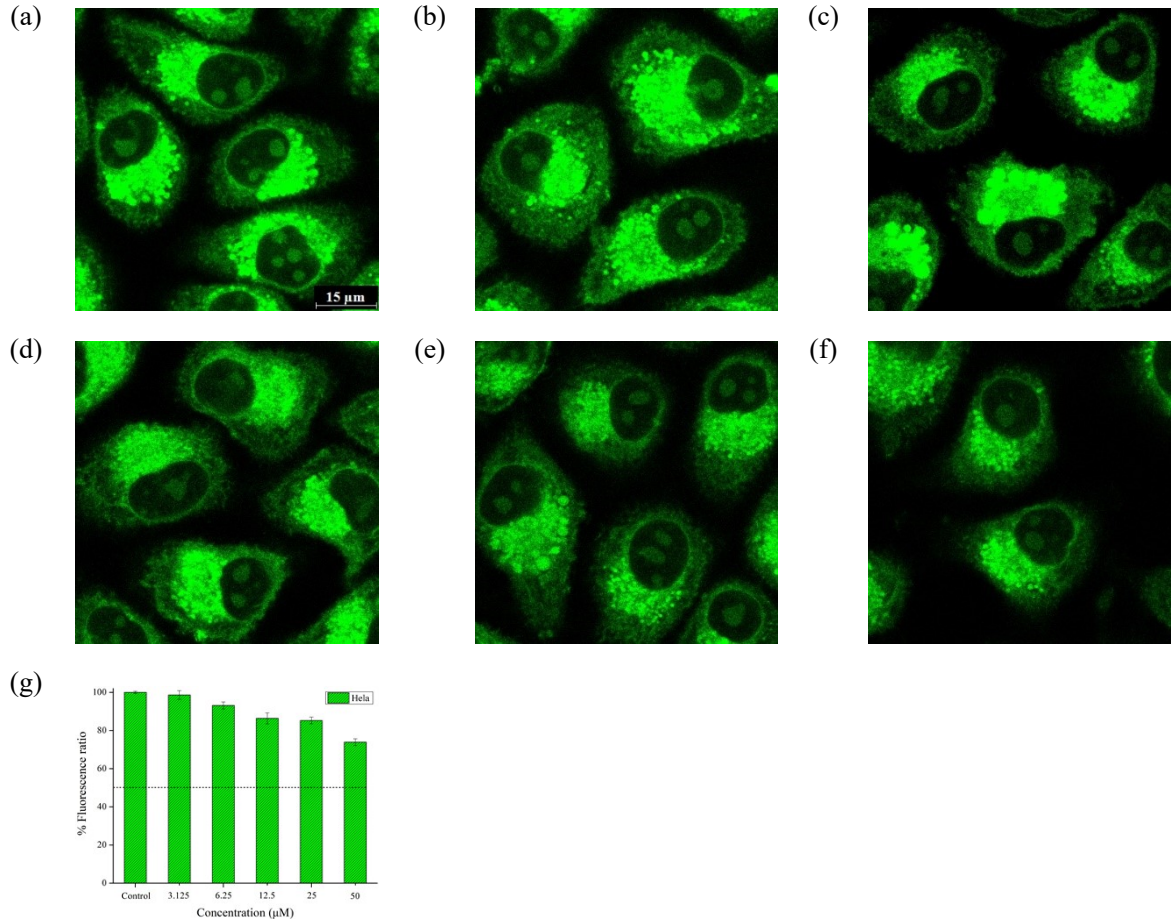

Fig. S69. (a-f) LysoSensor Green DND-189 (1.0 μM, 1 h) staining of (a) untreated HeLa cells and (b-f) HeLa cells treated with compound **2** at the concentrations of (b) 3.125 μM; (c) 6.25 μM; (d) 12.5 μM; (e) 25 μM and (f) 50 μM for 4 h, respectively. Green fluorescence: λ_{ex} BP 470/40 nm, λ_{em} BP 525/50 nm. (g) Graph of the LysoSensor Green DND-189 fluorescence against the concentrations of compound **2**.

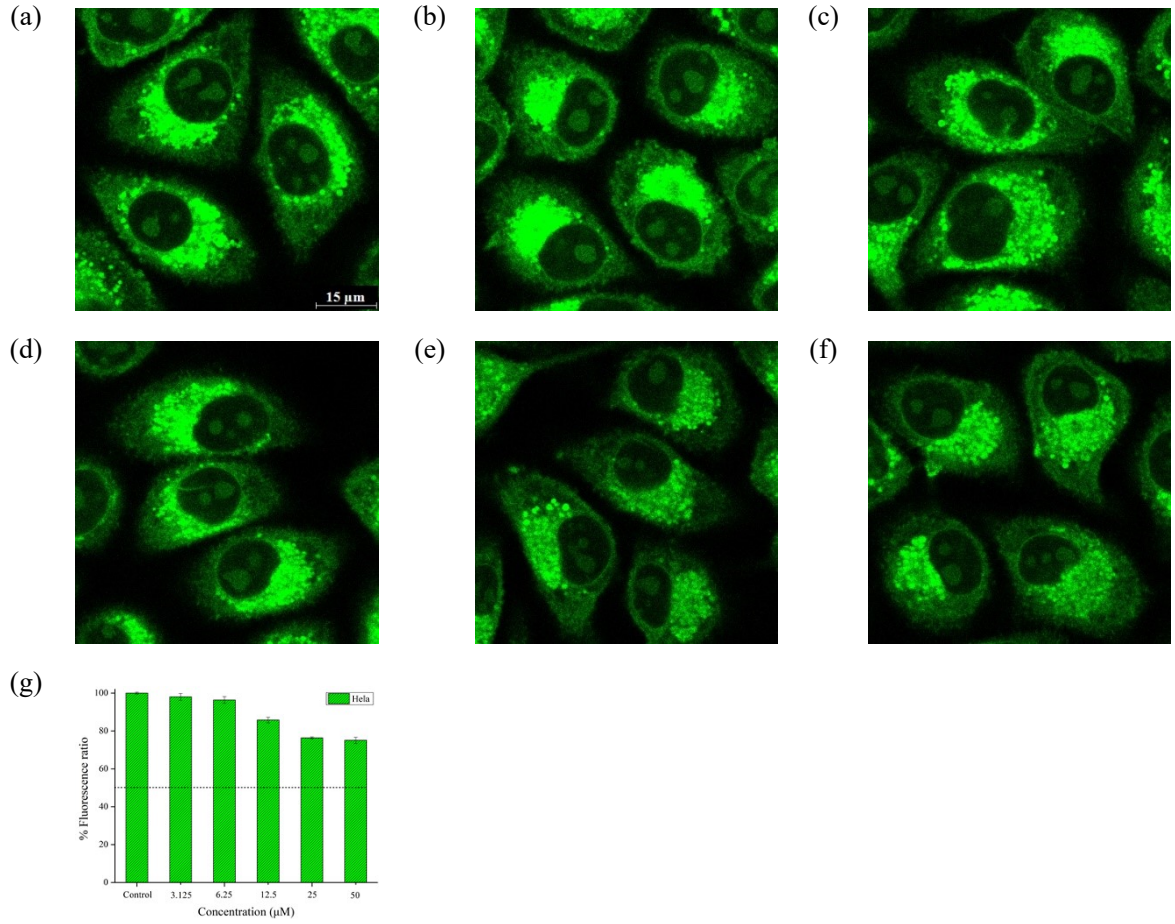

Fig. S70. (a-f) LysoSensor Green DND-189 (1.0 µM, 1 h) staining of (a) untreated HeLa cells and (b-f) HeLa cells treated with compound **3** at the concentrations of (b) 3.125 µM; (c) 6.25 µM; (d) 12.5 µM; (e) 25 µM and (f) 50 µM for 4 h, respectively. Green fluorescence: λ_{ex} BP 470/40 nm, λ_{em} BP 525/50 nm. (g) Graph of the LysoSensor Green DND-189 fluorescence against the concentrations of compound **3**.

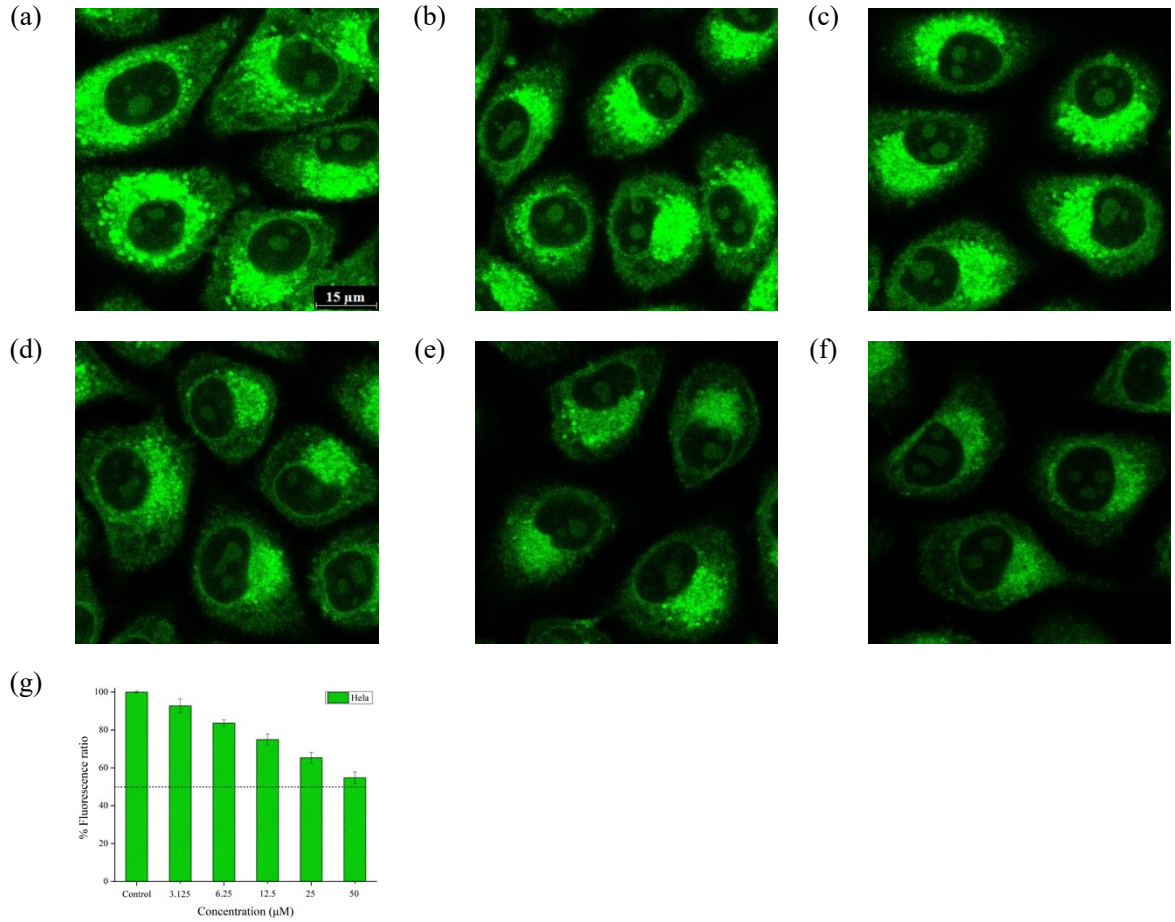

Fig. S71. (a-f) LysoSensor Green DND-189 (1.0 µM, 1 h) staining of (a) untreated HeLa cells and (b-f) HeLa cells treated with compound **4** at the concentrations of (b) 3.125 µM; (c) 6.25 µM; (d) 12.5 µM; (e) 25 µM and (f) 50 µM for 4 h, respectively. Green fluorescence: λ_{ex} BP 470/40 nm, λ_{em} BP 525/50 nm. (g) Graph of the LysoSensor Green DND-189 fluorescence against the concentrations of compound **4**.

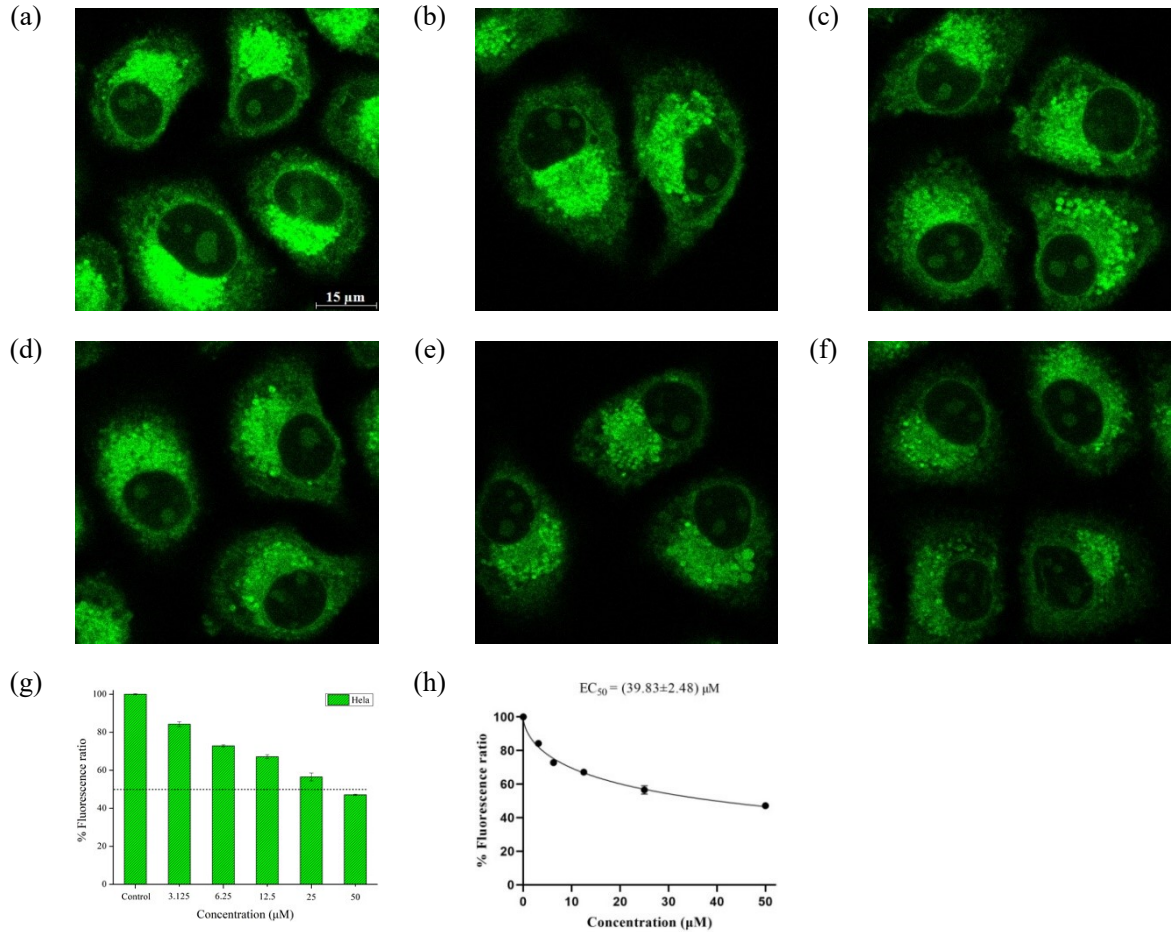

Fig. S72. (a-f) LysoSensor Green DND-189 (1.0 μM, 1 h) staining of (a) untreated HeLa cells and (b-f) HeLa cells treated with compound **5** at the concentrations of (b) 3.125 μM; (c) 6.25 μM; (d) 12.5 μM; (e) 25 μM and (f) 50 μM for 4 h, respectively. Green fluorescence: λ_{ex} BP 470/40 nm, λ_{em} BP 525/50 nm. (g) Graph of the LysoSensor Green DND-189 fluorescence against the concentrations of compound **5**. (h) Curve fitting of the LysoSensor Green DND-189 fluorescence against the concentrations of compound **5**.

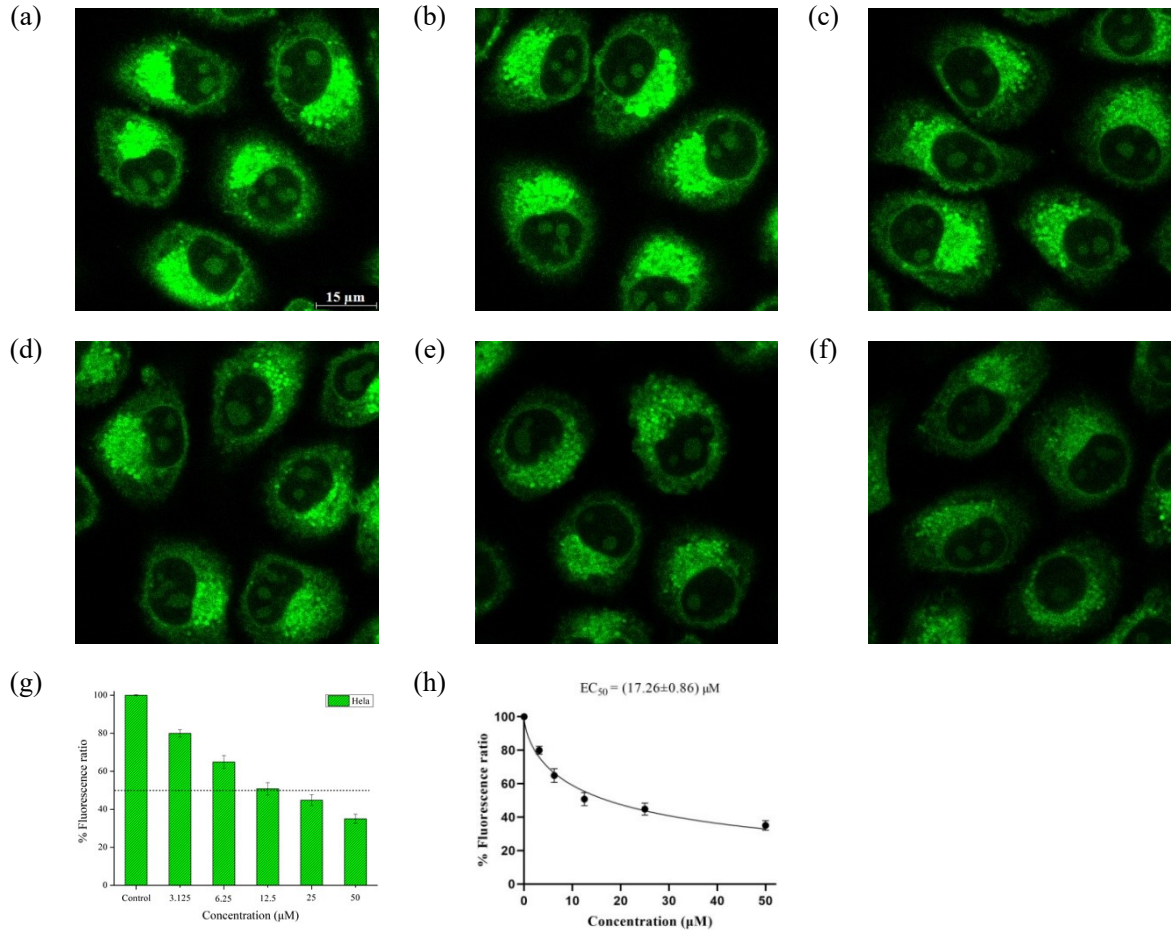

Fig. S73. (a-f) LysoSensor Green DND-189 (1.0 μM, 1 h) staining of (a) untreated HeLa cells and (b-f) HeLa cells treated with compound **6** at the concentrations of (b) 3.125 μM; (c) 6.25 μM; (d) 12.5 μM; (e) 25 μM and (f) 50 μM for 4 h, respectively. Green fluorescence: λ_{ex} BP 470/40 nm, λ_{em} BP 525/50 nm. (g) Graph of the LysoSensor Green DND-189 fluorescence against the concentrations of compound **6**. (h) Curve fitting of the LysoSensor Green DND-189 fluorescence against the concentrations of compound **6**.

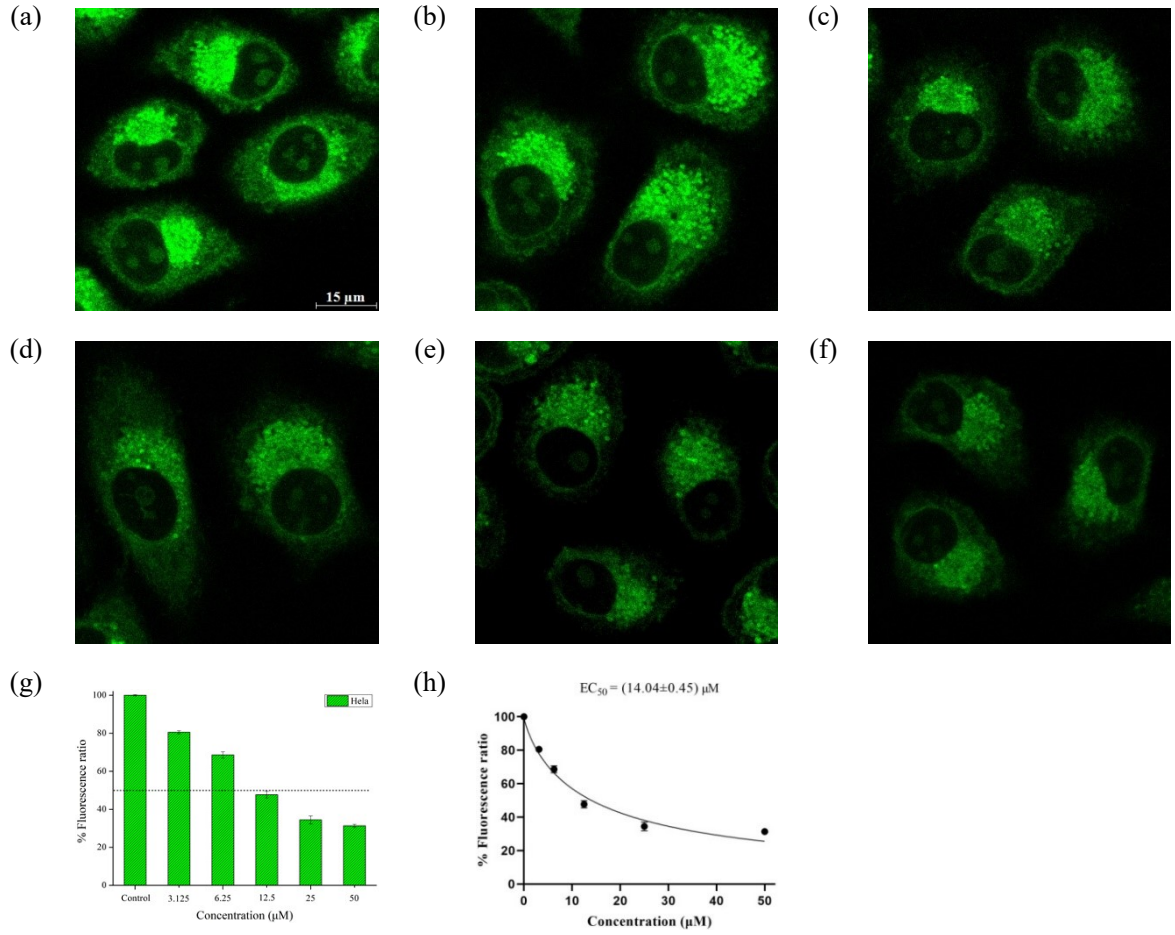

Fig. S74. (a-f) LysoSensor Green DND-189 (1.0 μM, 1 h) staining of (a) untreated HeLa cells and (b-f) HeLa cells treated with compound **7** at the concentrations of (b) 3.125 μM; (c) 6.25 μM; (d) 12.5 μM; (e) 25 μM and (f) 50 μM for 4 h, respectively. Green fluorescence: λ_{ex} BP 470/40 nm, λ_{em} BP 525/50 nm. (g) Graph of the LysoSensor Green DND-189 fluorescence against the concentrations of compound **7**. (h) Curve fitting of the LysoSensor Green DND-189 fluorescence against the concentrations of compound **7**.

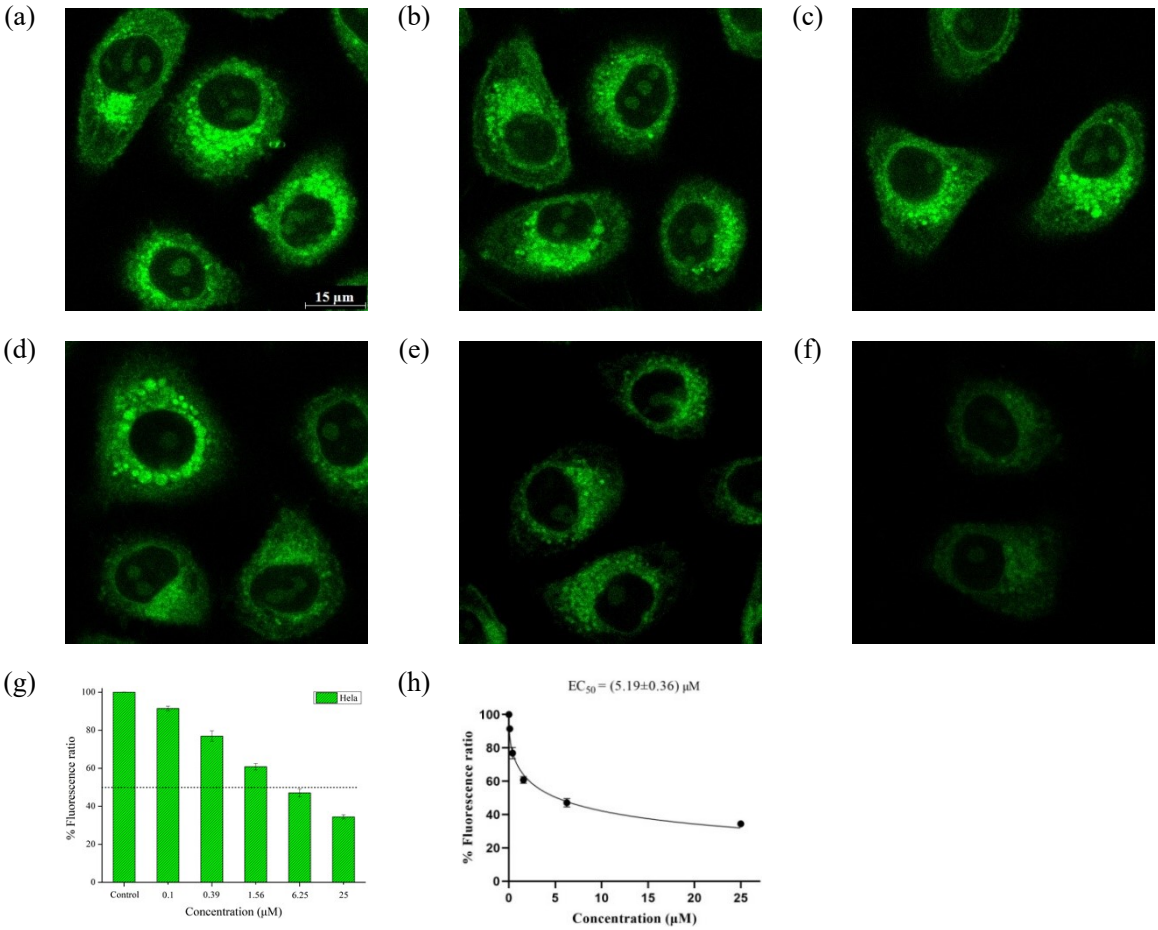

Fig. S75. (a-f) LysoSensor Green DND-189 (1.0 μM, 1 h) staining of (a) untreated HeLa cells and (b-f) HeLa cells treated with compound **8** at the concentrations of (b) 0.1 μM; (c) 0.39 μM; (d) 1.56 μM; (e) 6.25 μM and (f) 25 μM for 4 h, respectively. Green fluorescence: λ_{ex} BP 470/40 nm, λ_{em} BP 525/50 nm. (g) Graph of the LysoSensor Green DND-189 fluorescence against the concentrations of compound **8**. (h) Curve fitting of the LysoSensor Green DND-189 fluorescence against the concentrations of compound **8**.

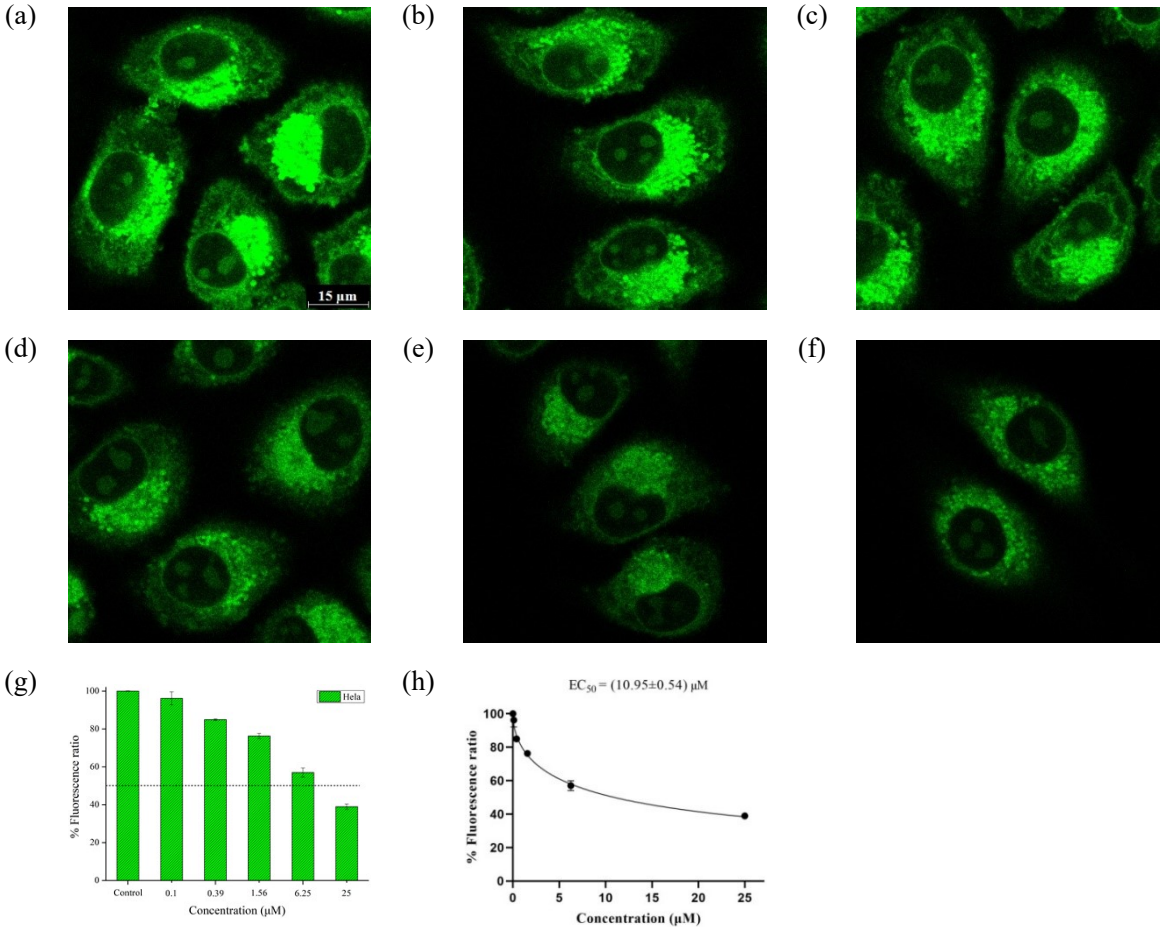

Fig. S76. (a-f) LysoSensor Green DND-189 (1.0 μM, 1 h) staining of (a) untreated HeLa cells and (b-f) HeLa cells treated with compound **9** at the concentrations of (b) 0.1 μM; (c) 0.39 μM; (d) 1.56 μM; (e) 6.25 μM and (f) 25 μM for 4 h, respectively. Green fluorescence: λ_{ex} BP 470/40 nm, λ_{em} BP 525/50 nm. (g) Graph of the LysoSensor Green DND-189 fluorescence against the concentrations of compound **9**. (h) Curve fitting of the LysoSensor Green DND-189 fluorescence against the concentrations of compound **9**.

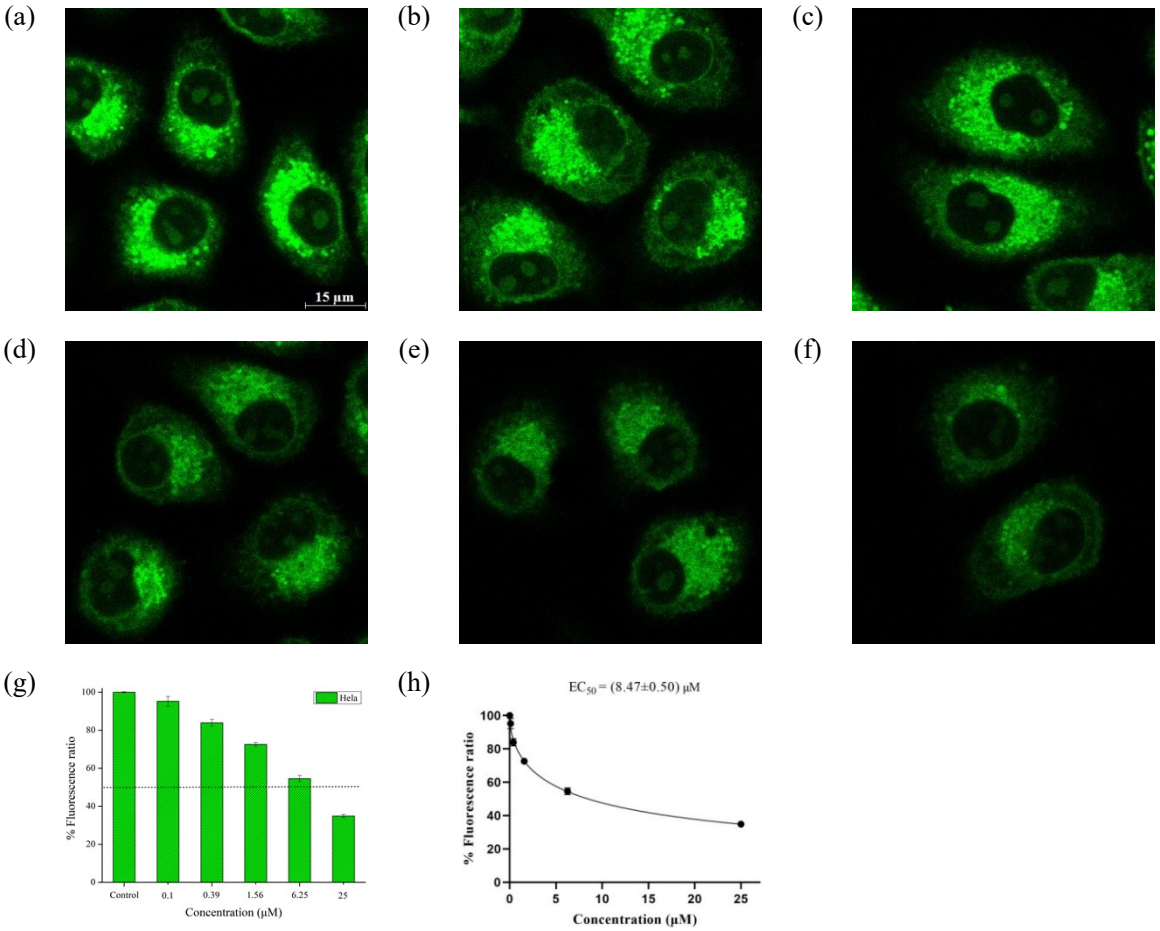

Fig. S77. (a-f) LysoSensor Green DND-189 (1.0 μM, 1 h) staining of (a) untreated HeLa cells and (b-f) HeLa cells treated with compound **10** at the concentrations of (b) 0.1 μM; (c) 0.39 μM; (d) 1.56 μM; (e) 6.25 μM and (f) 25 μM for 4 h, respectively. Green fluorescence: λ_{ex} BP 470/40 nm, λ_{em} BP 525/50 nm. (g) Graph of the LysoSensor Green DND-189 fluorescence against the concentrations of compound **10**. (h) Curve fitting of the LysoSensor Green DND-189 fluorescence against the concentrations of compound **10**.

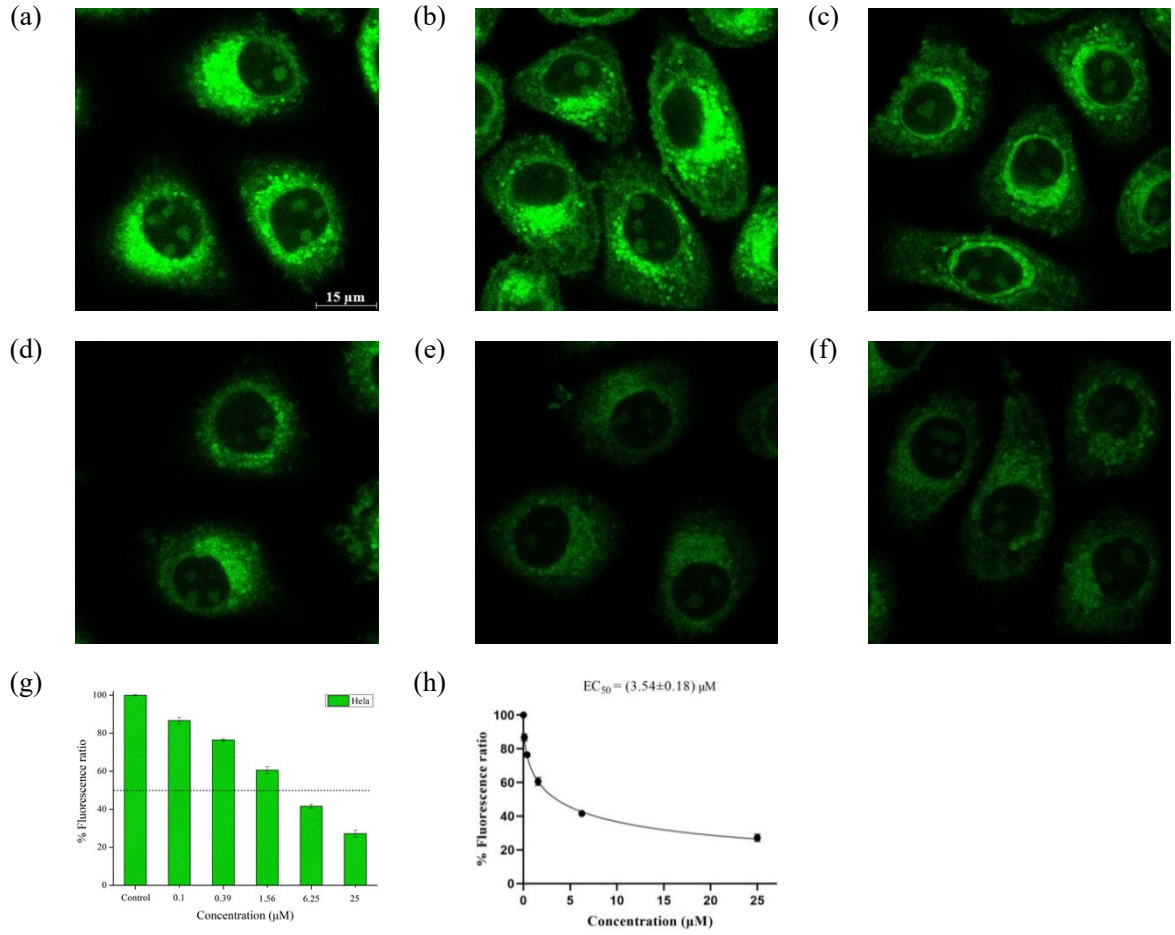

Fig. S78. (a-f) LysoSensor Green DND-189 (1.0 μM, 1 h) staining of (a) untreated HeLa cells and (b-f) HeLa cells treated with compound **11** at the concentrations of (b) 0.1 μM; (c) 0.39 μM; (d) 1.56 μM; (e) 6.25 μM and (f) 25 μM for 4 h, respectively. Green fluorescence: λ_{ex} BP 470/40 nm, λ_{em} BP 525/50 nm. (g) Graph of the LysoSensor Green DND-189 fluorescence against the concentrations of compound **11**. (h) Curve fitting of the LysoSensor Green DND-189 fluorescence against the concentrations of compound **11**.

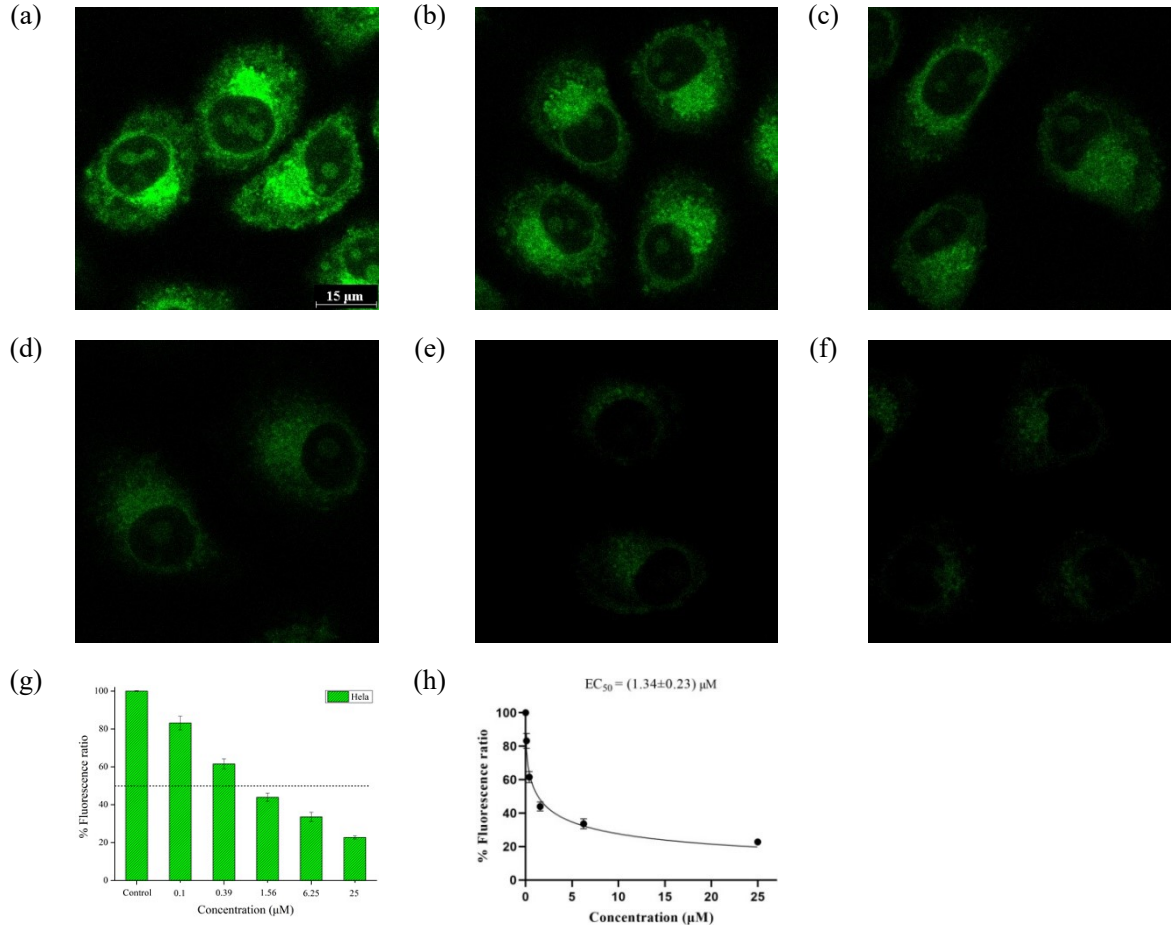

Fig. 79. (a-f) LysoSensor Green DND-189 (1.0 μM, 1 h) staining of (a) untreated HeLa cells and (b-f) HeLa cells treated with chloroquine phosphate at the concentrations of (b) 0.1 μM; (c) 0.39 μM; (d) 1.56 μM; (e) 6.25 μM and (f) 25 μM for 4 h, respectively. Green fluorescence: λ_{ex} BP 470/40 nm, λ_{em} BP 525/50 nm. (g) Graph of the LysoSensor Green DND-189 fluorescence against the concentrations of chloroquine phosphate. (h) Curve fitting of the LysoSensor Green DND-189 fluorescence against the concentrations of chloroquine phosphate.

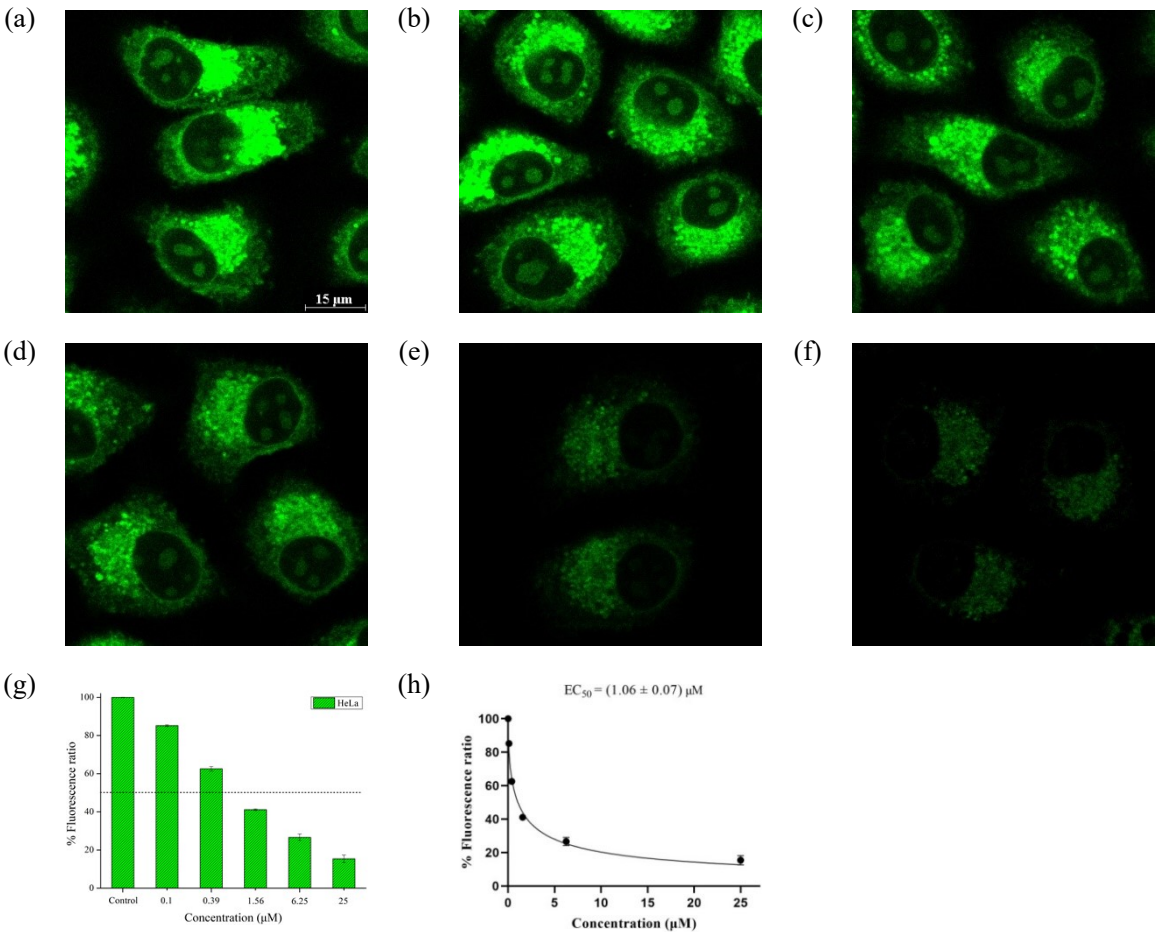

Fig. 80. (a-f) LysoSensor Green DND-189 (1.0 µM, 1 h) staining of (a) untreated HeLa cells and (b-f) HeLa cells treated with compound **A** at the concentrations of (b) 0.1 µM; (c) 0.39 µM; (d) 1.56 µM; (e) 6.25 µM and (f) 25 µM for 4 h, respectively. Green fluorescence: λ_{ex} BP 470/40 nm, λ_{em} BP 525/50 nm. (g) Graph of the LysoSensor Green DND-189 fluorescence against the concentrations of compound **A**. (h) Curve fitting of the LysoSensor Green DND-189 fluorescence against the concentrations of compound **A**.

7. BCECF-AM staining

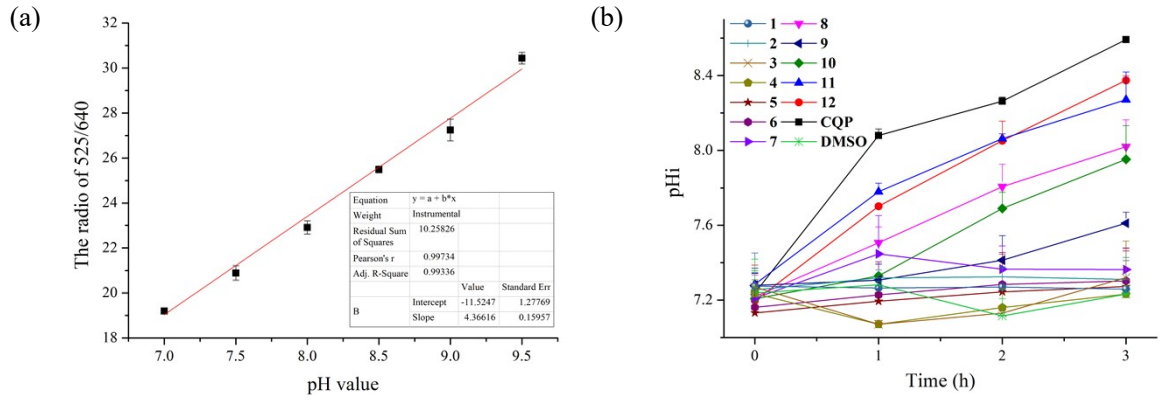

Fig. S81. (a) Standard curve of the emission wavelength 525/640 ratio of BCECF-AM corresponding to the pH value; (b) The intracellular pH (pH_i) change in HeLa treated with compounds **1**-**12** and chloroquine phosphate (CQP) over time. E_x: 485 nm, E_m: 525 nm and 640 nm.

8. Fluorescein-tetramethylrhodamine-labeled dextran staining

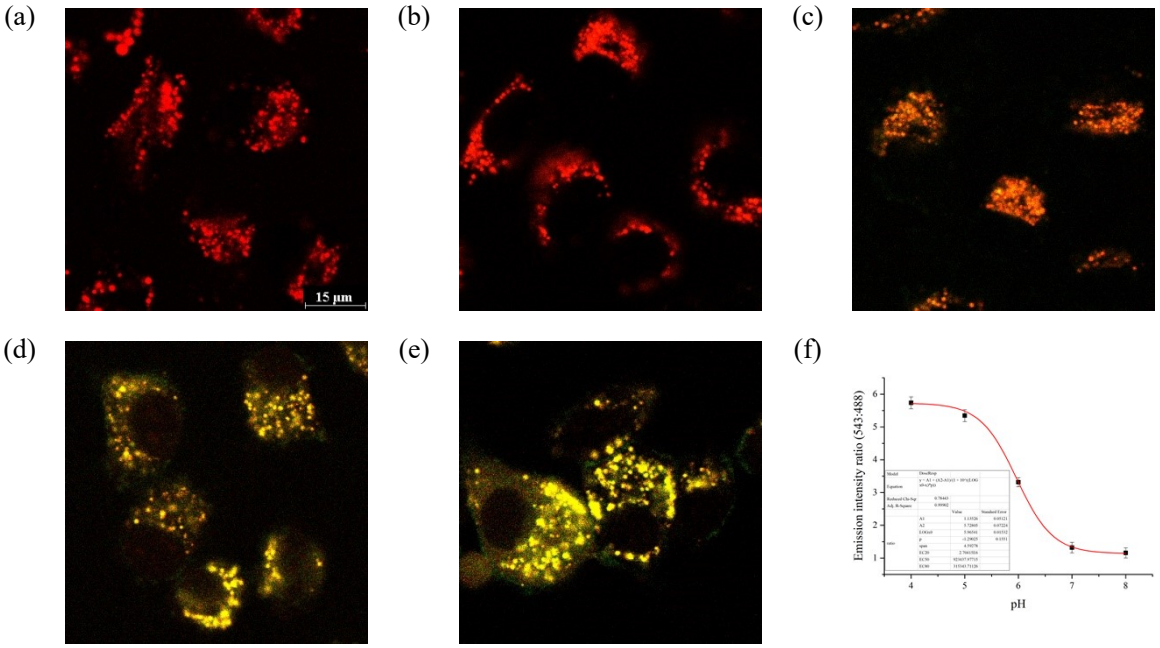

Fig. S82. (a-e) Staining plots of HeLa cells after 12 h of Fluorescein-tetramethylrhodamine-labeled dextran (0.2 mg/mL) staining and treatment with different pH calibration buffers. (a-e) HeLa cells treated with different pH standard solutions for 0.5 h, (a) 4.0; (b) 5.0; (c) 6.0; (d) 7.0 and (e) 8.0; (f) The pH titration curve of fluorescein-tetramethylrhodamine-labeled dextran. The fluorescein emission was calibrated using pH calibration buffers containing nigericin and valinomycin (mean ± s.d., n = 3).

9. MTT assay

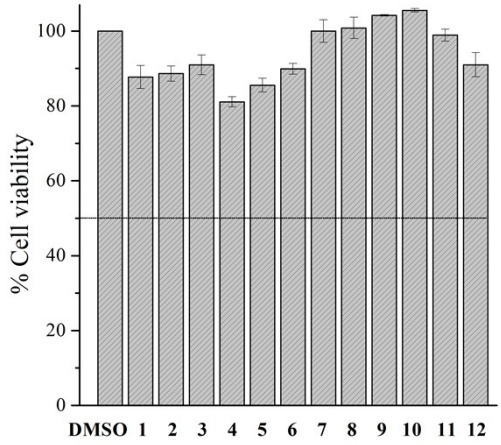

Fig. S83. Cell viability of compounds **1-12** (25 μM) toward HeLa cells (mean ± s.d., n = 3).

10. Western blotting

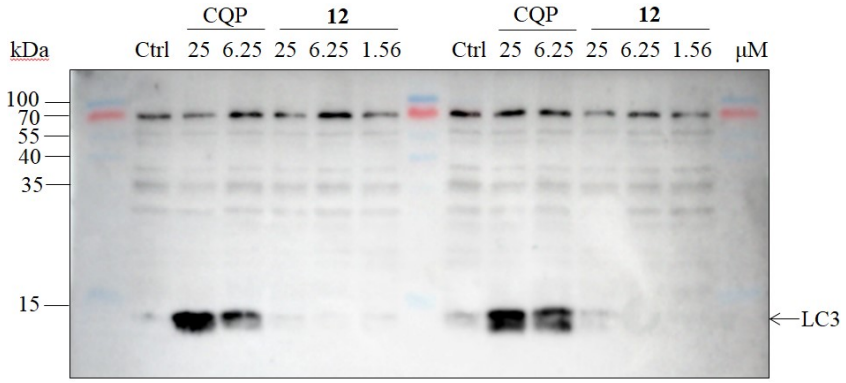

Fig. S84. Expanded and uncropped western blot panels of LC3 in HeLa cells after treatment with different concentration of compound **12** or chloroquine phosphate (CQP) for 24 h.

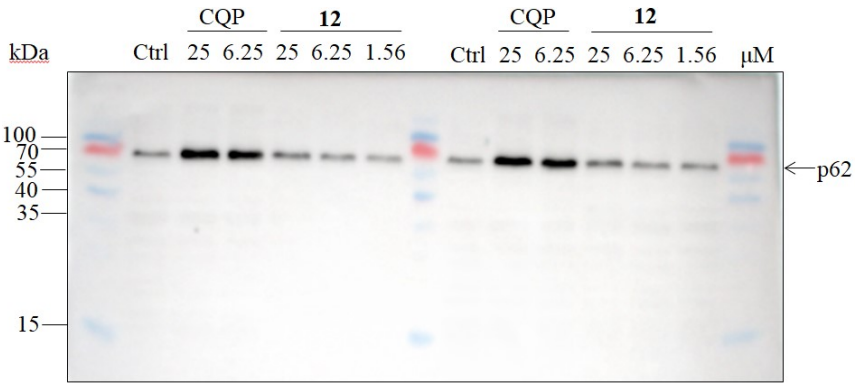

Fig. S85. Expanded and uncropped western blot panels of p62 in HeLa cells after treatment with different concentration of compound **12** or CQP for 24 h.

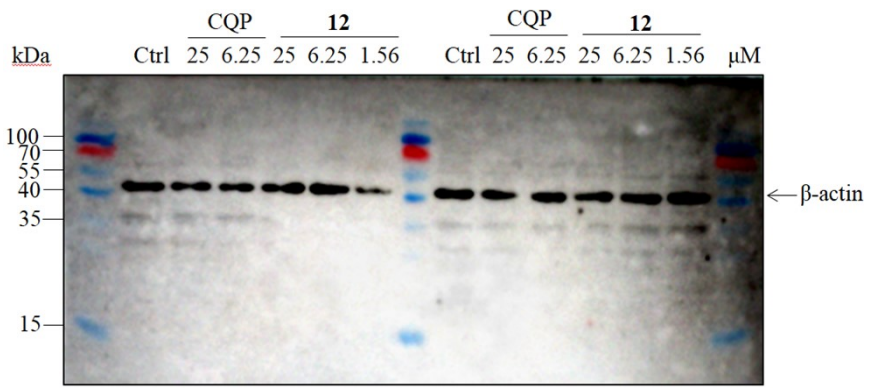

Fig. S86. Expanded and uncropped western blot panels of β-actin in HeLa cells after treatment with different concentration of compound **12** or CQP for 24 h.

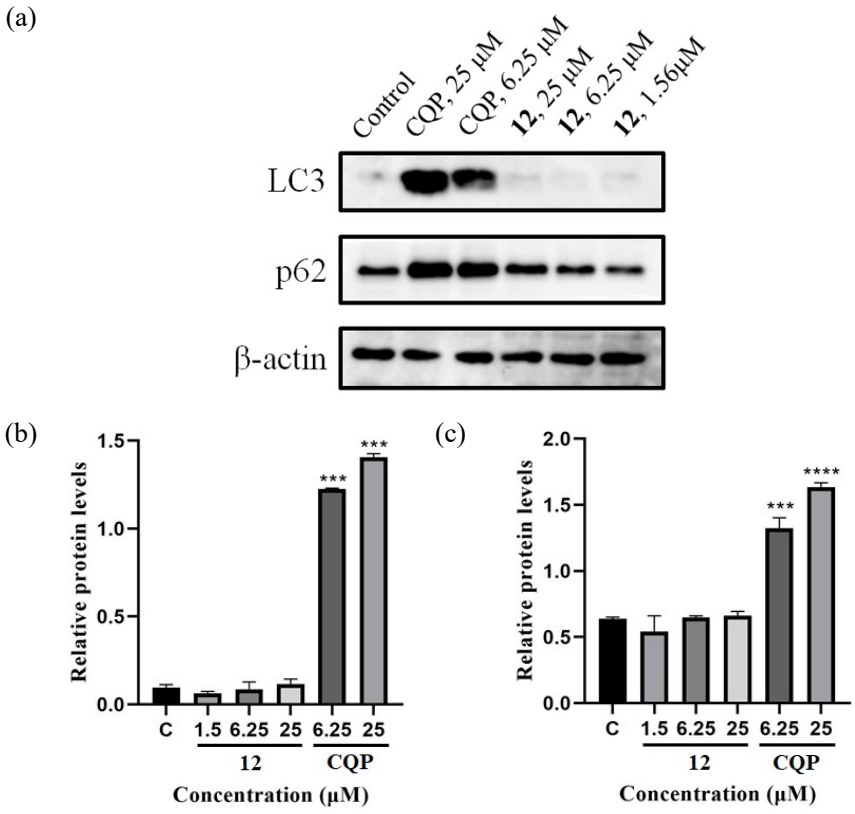

Fig. S87. Protein expression levels of LC3 and p62 in HeLa cells after treatment with different concentration of compound **12** or chloroquine phosphate (CQP) for 24 h. The data for (b) and (c) are represented as mean ± s.d. (n = 3), ***$p < 0.001$, ****$p < 0.0001$.